



The Assessment of Mitochondrial Function and Metabolic Activity in Pancreatic Progenitor Derived Hepatocytes

Emily Hudson

BSc(Hons), MRes.

Thesis submitted for the degree of Doctor of Philosophy

Newcastle University

Faculty of Medical Sciences

Institute of Cellular Medicine

September 2016

Declaration

I hereby declare that this thesis has been composed by myself and has not been submitted in any previous application for a degree. The work presented has been performed by myself, unless otherwise stated. All sources of information have been appropriately acknowledged by means of reference.

Abstract

Hepatocytes are the primary cell type of the liver, they play a key role in drug toxicity and therefore represent an ideal model for preclinical toxicity testing. However, current primary hepatocyte models resist *in vitro* proliferation and immortalised models are often not fully metabolically competent. One solution is the rodent B-13 cell line which forms hepatocyte-like B-13/H cells in response to glucocorticoid treatment. This thesis aimed to investigate the metabolic activity of B-13/H cells and assess the role of mitochondrial dysfunction in cytotoxicity. Cells were challenged with the anti-diabetic drug, troglitazone, which was withdrawn from the market following reports of liver injury, mitochondrial liabilities have since been associated with its toxicity. Extracellular flux analysis showed that basal levels of respiration were comparable between B-13 and B-13/H cells, however, reserve capacity was 5-fold greater in the B-13/H cells. In response to troglitazone, there was a concentration dependent decrease in oxygen consumption rate in B-13/H cells compared to a stimulation of respiration in B-13 cells and a concomitant increase in lactate levels and oxygen demand for ATP production. After 24 hours troglitazone treatment, there was a concentration dependent decrease in B-13/H viability. B-13 cell viability was unaffected. A larger baseline reserve capacity suggested a greater mitochondrial mass in B-13/H cells concomitant with a greater role in metabolism, similarly, B-13/H cells were more susceptible to troglitazone than B-13 cells. A drop in oxygen consumption rate suggested that there was mitochondrial dysfunction; this was supported by a drop in total ATP levels. In B-13 cells, troglitazone had a stimulatory effect on respiration and a concentration dependent increase in lactate suggested a switch from oxidative phosphorylation to glycolysis. The data presented indicate that B-13/H cells could potentially form the basis of a toxicity screening platform. This work could also underpin the development of a human equivalent model.

Acknowledgements

Firstly, I would like to thank my supervisor, Dr. Philip Manning for continued support and guidance throughout this project. I also offer my gratitude to the MRC for my MRC studentship, without which this project would not have been possible.

Special thanks to Dr. Aurora Gomez-Duran whose technical training and support were second-to-none. Without her expertise this process would have been much more difficult. I would also like to thank Dr. Philip Probert for his help with the B-13/H cells and to Dr. Emma Fairhall for kindly donating her time to setting up the H-13 and H-14 experiments.

To Hannah, Gina and Cara thank you for being there to lend a hand, an ear or sometimes a shoulder to cry on, my utmost gratitude for always understanding.

To my mum, dad and Liv, thank you for keeping me focussed and always believing I could do this even when I wasn't so sure.

Finally, to Alex, for unrelenting encouragement, being right by my side through the ups and the downs of the last four years but mostly for showing me that there is a life beyond science.

Contents

Declaration.....	i
Abstract.....	ii
Acknowledgements.....	iii
List of Figures	ix
List of Abbreviations.....	xi
Chapter 1: Introduction.....	1
1.1 Hepatocytes and the liver.....	2
1.2 Preclinical Toxicology.....	2
1.2.1 In silico studies.....	3
1.2.2 Safety Pharmacology.....	3
1.2.3 Genetic toxicology.....	3
1.2.4 General toxicology	3
1.3 Current Models for Toxicity Testing.....	4
1.3.1 The 3Rs	4
1.3.2. Human Hepatocytes	5
1.3.3 Immortalised Cell Lines.....	6
1.3.4 Embryonic Stem Cells.....	9
1.3.5 Induced Pluripotent Stem Cells.....	9
1.4 B-13/H Cells.....	11
1.4.1 Origins of the B-13/H Cell Line	11
1.4.2 Mechanism of Differentiation	11
1.4.3 Functional Similarity of B-13/H Cells to Hepatocytes.....	13
1.4.4 Human Equivalents of B-13/H Cells.....	13
1.5 Mitochondria.....	15
1.5.1 Mitochondrial Structure and Function	15
1.5.2 Cellular Respiration.....	15
1.5.3 The Electron Transport Chain.....	16

1.5.4 Free Radical Production	17
1.6 Mitochondrial Toxicity.....	18
1.6.1 Drug Induced Liver Injury.....	18
1.6.2 Mitochondrial Susceptibility to Damage	19
1.7 Mechanisms of Drug Induced Mitochondrial Damage.....	19
1.7.1 Mitochondrial Permeability Transition Pore Opening	20
1.7.2 Impairment of Oxidative Phosphorylation	21
1.7.3 Inhibition of Fatty Acid Oxidation	21
1.7.4 Oxidative Stress.....	21
1.8 Oxidative Damage.....	22
1.8.1 Protein Damage	22
1.8.2 Lipid Damage.....	22
1.8.3 DNA Damage.....	22
1.8.4 Anti-Oxidants	22
1.8.5 Paracetamol Toxicity.....	23
1.9 Troglitazone	24
1.9.1 Mechanism of Action.....	24
1.9.2 Mechanism of Toxicity	25
1.9.3 Apoptosis	28
1.9.4 Why was toxicity not predictable?.....	29
1.9.5 New Applications of Troglitazone.....	29
1.10 Study Objectives	30
1.11 Statistical Analysis	31
1.12 References.....	32
Chapter 2: Simultaneous Intracellular and Extracellular ROS Detection	39
2.1 Introduction	40
2.1.1 Physiological ROS Production	40
2.1.2 Methods of ROS Detection	41

2.1.3 Aims.....	45
2.2 Methods	47
2.2.1 Materials	47
2.2.2 Cell Culture	47
2.2.3 Long Term Cell Storage.....	48
2.2.4 Cell Stock Revival	48
2.2.5 Electrode Preparation	48
2.2.6 Electrode Calibration.....	48
2.2.7 Cellular Superoxide Measurement in B-13 and B-13/H Cells	49
2.2.8 Nanosensor Production	49
2.2.9 pH Nanosensor Calibration.....	50
2.2.10 Free Dye ROS Assay.....	50
2.2.11 Resazurin Cell Viability Assay	51
2.3 Results	52
2.3.1 Calibration of Superoxide response using Electrochemistry	52
2.3.2 Stimulated Extracellular O ₂ ⁻ Production in B-13 and B13/H Cells	52
2.3.3 Development of PEBBLE nanosensors for the detection of intracellular ROS based on a pH sensor proof of concept.	55
2.3.4 Toxicity of PEBBLE nanosensors	57
2.3.5 ROS measures using DCFDA Free Dye	58
2.3.6 ROS measures using PEBBLEs in Ethanol Treated Cells	58
2.4 Discussion.....	60
2.5 References.....	66
Chapter 3: Drug Induced Cytotoxicity and Antioxidant Treatment	68
3.1 Introduction	69
3.1.1 Thiazolidinediones	69
3.1.2 Antioxidants	71
3.1.3 Aims.....	75

3.2 Methods	76
3.2.1 Materials	76
3.2.2 Cell Culture	76
3.2.3 Resazurin Cell Viability Assay	76
3.2.4 Antioxidant Effect on Cell Viability.....	76
3.3 Results	77
3.3.1 Menadione Cytotoxicity and antioxidant effects in B-13 and B-13/H cells..	77
3.3.2 Troglitazone Cytotoxicity and Antioxidant effects in B-13 and B-13/H cells	79
3.4 Discussion.....	84
3.5 References.....	89
Chapter 4: Extracellular Flux Analysis to Determine Differences in the Metabolic Profile of B-13 and B-13/H Cells.....	92
4.1 Mitochondrial Role in DILI	93
4.1.1 Consequences of Mitochondrial Impairment.....	93
4.1.2 Current Technologies for Measuring Mitochondrial Respiration	95
4.1.3 Aims.....	99
4.2 Methods	101
4.2.1 Materials	101
4.2.2 Cell Culture	101
4.2.3 Seahorse Extracellular Flux Optimisation	101
4.2.4 Mitochondrial Stress Test	102
4.2.5 Normalisation for Protein Content.....	103
4.2.6 ATP Quantification.....	103
4.2.7 Lactate Quantification	104
4.3 Results	105
4.3.1 Optimisation of Extracellular Flux Analysis	105
4.3.2 The Effect of Troglitazone on Mitochondrial Respiration.....	106

4.3.3 Cellular ATP levels in Response to Troglitazone	110
4.3.4 Lactate Production Following Troglitazone Treatment	110
4.4 Discussion.....	112
4.5 References.....	117
Chapter 5: Human Equivalents.....	120
5.1 Introduction	121
5.1.1 Extrapolation of animal data to humans.....	121
5.1.2 Aims.....	125
5.2 Methods	126
5.2.1 Materials	126
5.2.2 Cell Provision	126
5.2.3 HPAC Cell Culture	126
5.2.4 H-13 and H-14 Cell Culture.....	126
5.2.5 Resazurin Cell Viability Assay	127
5.2.6 ATP Quantification	127
5.3 Results	128
5.4 Discussion.....	134
5.5 References.....	138
Chapter 6: General Discussion.....	141
6.1 General Discussion	142
6.2 References.....	148

List of Figures

Figure 1.1: The Electron transport chain.....	17
Figure 1.2: ROS production and anti-oxidant mechanisms	23
Figure 2.1: Electrochemical measures of O_2^-	43
Figure 2.2: representation of PEBBLE nanosensor	45
Figure 2.3: Calibration of the gold electrode to superoxide in a stirred system.	52
Figure 2.4: Current response of B-13/H cells to ethanol.....	53
Figure 2.5: O_2^- production by B-13/H cells during the transdifferentiation process following stimulation with 5% v/v ethanol	53
Figure 2.6: Current production from B-13 and B-13/H cells treated with menadione	54
Figure 2.7: Example electrochemistry trace	55
Figure 2.8: Calibration of pH sensitive nanosensors FAM and Oregon green.....	55
Figure 2.9: Calibration curve of DCFDA free dye	56
Figure 2.10: Calibration curve of DCFDA PEBBLE nanosensors.....	57
Figure 2.11: Cell viability following exposure to blank nanosensors.....	57
Figure 2.12: ROS production in response to treatment with menadione	59
Figure 3.1: The structure of thiazolidinediones.....	70
Figure 3.2: Schematic representation of lipid peroxidation.....	73
Figure 3.3: B-13 and B-13/H cell viability following menadione treatment.....	78
Figure 3.4: Antioxidant effects of catalase and SOD on B-13 cells.	79
Figure 3.5: Antioxidant effects of catalase and SOD on B-13/H cells.....	79
Figure 3.6: B-13 and B-13/H cell viability following troglitazone treatment	81
Figure 3.7: The effect of stage of differentiation on susceptibility to troglitazone.....	82
Figure 3.8: Effect of a range of concentrations of catalase on the viability of B-13/H cells	83
Figure 3.9: Effect of a range of concentrations of Co-enzyme Q10 on the viability of B-13 and B-13/H cells	83
Figure 4.1: The parameters of mitochondrial respiration that can be assessed using a mitochondrial stress test and illustration of a XF microplate and sensor cartridge .	98
Figure 4.2: Optimisation of Mitochondrial Stress Test.....	105
Figure 4.3: Effect of different concentrations of troglitazone on mitochondrial respiration following 24-hour incubation	107
Figure 4.4: Effect of different concentrations of troglitazone on mitochondrial functions following 24 hr incubation.....	109

Figure 4.5: Cellular ATP level in response to 1hr troglitazone treatment..... 110

Figure 4.6: Effect of troglitazone on lactate production in B-13 and B-13/H cells. ... 111

Figure 5.1: The comparison of troglitazone toxicity in H-13 with their undifferentiated counterparts over 24 hours..... 130

Figure 5.2: The comparison of troglitazone toxicity in H-14 with their undifferentiated counterparts over 24 hours..... 131

Figure 5.3: Comparison of troglitazone toxicity after 24-hour exposure between rodent and human cells lines..... 132

Figure 5.4: ATP levels in H-13 and H-14 cells treated with troglitazone for 1 hour. 133

List of Abbreviations

ADP	Adenosine diphosphate
ALT	Alanine transaminase
AST	Aspartate transaminase
ATP	Adenosine triphosphate
B-13	AR42J-B-13 cell
B-13/H	B-13 derived hepatocyte-like cell
BSA	Bovine serum albumin
C/EBP	CCAAT/enhancer-binding protein
CoQ10	Co-enzyme Q10
CPS1	Carbamoyl-phosphate synthetase 1
CYP450	Cytochrome P450
Cyt c	Cytochrome c
DCFDA	2',7' –dichlorofluorescein diacetate
DEX	Dexamethasone
DI	Deionised
DILI	Drug induced liver injury
DMEM	Dulbecco's modified eagle medium
DMPO	5,5-Dimethyl-1-Pyrroline-N-Oxide
DMSO	Dimethyl sulfoxide
DNA	Deoxyribonucleic acid
DTSSP	3,3'-Dithiobis(sulfosuccinimidylpropionate)
ECAR	Extracellular acidification rate
EDTA	Ethylenediaminetetraacetic acid
EPR	electron paramagnetic resonance
ETC	Electron transport chain
FAD	flavin adenine dinucleotide
FAM	5' 6-FAM (Fluorescein)
FBS	Foetal bovine serum
FCCP	Carbonyl cyanide-4-(trifluoromethoxy)phenylhydrazone
FIT-C	Fluorescein isothiocyanate
GR	Glucocorticoid receptor
GSH	Glutathione
GST	Glutathione transferases

HNF	Human nuclear factor
HPAC	Human pancreatic acinar cells
iPS	Induced pluripotent stem cell
JNK	c-Jun N-terminal kinases
KEL-F	Polychlorotrifluoroethylene
LC50	Lethal concentration required to kill 50% of the population
MPT	Mitochondrial permeability transition
mRNA	Messenger RNA
mtDNA	Mitochondrial DNA
NADH	Nicotinamide adenine dinucleotide
NADPH	Nicotinamide adenine dinucleotide phosphate
NAPQI	N-acetyl-p-benzoquinoneimine
NC3Rs	National Centre for 3Rs
NCE	New chemical entity
NOX	Nitric Oxide
PBS	Phosphate buffered saline
PEBBLE	Probe encapsulated by biologically localised embedding
PMA	phorbol 12-myristate 13-acetate
PPARγ	Peroxisome proliferator-activated receptor γ
PPRE	PPAR response element
ROS	Reactive oxygen species
RXR	Retinoid X receptor
SGK1	Serum/glucocorticoid regulated kinase 1
SOD	Superoxide dismutase
TAMRA	5-Carboxytetramethylrhodamine
TEMED	Tetramethylethylenediamine
TZD	Thiazolidinedione
UGT	UDP glucuronosyl-transferases
XF	Extracellular flux
XOD	Xanthine oxidase

Chapter 1: Introduction

1.1 Hepatocytes and the liver

The liver is the largest visceral organ in the body and represents approximately 2% of adult body weight. The liver has two main vascular systems, the first is supplied by the hepatic artery and the second by the portal vein (Malarkey *et al.*, 2005). The portal vein drains from the gastrointestinal tract and as such is enriched with nutrients from the intestine. This subsequently means that the liver is also vulnerable to high exposure from orally ingested xenobiotics and plays a vital role in the biotransformation and metabolism of exogenous substances. The liver is made up of approximately 15 different cell types, of which, hepatocytes are the most abundant, which represent approximately 60% of total cell content of the liver and 80% of total liver volume (Ishibashi *et al.*, 2009).

Hepatocytes are responsible for the majority of liver function and are the primary cells in which drug metabolism occurs due to their high content of phase I and II metabolic enzymes as well as high expression of uptake and efflux transporter proteins and therefore hepatocyte cell models play a huge role in preclinical studies as they can provide a useful high throughput screen for the assessment and understanding of the diverse mechanisms by which a compound can elicit toxic outcomes (Ishibashi *et al.*, 2009).

1.2 Preclinical Toxicology

The drug development process consists of four main phases: early discovery, late discovery, preclinical and clinical. Preclinical toxicity testing is vital in understanding or predicting adverse responses to potential new drug candidates both at therapeutic and supra-therapeutic doses to ensure the safety of participants in human clinical trials. Safety studies are crucial in the drug development process; in recent years the failure to predict toxicity has overtaken lack of efficacy as the primary reason for drug attrition. In 1991 40% of drugs that dropped out of the development process were due to poor pharmacokinetics or bioavailability, by 2000 this had been reduced to less than 10% with the development of better *in vitro* predictive systems (McKim Jr, 2010).

In recent years there has been a push to update the tools used to predict toxicity and to align the search for toxicity with the search for new compounds so that toxicity issues can be established earlier in the process to reduce the costs incurred with dropping a compound further in the development stages (McKim Jr, 2010). Broadly

speaking there are 4 main arms of exploratory safety studies: *in silico*, safety pharmacology, general toxicology and genetic toxicology.

1.2.1 *In silico studies*

In silico studies are initial computational predictions of a drug's toxicological potential based on its chemical structure. It is useful early on in the drug development process as many compounds can be screened quickly to identify leads and prioritise certain structures. However, the utility of *in silico* testing is restricted by the size of the database meaning it is not a fully comprehensive predictive system and it also lacks the ability to detect complex outcomes (Ahuja and Sharma, 2014).

1.2.2 *Safety Pharmacology*

The focus of safety pharmacology testing is to assess potential undesirable toxic effects in major physiological systems, predominantly, cardiovascular, central nervous system, respiratory, renal and gastro intestinal. By assessing functional end-points the results of safety pharmacology studies can inform testing by ruling out further studies with a drug that has a problematic profile at this stage. If these tests can be performed using high throughput *in vitro* screens, then it also reduces the number of animals required for further endpoint testing (Hamdam *et al.*, 2013).

1.2.3 *Genetic toxicology*

Genotoxicity studies provide a short term surrogate for longer term carcinogenicity studies and aim to understand if a drug candidate will be mutagenic. Mutagenicity tests identify whether a compound has the potential to cause chromosomal aberrations or DNA damage in the form of structural aberrations to DNA such as deletions, insertions, duplications or translocations as well as changes to the base sequence the results of which suggest the potential for the compound to be carcinogenic. Carcinogenicity studies are not part of the standard battery of tests unless a drug is expected to be required chronically or to treat a recurring condition (Ahuja and Sharma, 2014).

1.2.4 *General toxicology*

General toxicology tests aim to identify the maximum tolerated dose and to subsequently establish a dose range for the drug candidate. General toxicology also explores the toxicokinetics of a drug candidate by using cytotoxicity screens to

provide mechanistic information regarding a drug's bioactivation, mode of metabolism and potential toxic effects. It is at this stage when hepatocyte models are used as they can provide useful information about the mechanism(s) by which a molecule causes toxicity. Hepatocytes also allow for rapid, high throughput screening and when used with a panel of cell lines can provide accurate and reproducible data in a cost-effective manner (Ahuja and Sharma, 2014).

1.3 Current Models for Toxicity Testing

For many years' *in vitro* cell models have frequently been used for the determination of liver toxicity in pre-clinical regulatory toxicology experiments as well as for disease modelling. Cell models provide a useful tool early in the drug development process for high throughput screening of potential new chemical entities because they can be grown quickly and in volume. Cell lines can be easily manipulated depending upon the particular toxicity being studied, making choosing a subsequent animal model more accurate as *in vitro* models help to identify any species specific toxicities (Ahuja and Sharma, 2014). As a result, a wealth of cell and tissue models have been developed that can be tested in conjunction as a panel to provide an overview of chemical toxicity. Amongst the most commonly used cell lines are the HepG2 and HepaRG which are derived from human liver tissue and immortalised. It is estimated that approximately only 1 in 10,000 chemicals that enter into the discovery process ever make it to the market and 40% of new chemical entities that enter preclinical safety testing will fail because of toxicity issues, indicating that there is still a need for more accurate and reliable predictive methods (McKim Jr, 2010). The issue is further compounded by the drive to reduce testing in whole animals, with the introduction of the National Centre for 3Rs (NC3Rs) initiative it is more important than ever that new methods can be developed utilising cell based *in vitro* models.

1.3.1 The 3Rs

In 2004, the UK government established the NC3Rs in order to highlight the importance of animal welfare in research by producing a range of resources in order to educate researchers and funding 3Rs related research (Perry and Joynson, 2007). The 3Rs are guiding principles for the ethical use of animals in medical research, described by M. S. Russell and R. L. Burch in 1959 and stand for replacement, reduction and refinement and suggest that where possible the use of animals must be completely avoided (replacement), when this is not possible, studies must be

designed to use as few animals as possible (reduction) and at all times the welfare of the animal must be paramount; the methods used in the study must be adapted to ensure as little pain and distress as possible is experienced by the animal (refinement) (Holmes *et al.*, 2010).

In the UK, regulations for animal research are some of the strictest in the world. Researchers must obtain a number of government licenses before any work using animals can be performed and a comprehensive justification of the use of animals and cost-benefit analysis must be provided before work can begin. This includes demonstration that the 3Rs (reduction, replacement and refinement) have been considered (Perry and Joynson, 2007). Since the inception of animal models, medical research has advanced rapidly; sophisticated predictive *in silico* models and tissue models have been developed, making widespread use of whole animals less relevant in many areas of scientific research (Holmes *et al.*, 2010).

There are currently many alternative models for use instead of animals in all areas of medical research including primary models of human hepatocytes as well as immortalised cell lines and even liver microsomal fractions for studies of particular organelle functions. In pre-clinical toxicity testing, however, the issue of alternative models is more complex as the results obtained need to be predictive of human response to a chemical compound and as such liver cell models are rather more challenging to replace. However, when combined, different models can form a useful platform for establishing toxic effects.

1.3.2. Human Hepatocytes

A whole liver perfusion would be the ideal model for predicting drug induced liver injury (DILI) as it retains all original cell types and structure thus allowing for a response that is as close to the *in vivo* situation as possible. However, due to the scarcity of liver tissue for research, it cannot be obtained on demand and any experimental replicates are often from different donors and as such do not always provide consistent responses. Furthermore, any good quality livers are reserved for transplantation (Wallace *et al.*, 2010).

Human hepatocytes are considered the “gold standard” for drug metabolism and toxicity studies as they are fully competent metabolic cells derived from human liver tissue. Unfortunately, supply is limited and small fragments of tissue are often

variable in quality (Castell *et al.*, 2006). Furthermore, hepatocytes do not proliferate *in vitro* and thus cannot be expanded because they are resistant to subculture (Probert *et al.*, 2014).

Human hepatocytes do, however, present an adult phenotype and express functional phase I and II enzymes as well as enzyme co-factors and will respond to CYP inducers providing an overall metabolic profile of a compound (Castell *et al.*, 2006). A particular advantage human hepatocytes have over immortalised cell lines is that they show phenotypic variation dependent on the CYP expression of the individual hepatocyte donor; there will potentially be polymorphisms due to diet, age, social habits such as smoking and drinking as well as changes due to the donors' exposure to other drugs. This means that during the drug screening process susceptible individuals based upon genotype are more likely to be discovered. However, such variation in hepatocytes can also lead to variation in cell viability and attachment, making experimentation difficult (Castell *et al.*, 2006).

Long term drug toxicity studies are problematic in human hepatocytes as their phenotype is not stable in culture for more than a few days. CYP expression can become down regulated over time meaning that studies are restricted to acute dosing and chronic analysis is not possible (Castell *et al.*, 2006). Furthermore, routine testing is often hindered due to lack of access to fresh human hepatocytes. Additionally, there is often considerable variation in CYP expression between batches of isolated hepatocytes. This is largely due to the fact that cells are often significantly damaged prior to isolation because they have come from patients who have been on long term treatment which has caused hepatotoxicity and cellular damage. Furthermore, age, environmental factors and lifestyle factors such as drinking alcohol and smoking can all contribute to an altered CYP profile (Maes *et al.*, 2016). Consequently, generating reproducible and consistent data from human hepatocytes is often challenging (Rodríguez-Antona *et al.*, 2002).

1.3.3 Immortalised Cell Lines

Hepatic cell lines derived from human hepatomas are among the most commonly used hepatic cell lines as they are able to grow continuously in simple growth media, have an unlimited life span and a stable phenotype. These reasons along with their ease of availability make them an attractive option for hepatocyte studies and due to

the frequency with which they are used have become standardised across labs, making cross-comparison easier (Castell *et al.*, 2006).

The HepG2 line is a commonly used hepatocyte cell line as it exhibits many liver specific functions and has expression of some liver specific enzymes. However, the cells do not provide a useful predictive model as they lack functional expression of nearly all CYP enzymes. HepG2 cells only show a similar susceptibility as human hepatocytes to drugs that do not require metabolism such as amiodarone and chlorpromazine (Guillouzo *et al.*, 2007).

In contrast the HepaRG cell line has been reported as being much closer in CYP expression to human hepatocytes than the HepG2 cells (Guillouzo *et al.*, 2007; Hart *et al.*, 2010; Gerets *et al.*, 2012). HepaRG cells were originally derived from a female hepatocarcinoma patient. At sub-confluence they are proliferative but retain an undifferentiated form. With the addition of differentiation inducing media (William's E media supplemented with 10% FCS, 100 units/ml penicillin, 100 µg/ml streptomycin, 5 µg/ml insulin and the addition of 2% DMSO and 50 µM hydrocortisone for differentiation) the cells will differentiate into hepatocytes or biliary epithelial cells at which point they will remain stable for several weeks (Hart *et al.*, 2010). Interestingly, both undifferentiated and differentiated HepaRG cells show similar functionality to primary human hepatocytes, however, when differentiated there is an up regulation of drug metabolising enzymes. It has been reported that at the mRNA level, HepaRG cells express most phase I genes, including CYP1A2, CYP2B6, CYP2C9, CYP2E1 and CYP3A4 as well as most phase II genes, including UGT1A1, GSTA1, GSTA4 and GSTM1 (Hart *et al.*, 2010; Gerets *et al.*, 2012). The level of mRNA present of phase I and II enzymes was found to be comparable to that of primary human hepatocytes and were similarly as inducible using β-naphthoflavone to induce CYP1A2, PB for CYP2A6 and rifampicin for CYP3A4. CYP3A4 and CYP2B6 were found to be particularly highly inducible in the HepaRG cells and at much more consistent levels than those found in primary human hepatocytes (Gerets *et al.*, 2012). As mentioned previously, HepG2 cells show low expression of CYP enzymes and are poorly inducible. The only inducible gene found is CYP1A1 which is typically only expressed in the foetal liver *in vivo*. This suggests that HepG2 cells do not retain an adult phenotype and would explain why cells have low metabolic capacity (Gerets *et al.*, 2012). Changes in gene expression that occur during processes such

as differentiation are mostly controlled at a transcriptional level (Ramji and Foka, 2002). Liver specific gene expression in adult hepatocytes relies upon four families of transcription factors; C/EBP, HNF-1, HNF-3 and HNF-4 (Rodríguez-Antona *et al.*, 2002). It has been suggested that a decrease in these liver enriched transcription factors causes a downregulation of CYP expression during culture. One of the most commonly expressed transcription factors in the regulation of CYP enzymes in the liver is C/EBP- β . C/EBP- β can be transcribed in a full length form or a truncated form. It has been found that the truncated form lacks the specific domain which causes the activation of CYP transcription and furthermore, antagonises the full length form. This means that, when the truncated form is dominant, not only are functional CYP enzymes unable to be transcribed but they are also inhibited from being transcribed by functional C/EBP- β (Rodríguez-Antona *et al.*, 2002).

Unfortunately, although the CYP mRNA levels are comparable to primary human hepatocytes and they show a similar level of induction this does not correlate with functionality. The enzyme activity in HepaRG cells is much lower than primary human hepatocytes and is more comparable to the enzyme activity found in HepG2 cells. Gerets *et al* reported that in order to achieve comparable LC50 values with primary human hepatocytes, higher concentrations and longer incubation times were required with HepaRG cells. It was suggested that this could be because in HepaRG cells, higher levels of basal CYP may be required in order to successfully metabolise drugs, it is also possible that the cells express more phase II than phase I enzymes and thus drugs are more efficiently metabolised by alternative pathways that do not generate toxic metabolites (Gerets *et al.*, 2012).

Immortalised cell lines such as HepG2 and HepaRG are an attractive option when looking for a hepatocyte cell line to study as they are readily available, easy to culture, they are proliferative, do not de-differentiate in culture and have a stable phenotype. However, while they address many of the issues found with primary hepatocytes they may not be suitable for toxicity profiling of drug compounds as they may underestimate toxicity due to a reduced or dysfunctional cytochrome P450 profile.

In order to overcome the limitations of immortalised lines a lot of work in recent years has focussed on the development of new ways in which to generate human hepatocytes using stem cells. Because of their human physiology, stem cells could

be useful in regenerative medicine as well as predicative toxicity studies and disease modelling, thus offering huge potential.

1.3.4 Embryonic Stem Cells

Embryonic stem cells are pluripotent cells derived from the inner cell mass of a blastocyst. This means that upon exposure to specific growth factors the cells can be directed towards any cell lineage in the body and have the potential for continuous differentiation *in vitro* (Zhang *et al.*, 2013). The aim is to derive fully functioning adult human hepatocytes from pluripotent embryonic cells, however, as there is no standardised method for doing this, the procedure is still being refined. Similarly, once the cells have differentiated there is currently no set method for the characterisation of the cells to determine how like primary human hepatocytes the derived cells are. This would not only be important in order to assure batch to batch consistency in cells but also to ensure comparable results between labs using the same cells. Currently the cells are assessed based on the purity of the batch i.e. the proportion of mature hepatocyte like cells present, and their gene expression profile. Similar to the HepG2 and HepaRG cells mentioned in Section 1.1.3, a fully functioning and inducible CYP profile is yet to be seen in any successfully derived hepatocyte like cells (Kia *et al.*, 2013). Additionally, there are many ethical concerns with the use of embryos because the isolation of the inner cell mass results in the destruction of the embryo and thus progress in this field is often very slow (Zhang *et al.*, 2013).

1.3.5 Induced Pluripotent Stem Cells

Pluripotent cells are able to differentiate into any cell derivative of the 3 germ layers (endoderm, mesoderm and ectoderm). Therefore, when these cells are exposed to certain growth factors and hormones they can be directed down a particular differentiation pathway and as a result form any cell type within the body.

Pluripotency can be induced in cells by transducing particular genes that cause the cells to revert to endoderm cells. iPS cells were first used to generate human hepatocytes in 2004 by Song *et al.* (Song *et al.*, 2009). Endoderm induction was initiated by transduction of a lentivirus containing the genes Oct-4, Sox-2, Klf4 and Utf1 into human fibroblasts. Following induction of pluripotency, the cells could then be directed down a hepatocyte differentiation pathway by culture in hepatocyte culture medium containing specific fibroblast growth factors. Following 21 days

differentiation the resulting cells exhibited liver specific functions such as albumin secretion, urea production and cytochrome P450 activity as well as expression of specific hepatic markers such as albumin (Song *et al.*, 2009).

Hepatocytes generated in this way are comparable to human embryonic stem cell derived hepatocytes without the ethical implications. Furthermore, they proliferate extensively and therefore are preferential to human hepatocytes extracted from liver tissue. Finally, iPS technology could be harnessed to produce patient specific cells allowing for their transplantation *in vivo*, however, this is currently not possible as the cells do not expand *in vivo* (Zhang *et al.*, 2013). There are also additional concerns over the use of iPS cells in humans as their production requires the use of viral vectors which could potentially introduce genomic insertions of exogenous sequences into the DNA of hepatocytes which could potentially pose a tumour risk in humans (Kia *et al.*, 2013). It has also been highlighted that iPS cells may retain epigenetic memory and overcoming this represents another challenge of developing a genetically stable model. Epigenetic memory is the term given to cells that return to the original phenotype of the parent cells, thought possibly to be due to incomplete DNA methylation (Kia *et al.*, 2013).

Stem cells have huge potential not only in academic research but also clinically. It is possible that if a stable cell line can be generated, hepatic like stem cells could have the necessary functional genotype that would allow them to be used in regenerative medicine. While huge steps have been taken to achieve this there are still many remaining challenges, not least that the production of hepatocyte equivalents from stem cells is very expensive.

Over the past decade, work has been done to develop a novel cell line derived from the pancreatic acinar cells of rats following the observation that simple steroid treatment caused the cells to transdifferentiate into hepatocyte like cells. Creating hepatocytes via this method has been reported as being an estimated 5 million times cheaper than generating hepatocytes from stem cells (Probert *et al.*, 2014). If the mechanisms behind this transdifferentiation could be established and harnessed it could pave the way for a human equivalent.

1.4 B-13/H Cells

1.4.1 Origins of the B-13/H Cell Line

B-13 cells are a sub-clone of the exocrine pancreatic AR42J cell line developed from rat adenocarcinoma cells. The AR42J cell line, which is still used today in exocrine pancreas research, was created by treating inbred Wistar/Lewis rats with the naturally occurring antibiotic, azaserine, known to be capable of producing carcinomas and isolating the cells from the pancreatic tumours. The Kojima lab developed the B-13 sub-clone in 1996 by treating AR42J cells with hepatocyte growth factor and activin A. Following treatment, it was found that the cells that were able to differentiate into insulin producing, endocrine, β -like pancreatic cells *in vitro* (Probert *et al.*, 2015). In 2000, Shen *et al.* reported that, following glucocorticoid treatment, there was a distinct change in phenotype as cells altered from pancreatic to hepatic morphology (Shen *et al.*, 2000). This observation was later confirmed with studies that showed these hepatic like cells to express certain hepatic specific genes (Tosh *et al.*, 2002a; Tosh *et al.*, 2002b). This work was built upon in 2003 by the Wright group, it was demonstrated that following 12 days of treatment with dexamethasone, B-13/H cells expressed significant levels of 4 constitutively expressed cytochrome P450 enzymes- CYP2C11, CYP2A, CYP2E1 and CYP3A1, which were undetectable in B-13 cells. Furthermore, for the first time it was found that the CYP enzymes expressed were also found to be metabolically active as B-13/H cells were sensitive to the hepatotoxin, paracetamol. Paracetamol metabolism is dependent upon CYP2E1 activity in order to be toxic. This enzyme metabolises paracetamol to the electrophilic intermediate, N-Acetyl-p-benzoquinone imine (NAPQI). Observation of paracetamol-dependent toxicity in B13-H cells could, therefore, suggest the presence of functionally active CYP2E1 (Marek *et al.*, 2003).

1.4.2 Mechanism of Differentiation

B-13 cells readily proliferate in basic cell culture media supplemented with serum. There are no additional growth factors or culture modifications required. The cells will grow and expand on plastic substrate but will not grow in agar. This suggests that B-13 cells have anchorage dependent growth and are potentially non-cancerous (Fairhall *et al.*, 2013a). To transdifferentiate the cells from B-13 to B-13/H 10nM dexamethasone is added to the media. This is the only media supplement that is required to initiate the transdifferentiation process. Conversion takes between 7-14

days and following this period >80% of cells will have trans-differentiated, remaining cells maintain a B-13 phenotype (Fairhall *et al.*, 2013a).

B-13 cells respond to dexamethasone treatment through the glucocorticoid (GR) receptor. Many other glucocorticoids work via the GR receptor and will elicit a similar initiation of transdifferentiation in B-13 cells as dexamethasone. Dexamethasone was preferentially chosen, however, due to its high specificity for the GR receptor and rapid metabolism (Probert *et al.*, 2015). Other classes of steroids, such as mineralocorticoids, fail to initiate trans-differentiation. Furthermore, glucocorticoids that can act via mineralocorticoid receptors also fail to elicit a response, suggesting that it is a very specific glucocorticoid mediated process. Glucocorticoids have wide ranging metabolic actions *in vivo* and promote gluconeogenesis, lipolysis and protein breakdown as well as immunosuppressant and anti-inflammatory effects. However, perhaps more relevant when trying to understand B-13 differentiation, glucocorticoids are also known to have a developmental role in the foetus in tissue maturation (Probert *et al.*, 2015).

While the full mechanism behind the transdifferentiation process is yet to be established, it is thought to be, in part, due to changes in expression of the serum and glucocorticoid kinase (SGK1) gene. Microarray studies have shown that SGK1 has the highest induced transcript in response to dexamethasone treatment of 5000 transcripts (Probert *et al.*, 2015). The SGK1 gene encodes for serum and glucocorticoid-regulated kinase 1 (Sgk1). It is an enzyme involved in ion channel regulation, mediating a stress response to low sodium salt levels by promoting reabsorption in the kidney (Wallace *et al.*, 2010). It is thought that Sgk1 is able to cross talk with the Wnt signalling pathway which leads to an inhibition of Wnt signalling activity and promotes induction of C/EBP- β (Fairhall *et al.*, 2016). C/EBP- β is an enhancer binding protein that promotes proliferation, differentiation, metabolism and inflammation, primarily in hepatocytes, adipocytes and haematopoietic cells (Ramji and Foka, 2002). It was found that Wnt signalling was highly active in B-13 cells and inhibition of this pathway alone was enough to initiate transdifferentiation into B-13/H phenotype. While it is thought that SGK1 expression provides the link between initial GR receptor activation and subsequent Wnt signalling repression its importance in pancreatic cell transdifferentiation is unclear. SGK1 has a clear

functional role in the kidney but its utility and significance in other tissues remains to be fully understood (Wallace *et al.*, 2010).

1.4.3 Functional Similarity of B-13/H Cells to Hepatocytes

Initial studies into the similarity of B-13/H cells to hepatocytes focussed on immunofluorescence detection of genes. While this provided excellent preliminary data to suggest these cells were potentially hepatocyte-like, functionality was not assessed. In 2003 the Wright group established that the CYP enzymes expressed by B13/H cells were functional and this work was built upon in a further study that aimed to establish a potential use for B-13/H in toxicity and genotoxicity studies. Cytochrome P450 induction, toxin susceptibility and transporter gene expression were studied further and it was found that regulation of major CYP families remained intact and that functional transport across cell membranes was detected. The expression of transporter mRNAs was upregulated relative to B-13 levels and some were expressed at levels similar to those found *in vivo*, although most were below levels seen in the adult rat liver. CYP3A enzymes were significantly functional and inducers of the nuclear receptor that upregulates CYP3A expression, PXR, were found to be effective (Probert *et al.*, 2014). There were however, some major differences seen between the B-13/H cells and hepatocytes. CYP2B1 mRNA was present, it was not, however, translated into functional protein, similarly other CYP2B isoforms show low levels of activity. CYP1A2 was not expressed in the B-13/H cells, however, it was successfully genetically engineered to be expressed and in doing so humanised the line, demonstrating that the B-13 cell line can be readily manipulated to suit the needs of the experiment (Probert *et al.*, 2014).

1.4.4 Human Equivalents of B-13/H Cells

It was hypothesised that B-13 cells are hyper-responsive to GR receptor activation due to over induction or sustained exposure to elevated SGK1. If the genetic mechanism behind the response can be deciphered and reproduced in a human cell line, there is the possibility that a B-13/H human equivalent can be established.

The significance of a human equivalent would mean that the potential of these cells would go beyond the lab and possibly have clinical applications (Fairhall *et al.*, 2016).

It has been reported by Fairhall *et al.* that these mechanisms do exist in humans, *in vivo* (Fairhall *et al.*, 2013b). Pancreatic tissue samples from patients that had been

treated with systemic glucocorticoids for at least 20 years were compared to control samples where there had been no long-term therapy. It was found that the hepatic specific markers, CPS1 and albumin were expressed in the pancreatic cells of patients on glucocorticoid therapy at levels normally seen in the liver. Furthermore, enzymes expressed at high levels in the liver such as CYP3A4 were also discovered at high levels in the pancreatic cells. In the control cells, from patients with no glucocorticoid therapy, CPS1, albumin and CYP3A4, were undetectable. This suggested that the pathophysiological response exists in humans and could possibly be harnessed as a cell line. Further experiments showed that when these pancreatic cells were grown in culture with dexamethasone treatment, the control cells began to show hepatic markers at the mRNA level and the cells from patients with glucocorticoid therapy retained the expression of pre-existing markers. This suggested that there is potential for continued culture of these cells and development of a novel hepatic cell line (Fairhall *et al.*, 2016).

Unpublished work has shown that there is potential for Human Pancreatic Acinar Cells (HPACs) to be used as a progenitor to hepatocyte-like cells using DEX treatment identical to that used on B-13 cells to stimulate trans-differentiation. Currently, there are two different HPAC variants that are being studied both of which have been transfected with a different human growth factor in order to help maintain a hepatocyte-like genotype; H-13 cells are human equivalents transfected with HNF-4a and H-14 cells are human equivalents transfected with HNF-1a (Fairhall, 2013).

B-13/H cells represent a cell line that provides an on demand and unlimited supply of functional hepatocytes for the screening of drug toxicity and metabolism. However, it is important to bear in mind that once the cells have differentiated from their B-13 phenotype they stop proliferating and subsequently there is also not 100% conversion. Yield is very high, >80%, however there remains a sub population that is resistant to differentiation and continues to proliferate (Wallace *et al.*, 2010). While there is a lack of expression of some functional CYP metabolising enzymes, it has been shown that there is near functional comparability of B-13/H cells to hepatocytes including functional CYP3A isoform which, *in vivo*, is one of the most commonly implicated isoforms in xenobiotic metabolism and liver specific enzymes, such as albumin, are expressed as well. It is important when assessing drug toxicity *in vitro*

that responses are comparable to *in vivo* as they are a predictive assessment of human susceptibility.

At a time when adverse drug reactions are the leading cause of drug attrition in the UK and the reduction of whole animal studies is of paramount importance, finding an *in vitro* cell model that is capable of predicting human response is more relevant than ever before. A model cell line needs to be capable of high throughput screening of compounds, thus needs to be able to be produced in large quantities that are genetically uncompromised and have batch to batch comparability in order to generate reliable predictive data. B-13/H cells represent a cost effective and functional platform that has potential to provide the basis for a human equivalent to be developed.

1.5 Mitochondria

1.5.1 Mitochondrial Structure and Function

Mitochondria are often described as the powerhouse of the cell. They produce energy in the form of ATP which is used by all other cells in the body to function and survive. Mitochondria are a two membraned organelle; an outer membrane and an inner membrane that surrounds a matrix. The smooth outer membrane is highly permeable as it contains a large channel forming protein that is permeable to any molecule of 10,000 daltons or less. This makes it susceptible to the transport of xenobiotics as well as endogenous compounds. The inner membrane is highly folded into structures called cristae to maximise the surface area available for oxidative phosphorylation. The inner membrane also contains the proteins of the electron transport chain (ETC) required to generate ATP embedded within it. The mitochondrial matrix also contains the mitochondria's own genome which consists of the circular mtDNA and transcripts that encode for 13 proteins required for oxidative phosphorylation (Alberts, 2002).

1.5.2 Cellular Respiration

Cellular respiration is a multi-step process, the first part of which, glycolysis, does not occur in the mitochondria itself but in the cytoplasm of the cell. Glycolysis is the process by which a glucose molecule, with 6 carbon atoms, is broken down into 2 pyruvate molecules each with 3 carbon atoms as a priming reaction before entry into the mitochondria. While the reaction itself is able to generate energy as ATP it is not

very efficient and for every 4 ATP molecules generated from glycolysis an input of 2 ATP molecules is required. The pyruvate molecules enter into the mitochondrial matrix where they undergo a link reaction which decarboxylates and dehydrogenates the pyruvate molecules to 2 carbon acetate molecules. Coenzyme A accepts acetate to form acetyl coenzyme A which is then able to enter the Krebs cycle (Alberts, 2002).

The purpose of the Krebs cycle is to reduce carrier molecules which can be used to transport hydrogen to the ETC. Acetate is added to oxaloacetate to form citrate which is sequentially oxidised in a series of decarboxylation and dehydrogenation reactions before regenerating oxaloacetate (Dashty, 2013). The first decarboxylation and dehydrogenation of citrate forms α -ketoglutarate, a 5 carbon compound. The lost carboxy group forms carbon dioxide and the hydrogen atom reduces a molecule of the carrier, NAD to form NADH. α -ketoglutarate is decarboxylated and dehydrogenated to the 4 carbon compound, succinate, forming another molecule of NADH. Succinate is oxidised to fumarate, the by-product of which is a molecule of reduced FAD (FADH₂). Fumarate is hydrated to form malate which in turn is dehydrogenated to regenerate oxaloacetate and produce another molecule of NADH. The energy carried by the activated hydrogen as part of NADH and FADH₂ is used to generate ATP in the ETC (Alberts, 2002; Dashty, 2013).

1.5.3 The Electron Transport Chain

The ETC is the final step in mitochondrial respiration (figure 1.1). It is here that the most ATP can be generated. NADH and FADH₂ carrier molecules need to be oxidised in order to release their energy, however the hydrogen atoms that NADH and FADH₂ carry are not directly transferred to oxygen. Instead, it is the electrons that are transferred through a series of protein complexes until they reach the final electron acceptor, molecular oxygen, to generate water as seen in figure 1.1 (Dashty, 2013). The four protein complexes: I, II, III and IV, are embedded within the inner mitochondrial membrane. Electrons from NADH enter the ETC at complex I whereas electrons from FADH₂ enter at complex II. Co enzyme Q is a lipid soluble molecule that transports the electrons from complexes I and II to complex III. From complex III electrons are transported to complex IV via cytochrome C. At complex IV electrons are transferred to molecular oxygen to generate water. Electron transport is coupled to the transport of protons out of the matrix and into the intermembrane space.

Protons are electrically charged so there is a generation of an electrochemical gradient which can be utilised for the generation of ATP. Because the phospholipid bilayer is impermeable to ions the passage of protons back into the matrix can only occur through a protein channel. A fifth protein complex- ATP synthase, catalyses the synthesis of ATP from ADP by utilising this gradient and transporting protons back into the matrix down the electrochemical concentration gradient (Cooper, 2000).

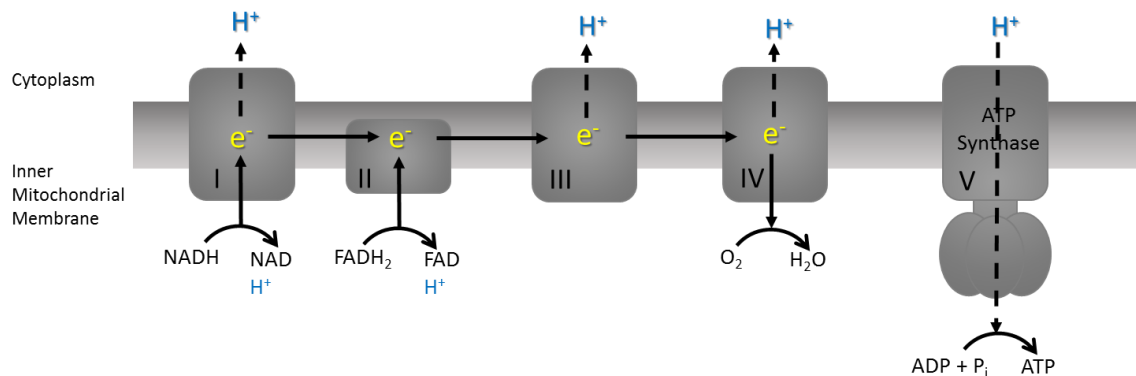


Figure 1.1 The Electron Transport Chain. The electron transport chain is found in the inner mitochondrial membrane of mitochondria. It is the process by which most of a cell's energy, in the form of ATP, is produced. Electrons are transferred to the electron transport chain by carrier molecules NADH and FADH₂ then passed down a series of complexes (I to IV). Electron transport is coupled to the movement of hydrogen ions out of the matrix creating an electrochemical gradient which is harnessed at complex V (ATP-synthase) where it is driven down the concentration gradient, through the protein channel, to synthesise ATP from ADP. Adapted from (Ow et al., 2008)

1.5.4 Free Radical Production

The ETC is not 100% efficient. Electrons can leak from complexes and can prematurely cause the one electron reduction of oxygen to the superoxide free radical (O₂⁻) (Hamanaka and Chandel, 2010). A free radical is an atom or molecule with unpaired electrons making them highly reactive and unstable. If a free radical specifically contains oxygen it is known as a reactive oxygen species (ROS). Mitochondria are the biggest source of physiological ROS and complexes I, II and III are all capable of prematurely reducing oxygen (Deavall et al., 2012). Under normal physiological conditions, O₂⁻ is catalysed to hydrogen peroxide (H₂O₂) by manganese superoxide dismutase (Mn-SOD) in the mitochondria. Hydrogen peroxide is a reactive non-radical species that is reduced to water by the antioxidant, glutathione. However, when a cell is stressed and there are excessive levels of superoxide it is possible that H₂O₂ undergoes another reaction, known as Fenton's reaction, and

generate the highly reactive hydroxyl radical ($\text{OH}\cdot$). Under normal conditions, free iron is sequestered into ferritin clusters and kept in a reduced state, however, these clusters can be oxidised by O_2^- , releasing Fe^{2+} ions which participate in the Fenton's reaction by catalysing the formation of $\text{OH}\cdot$ from H_2O_2 (figure 1.2). Hydroxyl radicals are extremely reactive and damaging, however, due to an extremely short half-life ($\sim 10^{-9}$ s) only react close to the site of their formation (Valko *et al.*, 2007). The physiological leakage of O_2^- , therefore, has important consequences for mitochondrial drug induced liver injury, as it presents a possible initial site for subsequent oxidative stress.

1.6 Mitochondrial Toxicity

1.6.1 Drug Induced Liver Injury

Drug induced liver injury (DILI) is a severe and off target response to a drug, it is a broad term that describes many manifestations within the liver, the most common of which is hepatocyte death after drug ingestion. DILI can be predictable, as is the case with paracetamol, or unpredictable, as is the case with idiosyncratic DILI. Idiosyncratic toxicities occur at therapeutic pharmacological doses and are defined by their delayed onset and rare occurrence, less than 1 in 10,000 patients. An idiosyncratic response is not a single mechanism of toxicity, and, again, is a term that describes all unexpected toxicities (Dyken and Will, 2007). Idiosyncratic DILI is one of the major reasons for cessation of new drug development as well as discontinuation of current marketed treatments. It presents a major problem for drug companies not only financially but also because of the difficulty in predicating toxic outcomes during drug development due to the elusive nature of the mechanisms of toxicity. These may be due to the intrinsic chemistry of the drug or individual variation in patients due to acquired or genetic factors (Boelsterli and Lim, 2007). One of the most common reasons underlying DILI is mitochondrial dysfunction. Mitochondria play a fundamental role in energy production through ATP generation and as such are often a major target of toxicity. The mechanisms through which mitochondrial dysfunction can occur are varied and can lead to severe pathologies in patients. If the process of energy production is disrupted the consequences can lead to the necrosis or apoptosis of hepatocytes causing cytolytic hepatitis which can ultimately result in liver failure. It is, therefore, vitally important that mitochondrial abnormalities

are investigated in the drug development process in order to prevent such severe consequences in patients (Labbe *et al.*, 2008).

1.6.2 Mitochondrial Susceptibility to Damage

The unique structure of mitochondria make them particularly susceptible to toxic insult. The inner mitochondrial membrane contains the cells cytochrome P450 enzymes, which play a crucial role in the metabolism, and sometimes activation, of drug compounds to potentially toxic metabolites. Rather than cholesterol, the inner mitochondrial membrane contains a high level of a lipid called cardiolipin, which is almost exclusively found here. As a lipid it contains a high level of unsaturated carbon bonds that are vulnerable to oxidation by ROS. Cardiolipin has a high affinity for lipophilic drugs and their binding brings the drug molecules in close proximity to the ETC and mtDNA (Boelsterli and Lim, 2007).

The structure of mtDNA makes it particularly vulnerable to damage, its small circular form lacks the protective structure of histone packaging and repair mechanisms that can be found in nuclear DNA. The lack of histone protection means that mtDNA is exposed to oxidative damage from ROS (Meyer *et al.*, 2013). The knock-on effect of damaged mtDNA is a failure in the mechanism of replication and translation of mitochondrial complexes. This has severe consequences for electron transport which becomes inhibited and as such there is an increase in the build-up and release of O_2^- . As a state of oxidative stress develops, mtDNA will become further damaged by the O_2^- , and a vicious cycle develops (Boelsterli and Lim, 2007).

Besides energy production, mitochondria also play an important role in the initiation of cell death via apoptosis. Mitochondria contain inactivate 'death proteins' (one of which is cytochrome *c*) in the inter membrane space. When a cell is stressed, these proteins become activated and translocate to the nucleus where protease cascades can be initiated and apoptosis or necrosis follows (Boelsterli and Lim, 2007).

1.7 Mechanisms of Drug Induced Mitochondrial Damage

It is often difficult to determine the mechanisms behind observed DILI as damage can occur via many different routes and in many different regions of the liver, however, frequently, mitochondrial damage is implicated. Mitochondrial damage itself is also difficult to understand as the effects can be subtle and go undetected for a long time before serious pathology emerges. This is due to the compensatory effect enabled by

the large numbers of mitochondria within liver cells. Furthermore, a drug itself may not be directly toxic to mitochondria and may require metabolism to a toxic metabolite before damage is caused (Begrache *et al.*, 2011). Most commonly, damage is seen at the mitochondrial permeability pore or at the level of the mitochondrial respiratory chain via inhibition of oxidative phosphorylation or inhibition of fatty acid oxidation.

1.7.1 Mitochondrial Permeability Transition Pore Opening

The mitochondrial permeability transition pore (MPTP) is a contact site between the outer mitochondrial membrane and the inner mitochondrial membrane. The role of the MPTP is unclear because, in healthy cells the pore remains closed and it is only under the influence of stressful stimuli such as increased cellular ROS or calcium that the pore opens. It is at this point that there is a cascade of other effects that can ultimately lead to cell death via apoptosis or necrosis (Pessayre *et al.*, 2012).

Opening of the pore leads to disruption of the proton gradient that is generated to drive ATP production. The passive re-entry of protons into the inner mitochondrial membrane bypasses ATP-synthase, uncouples oxidative phosphorylation and stops the production of ATP. Depletion of ATP ultimately results in bioenergetic failure of the cell. It is not only proton gradient dissipation that leads to cell damage. When the pore is open, it allows the passage of all small molecular weight molecules through the inner mitochondrial membrane and diminishing the gradients present between mitochondria and cytosol whilst retaining all larger protein molecules in their respective cellular compartments. This drives an osmotic force as the protein concentration within the mitochondrial matrix is greater than in the outer membrane space. This influx of water causes the mitochondria to swell and the cristae inside to unfold. When the pressure of the swollen matrix gets too high the outer mitochondrial membrane can rupture and release pro-apoptotic proteins which have the potential to initiate cell death signalling (Halestrap, 2009; Pessayre *et al.*, 2012). The exact mechanisms by which drugs can initiate the opening of the MPTP are largely unknown but it is thought that there are three likely routes by which opening can be initiated: a) direct interaction of the drug with the pore, b) as a result of oxidative stress causing oxidation of thiol groups present on components of the pore and c) activation of endogenous inducers such as JNK (Begrache *et al.*, 2011).

1.7.2 Impairment of Oxidative Phosphorylation

Uncoupling of oxidative phosphorylation occurs when a drug is able to inhibit the coupling of electron transport to the production of ATP through ATP synthase. A well-known example of a drug that is toxic via this mechanism is Carbonyl cyanide 4-(trifluoromethoxy) phenylhydrazone (FCCP). FCCP is a lipophilic weak acid that is membrane permeable in both its protonated and unprotonated state. FCCP is able to diffuse, in its protonated form, through the lipid membrane into the mitochondria matrix due to the mitochondrial membrane potential. In the matrix FCCP dissociates into an anion and a proton, the anion is able to diffuse back through the membrane and become protonated again. In this mechanism, electron transfer is not changed but there is no ATP production at the end of the chain (Labbe *et al.*, 2008). This not only means that ATP production is inhibited but that there is a greater opportunity for O_2^- build up and subsequent oxidative stress.

1.7.3 Inhibition of Fatty Acid Oxidation

Fatty acids are oxidised in the mitochondria during cellular respiration to yield fatty acyl-adenylate, which is then bound to co-enzyme A to produce acetyl-CoA for entry into the Krebs Cycle. If this process is damaged there is an accumulation of free fatty acids and triglycerides. This can occur directly, by drug inhibition of FAO enzymes or indirectly as a consequence of drug damage to the mitochondrial respiratory chain which becomes unable to regenerate oxidised co-factors (NAD^+ and FAD) that are required in the oxidation of fatty acids (Labbe *et al.*, 2008).

1.7.4 Oxidative Stress

As mentioned in section 1.6.2, mtDNA is highly susceptible to drug induced oxidative damage, this has a knock-on effect on the proteins transcribed, most of which form the ETC. If the ETC is damaged there can be an increased in production of O_2^- . Under normal physiological conditions ROS are not damaging to mitochondria as mitochondria contain a battery of antioxidants that are able to neutralise the ROS. However, in extreme circumstances, these antioxidant mechanisms can become overwhelmed. It is at this point that oxidative damage can occur (Deavall *et al.*, 2012).

1.8 Oxidative Damage

1.8.1 Protein Damage

The effects of protein damage are incredibly broad and varied due to the abundance and physiological roles of proteins. For example, enzymes such as kinases and phosphatases, DNA replication and transcription machinery and protein channels are all vulnerable to damage. There are susceptibility factors, however, such as the amino acid residues contained within the protein. Disulphide bonds, found between cysteine residues, for example, are particularly prone to ROS induced oxidation and cross linking, changing the tertiary structure of the protein and thus its ability to function. If the enzymes involved in oxidative phosphorylation become oxidised, then there are implications for mitochondrial respiration. It is likely that electron transport may become inhibited, ATP production will decrease and ultimately, cell death may follow (Deavall *et al.*, 2012).

1.8.2 Lipid Damage

Lipid damage by ROS is known as lipid peroxidation. This occurs when ROS oxidise unsaturated hydrocarbon bonds in lipid membranes forming lipid hydroperoxides. This increases the membranes fluidity and can cause inactivation of membrane receptors and enzymes (Deavall *et al.*, 2012).

1.8.3 DNA Damage

ROS react with DNA bases to form lesions, many of which are mutagenic if not repaired. The hydroxyl radical is able to react with DNA by addition to double bonds within DNA bases. Depending upon the location depends upon the nature of the adduct radical formed, for example, addition to the C5-C6 double bond of pyrimidines leads to the formation of C5-OH and C6-OH radicals with the C5-OH radical being reducing and the C6-OH radical being oxidising. One of the most well studied adducts is the C8-OH radical formed on adenine molecules giving rise to 8-OH-Gua which when oxidised, forms the stable product, 8-Oxo-2'-deoxyguanosine (8-oxo-dG). 8-oxo-dG is a well-established biomarker of oxidative stress and is widely studied *in vitro* (Cooke *et al.*, 2003).

1.8.4 Anti-Oxidants

The antioxidant defence system maintains the redox balance, preventing a state of oxidative stress from developing by reducing oxidising molecules so that they are no

longer harmful. Endogenous antioxidants can broadly be divided into 2 categories: enzymatic antioxidants, including SOD, catalase and glutathione peroxidase, and non-enzymatic antioxidants including vitamin E, glutathione and bilirubin (Oyewole, 2015). Antioxidants are widely distributed throughout the body and most are found in cellular cytosol, however there are some variants localised in mitochondria. Superoxide is removed from cells by a one electron transfer between O_2^- molecules forming molecular oxygen or H_2O_2 . This reaction is catalysed by SOD which is present as Cu-SOD or Zn-SOD in the cytosol or Mn-SOD in the mitochondria (Jaeschke *et al.*, 2012).

Figure 1.2 shows that H_2O_2 , while not a free radical, in the presence of free iron (Fe^{2+}) is capable of forming the OH^\bullet and the hydroxide ion (OH^-) which are highly reactive and can cause oxidative damage as previously mentioned. Ferritin, a metal chelator, is present in cells to prevent the formation of hydroxyl radicals and hydroxide ions by binding iron in its ferric state, stopping it from being reactive (Jaeschke *et al.*, 2012).

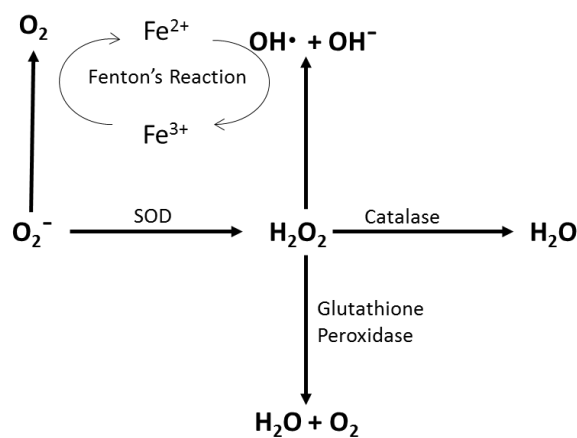


Figure 1.2: ROS production and anti-oxidant mechanisms. When there is superoxide leakage from the electron transport chain it is rapidly dismutated to form H_2O_2 , which, if not neutralised by catalase or glutathione peroxidase can lead to the production of OH^\bullet and OH^- which can subsequently go on to cause oxidative damage such as lipid peroxidation. Adapted from (Jaeschke *et al.*, 2012)

1.8.5 Paracetamol Toxicity

One of the most well studied drugs with associated mitochondrial toxicity is paracetamol. At its recommended dose, paracetamol is a safe and effective analgesic, however, in a situation of overdose, it can cause severe hepatotoxicity. It

is the most common cause of liver failure on both the UK and US and is a common indication for liver transplant. For a long time, its mechanism of action was controversial due to its varied effects within the cell.

When taken at normal doses 85-90% is metabolised by glucuronidation or sulphation and excreted into the urine, 2% enters into the urine unchanged and the remaining 8-13% undergoes phase I metabolism by CYP2E1 to form metabolite, N-Acetyl-p-benzoquinone (NAPQI) which is further metabolised by glutathione conjugation to a non-toxic metabolite (Lancaster *et al.*, 2014). In a situation of overdose, however, glucuronidation and sulphation pathways become saturated and metabolism is shifted towards CYP2E1 and consequently NAPQI can accumulate and as glutathione levels deplete, can reach toxic levels. NAPQI it is able to conjugate to sulphhydryl groups present on mitochondrial proteins and form protein adducts. This in turn leads to mitochondrial dysfunction due to membrane disruption and depletion of ATP production. As previously mentioned, if there is damage to the ETC there is a build-up of superoxide leakage and subsequent oxidative stress within the mitochondria. The reaction of ROS with other cellular components leads to mtDNA damage, mitochondrial permeability pore opening and a complete shut down in ATP production. Depending on the extent of the damage to the cell this can result in apoptosis or necrosis. In severe cases paracetamol overdose can lead to permanent liver damage (Lancaster *et al.*, 2014).

1.9 Troglitazone

Troglitazone was an oral anti-diabetic introduced to the market in 1997 for treatment of adult onset, insulin resistant, type II diabetes (Yokoi, 2010). However, in 2000, it was withdrawn from the market after reports of severe idiosyncratic hepatotoxicity (Yokoi, 2010). The main effects of Troglitazone are to decrease blood glucose levels by increasing glucose uptake in skeletal muscle but also to sensitise target tissues: hepatocytes, adipose tissue and skeletal muscle, to insulin and promote the anabolic effects of insulin. Troglitazone is a high affinity ligand of PPAR γ receptors, and it is through binding to these receptors that troglitazone has pharmacological effect (Hauer, 2002).

1.9.1 Mechanism of Action

Troglitazone was developed as part of a programme to produce new antioxidants with antilipidemic properties and this, in part, explains its chemical structure.

Troglitazone molecules contain the same chroman ring moiety as vitamin E (conferring antioxidant properties) attached to a thiazolidinedione ring (Smith, 2003). The structure of troglitazone means that it is highly lipophilic and consequently rapidly enters the cell and binds to PPAR γ receptors, with high affinity. PPAR γ receptors are predominantly expressed in white and brown adipose tissue and are found within the nucleus of the cell bound to a retinoid X receptor (RXR) forming a heterodimer. Upon troglitazone binding there is a conformational change in the PPAR γ -RXR complex and a co-repressor is displaced which allows for binding to PPAR γ response elements and subsequent activation of DNA sequences that control the expression of a number of genes involved in lipid metabolism thus mimicking the actions of insulin (Day, 1999).

1.9.2 Mechanism of Toxicity

The mechanism by which troglitazone elicits toxicity has been the source of controversy for many years and there have been many proposed theories without one clear pathway. When considering toxicity of a drug, it is pertinent to remember that it may not be the parent compound that causes damage. Troglitazone is metabolised by 3 main pathways: sulphation, glucuronidation and by phase II cytochrome P450 enzyme reactions (Yokoi, 2010). Sulphation is the main route of metabolism and sulphates account for approximately 70% of the troglitazone metabolites found in the plasma, along with glucuronide metabolites they are excreted into the bile and thus, the main route of excretion is faecal and not urinary (Smith 2003). The third metabolite is a quinone, formed from the oxidation of the chroman ring structure, a process metabolised predominantly by CYP3A4 (Yokoi, 2010).

Quinones are well-established cytotoxic compounds, their structure allows them to undergo redox cycling to generate ROS that have the potential to cause cellular damage such as lipid peroxidation and protein oxidation. The one electron reduction of a quinone molecule forms a semi-quinone radical species that can be subsequently oxidised by molecular oxygen, regenerating the parent quinone and forming a superoxide molecule in the process. The parent quinone is then free to cycle again resulting in the persistent generation of superoxide and consequently, secondary ROS in the form of hydrogen peroxide and hydroxyl radicals (Bolton *et al.*, 2000).

CYP3A4 is responsible for the formation of quinone metabolites in humans as it catalyses the formation of the quinone moiety from the chroman ring structure. The quinone can then be further metabolised to break the ring structure, generating even more electrophilic intermediates that can cause damage (Yokoi, 2010).

The paradox of troglitazone is that it was developed to have antioxidant properties that can neutralise ROS. This makes the detection of ROS *in vitro* very complicated, however, it is thought that the antioxidant properties of troglitazone can be exhausted and toxicity is elicited through simple intrinsic mechanisms similar to paracetamol. Narayan et al. found that when N1S1 Novikoff rat hepatoma cells were treated with troglitazone, concentration of 5 μM and above could induce oxidative stress (Narayanan *et al.*, 2003). An increase in O_2^- levels was concomitant with alteration to mitochondrial membrane potential and membrane peroxidation. It is thought that this is due to the formation of quinone moieties as described above. However, there is also a second mechanism postulated that could account for the development of oxidative stress, the 2 electron s-oxidation of the thiazolidinedione ring is also able to undergo redox cycling and generate superoxide. While Narayanan found evidence of oxidative stress it was also found that at equimolar concentrations the quinone metabolite was unable to induce a similar toxic response to the parent compound. This suggests that there may be a direct acting effect of troglitazone rather than quinone cycling (Narayanan *et al.*, 2003). Yamamoto et al. further supports this idea and found that while there was some toxicity seen with the quinone metabolite in HepG2 cells, the parent drug was more toxic (Yamamoto *et al.*, 2001). The idea that it is the parent drug rather than a reactive metabolite that contributes most to cytotoxicity is well supported (Kostrubsky *et al.*, 2000; Tettey *et al.*, 2001; Yamamoto *et al.*, 2001; Tirmenstein *et al.*, 2002) however, there is some evidence to corroborate the theory that cellular damage is a result of direct formation of ROS suggesting a limited role for quinone metabolites in toxicity. Masubchi et al. suggested that the ROS observed following troglitazone treatment could be secondary to mitochondrial permeability pore opening and mitochondrial damage and therefore not a direct mechanism of damage but a consequence (Masubuchi *et al.*, 2006).

There is huge inter-individual variation in functional capacity of drug metabolising enzymes and it is possible that this is responsible for the idiosyncratic nature of troglitazone toxicity. Cryopreserved human hepatocytes with low CYP3A4 activity

and more extensive sulphation capacity (therefore limited capacity for generation of quinone metabolite and increased sulphate conversion) have been shown to have high sensitivity to the cytotoxic effects of troglitazone. This suggests that there could be a susceptible genotype in which a subpopulation is more likely to have hepatotoxic effects but also that an increased level of troglitazone sulphate could also be damaging and high levels of CYP3A4 could be protective (Hewitt *et al.*, 2002). In agreement with these findings, Funk *et al.* found that, in male Wistar rats, the sulphate metabolite rather than the parent compound had greater impact on hepatobiliary elimination due to competitive inhibition of the bile salt export pump (BSEP), accumulation of toxic bile salts and mitochondrial damage due to their intrinsic detergent properties (Funk *et al.*, 2001).

Kostrubsky *et al.* investigated the action of troglitazone in human and porcine hepatocytes with the aim of identifying whether troglitazone or its sulphate metabolite was responsible for hepatotoxicity. Porcine hepatocytes were chosen because of their low sulphation capacity. It was found that following 2-hours treatment with troglitazone, concentrations of $\geq 25 \mu\text{M}$ produced an irreversible inhibition of protein synthesis and concentrations $\geq 50 \mu\text{M}$ were cytotoxic in human hepatocytes. In contrast, at $50 \mu\text{M}$ protein synthesis was reversible in porcine hepatocytes and concentrations of $100 \mu\text{M}$ were cytotoxic (Kostrubsky *et al.*, 2000). Toxicity correlated with an increase in un-metabolised troglitazone, suggesting that the parent drug was the cause of toxicity in human hepatocytes. The resistance to toxicity in porcine hepatocytes was attributed to high levels of glucuronide conjugation (Kostrubsky *et al.*, 2000).

HepG2 cells are known to have a low P450 profile and subsequently are a useful tool for assessing the involvement of P450 enzymes in drug metabolism. Tirmenstein *et al.* reported that treatment with troglitazone was cytotoxic, suggesting that the parent compound was more toxic than its metabolites (Tirmenstein *et al.*, 2002).

Mitochondrial dysfunction is often observed alongside troglitazone cytotoxicity suggesting a role for mitochondria in the mechanism of toxicity (Haskins *et al.*, 2001; Tirmenstein *et al.*, 2002; Rachek *et al.*, 2009; Hu *et al.*, 2015). Dan *et al.* reported significant inhibitory effects of troglitazone on the enzymatic activity of the ETC in HepaRG cells. Cells treated with troglitazone for 48 hours showed significantly lower levels of basal mitochondrial respiration than untreated control cells, the oxygen

consumed for production of ATP was almost entirely halted. Interestingly, levels of ATP, although reduced, were not completely inhibited. It was postulated that the cells switched to glycolysis as a compensatory mechanism of generating ATP. In addition to this, a subsequent decline in mitochondrial membrane potential and activation of pro-apoptotic caspase 3 was seen. Troglitazone at a concentration of 50 μM elevated cellular levels of ROS 2-fold, but this was considered a secondary effect to initial mitochondrial damage. ROS are able to cause structural changes in mitochondria and it was postulated that increased ROS levels initiated a vicious circle of toxic effects including mtDNA damage (Hu *et al.*, 2015). In concordance with this, Masubuchi *et al.* found that troglitazone induced the MPT pore and postulated that the toxic effects were a result of the direct effects of troglitazone on the ETC or MPT pore (Masubuchi *et al.*, 2006), similarly Rachek *et al.* found that significant mtDNA damage was associated with a drop in ATP concentration and overall decline in cell viability (Rachek *et al.*, 2009). Conversely, Bova *et al.* reported no significant change in ATP levels in HepG2 cells treated with troglitazone up to 100 μM despite seeing a marked reduction in membrane potential, indicative of cytotoxicity. This suggests that perhaps different cell lines have differing capacities to compensate via glycolysis (Bova *et al.*, 2005).

1.9.3 Apoptosis

Apoptosis is the most likely route of troglitazone induced cell death and has been observed in human and rodent cells lines (Haskins *et al.*, 2001; Yamamoto *et al.*, 2001; Bae and Song, 2003; Bova *et al.*, 2005). It has previously been shown that troglitazone causes concentration dependent depletion of ATP, opening of the MPT pore and a reduced membrane potential; these are all steps that can lead to the release of pro-apoptotic proteins and subsequent initiation of apoptosis. Experiments in HepG2 and Chang cells found that troglitazone can induce apoptosis via the classical c-Jun N-terminal protein kinase (JNK) pathway. Troglitazone directly activates JNK and p38 via a stress activated pathway. Subsequently, there is an increase in the pro-apoptotic proteins Bad, Bax and cytochrome c (Bae and Song, 2003). Apoptosis is an energy consuming process and therefore if ATP is depleted too much, or the compensatory mechanisms of glycolysis cannot produce enough additional ATP, then it is possible that hepatocytes can revert to necrosis as a mechanism of cell death instead of apoptosis and therefore it is possible that

troglitazone can induce apoptosis and necrosis dependent upon the availability of ATP (Smith, 2003).

While there are many possible mechanisms of toxicity reported for troglitazone, current literature suggests that troglitazone is a direct acting hepatotoxin that elicits cytotoxicity through causing mitochondrial damage due to dysfunction of respiration. The consequences of dysfunctional respiration are reduced cellular ATP and thus energy starvation in the mitochondria and loss of membrane potential which can initiate mechanisms of cell death including apoptosis and necrosis. There appears to be secondary generation of ROS which have widespread intracellular damaging effects including mtDNA binding which further damages the production of a healthy ETC resulting in a state of oxidative stress due to superoxide leakage. It is also possible that the damage can go undetected for long periods of time because the damage is silent as apoptosis does not raise serum liver enzymes (Smith, 2003).

1.9.4 Why was toxicity not predictable?

The effects of toxicity ultimately depended upon the cell model studied. There was some interspecies variation as well as variation due to differing expression of metabolic enzymes. Consequently, pinpointing the exact mechanism of damage is very challenging. Furthermore, in pre-clinical tests, no troglitazone toxicity was reported in whole animal studies. It has been postulated that this is due to physiologically normal rats being used and that potentially the humans in which toxicity was seen had impaired liver function due to their diabetic condition and thus decreased ability to metabolise troglitazone (Tirmenstein *et al.*, 2002).

1.9.5 New Applications of Troglitazone

Troglitazone was withdrawn from the market in 2000 after several reports of liver failure, however, there has been a resurgence in interest in the compound as it is thought its PPAR γ mediated effects could be harnessed in anti-cancer treatments to halt the division of tumour cells (Day, 1999). The theory is based upon the finding that PPAR γ is involved in cellular proliferation. The binding of different ligands to PPAR γ can initiate different downstream effects depending on whether they are inhibitory or stimulatory. As a result of the wide variation in responses to activation of PPAR γ the effects in cancer cells are complex and dependent upon the nature of the cancer (Fröhlich and Wahl, 2015). Positive effects of glitazones in anticancer therapy have been shown in colorectal cancer and bladder cancer (Mueller *et al.*,

2000; Ogino *et al.*, 2009). Conversely PPAR γ expression was found to be linked with poor prognosis in lung cancer and it has also been reported that there was no therapeutic effect in patients with early stage breast cancer (Theocharis *et al.*, 2002; Burstein *et al.*, 2003). Interestingly it has also been reported that there may be off target effects of troglitazone. It was found that troglitazone was able to elicit anti-tumour effects in cancers where PPAR γ expression was low possibly thought to be mediated by glitazone ability to inhibit pro-apoptotic proteins (Shiau *et al.*, 2005; Wei *et al.*, 2009).

A fuller understanding of the mechanisms involved in troglitazone toxicity may enable the drug to be redesigned and repurposed as a novel chemotherapy.

1.10 Study Objectives

One of the biggest challenges facing drug development today is reducing the high attrition rate of new chemical entities in the face of reducing the number of animal studies performed. Current hepatocyte cell models exist in order to do this, however, many are lacking a comprehensive drug metabolism profile. As such they are not suited to toxicity testing, where it is imperative that results are predictive of human response. New and more efficient cell models need to be developed that can be used for high through-put screening and can provide meaningful predictive data to ultimately enable the translation of laboratory findings into clinical practice.

Recently it has been reported that mitochondria are often implicated in the drug induced liver injury which is the major cause of drug attrition. Often mitochondrial dysfunction can be silent due to the compensatory effects of other mitochondria within the cells, however, ultimately, when damage is too great liver failure may result.

With this in mind the aims of my project were to:

- Study the effect of differentiation on mitochondrial function in B-13/H cells.
- Study the effect of differentiation on toxicity in B-13/H cells.
- Attempt to use B13/H cells in a novel drug screening platform for the intracellular and extracellular detection of reactive oxygen species.

- To discover if Troglitazone, a known hepatotoxin, is more toxic to B-13/H cells than B-13 cells?
- Investigate whether the results could be repeated in a human equivalent cell line: H-13 and H-14.

1.11 Statistical Analysis

Statistical significance between groups were determined using the Student's 2- tailed t-test, unless otherwise specified. Significance was achieved where $p < 0.05$.

1.12 References

- Ahuja, V. and Sharma, S. (2014) 'Drug safety testing paradigm, current progress and future challenges: An overview', *Journal of Applied Toxicology*, 34(6), pp. 576-594.
- Alberts (2002) *Molecular Biology of the Cell*. 4th edn. New York: Garland Science.
- Bae, M.A. and Song, B.J. (2003) 'Critical role of c-Jun N-terminal protein kinase activation in troglitazone-induced apoptosis of human HepG2 hepatoma cells', *Molecular Pharmacology*, 63(2), pp. 401-408.
- Begrache, K., Massart, J., Robin, M.A., Borgne-Sanchez, A. and Fromenty, B. (2011) 'Drug-induced toxicity on mitochondria and lipid metabolism: Mechanistic diversity and deleterious consequences for the liver', *Journal of Hepatology*, 54(4), pp. 773-794.
- Boelsterli, U.A. and Lim, P.L.K. (2007) 'Mitochondrial abnormalities-A link to idiosyncratic drug hepatotoxicity?', *Toxicology and Applied Pharmacology*, 220(1), pp. 92-107.
- Bolton, J.L., Trush, M.A., Penning, T.M., Dryhurst, G. and Monks, T.J. (2000) 'Role of quinones in toxicology', *Chemical Research in Toxicology*, 13(3), pp. 135-160.
- Bova, M.P., Tam, D., McMahon, G. and Mattson, M.N. (2005) 'Troglitazone induces a rapid drop of mitochondrial membrane potential in liver HepG2 cells', *Toxicology Letters*, 155(1), pp. 41-50.
- Burstein, H.J., Demetri, G.D., Mueller, E., Sarraf, P., Spiegelman, B.M. and Winer, E.P. (2003) 'Use of the peroxisome proliferator-activated receptor (PPAR) γ ligand troglitazone as treatment for refractory breast cancer: A phase II study', *Breast Cancer Research and Treatment*, 79(3), pp. 391-397.
- Castell, J.V., Jover, R., Martínez-Jiménez, C.P. and Gómez-Lechón, M.J. (2006) 'Hepatocyte cell lines: Their use, scope and limitations in drug metabolism studies', *Expert Opinion on Drug Metabolism and Toxicology*, 2(2), pp. 183-212.
- Cooke, M.S., Evans, M.D., Dizdaroglu, M. and Lunec, J. (2003) 'Oxidative DNA damage: Mechanisms, mutation, and disease', *FASEB Journal*, 17(10), pp. 1195-1214.
- Cooper (2000) *The Cell: A Molecular Approach*. 2nd edition. Sunderland (MA): Sinauer Associates.
- Dashty, M. (2013) 'A quick look at biochemistry: Carbohydrate metabolism', *Clinical Biochemistry*, 46(15), pp. 1339-1352.

- Day, C. (1999) 'Thiazolidinediones: A new class of antidiabetic drugs', *Diabetic Medicine*, 16(3), pp. 179-192.
- Deavall, D.G., Martin, E.A., Horner, J.M. and Roberts, R. (2012) 'Drug-induced oxidative stress and toxicity', *Journal of Toxicology*, 2012.
- Dykens, J.A. and Will, Y. (2007) 'The significance of mitochondrial toxicity testing in drug development', *Drug Discovery Today*, 12(17-18), pp. 777-785.
- Fairhall, E.A. (2013) *Hepatocyte generation from pancreatic acinar cell lines*. Newcastle University
- Fairhall, E.A., Charles, M.A., Probert, P.M.E., Wallace, K., Gibb, J., Ravindan, C., Soloman, M. and Wright, M.C. (2016) 'Pancreatic B-13 Cell transdifferentiation to hepatocytes is dependent on epigenetic-regulated changes in gene expression', *PLoS ONE*, 11(3).
- Fairhall, E.A., Charles, M.A., Wallace, K., Schwab, C.J., Harrison, C.J., Richter, M., Hoffmann, S.A., Charlton, K.A., Zeilinger, K. and Wright, M.C. (2013a) 'The B-13 hepatocyte progenitor cell resists pluripotency induction and differentiation to non-hepatocyte cells', *Toxicology Research*, 2(5), pp. 308-320.
- Fairhall, E.A., Wallace, K., White, S.A., Huang, G.C., Shaw, J.A., Wright, S.C., Charlton, K.A., Burt, A.D. and Wright, M.C. (2013b) 'Adult human exocrine pancreas differentiation to hepatocytes - Potential source of a human hepatocyte progenitor for use in toxicology research', *Toxicology Research*, 2(1), pp. 80-87.
- Fröhlich, E. and Wahl, R. (2015) 'Chemotherapy and chemoprevention by thiazolidinediones', *BioMed Research International*, 2015.
- Funk, C., Ponelle, C., Scheuermann, G. and Pantze, M. (2001) 'Cholestatic potential of troglitazone as a possible factor contributing to troglitazone-induced hepatotoxicity: In vivo and in vitro interaction at the canalicular bile salt export pump (Bsep) in the rat', *Molecular Pharmacology*, 59(3), pp. 627-635.
- Gerets, H.H.J., Tilmant, K., Gerin, B., Chanteux, H., Depelchin, B.O., Dhalluin, S. and Atienzar, F.A. (2012) 'Characterization of primary human hepatocytes, HepG2 cells, and HepaRG cells at the mRNA level and CYP activity in response to inducers and their predictivity for the detection of human hepatotoxins', *Cell Biology and Toxicology*, 28(2), pp. 69-87.
- Guillouzo, A., Corlu, A., Aninat, C., Glaise, D., Morel, F. and Guguen-Guillouzo, C. (2007) 'The human hepatoma HepaRG cells: A highly differentiated model for studies

of liver metabolism and toxicity of xenobiotics', *Chemico-Biological Interactions*, 168(1), pp. 66-73.

Halestrap, A.P. (2009) 'What is the mitochondrial permeability transition pore?', *Journal of Molecular and Cellular Cardiology*, 46(6), pp. 821-831.

Hamanaka, R.B. and Chandel, N.S. (2010) 'Mitochondrial reactive oxygen species regulate cellular signaling and dictate biological outcomes', *Trends in Biochemical Sciences*, 35(9), pp. 505-513.

Hamdam, J., Sethu, S., Smith, T., Alfirevic, A., Alhaidari, M., Atkinson, J., Ayala, M., Box, H., Cross, M., Delaunois, A., Dermody, A., Govindappa, K., Guillon, J.M., Jenkins, R., Kenna, G., Lemmer, B., Meecham, K., Olayanju, A., Pestel, S., Rothfuss, A., Sidaway, J., Sison-Young, R., Smith, E., Stebbings, R., Tingle, Y., Valentin, J.P., Williams, A., Williams, D., Park, K. and Goldring, C. (2013) 'Safety pharmacology - Current and emerging concepts', *Toxicology and Applied Pharmacology*, 273(2), pp. 229-241.

Hart, S.N., Li, Y., Nakamoto, K., Subileau, E.A., Steen, D. and Zhong, X.B. (2010) 'A comparison of whole genome gene expression profiles of HepaRG cells and HepG2 cells to primary human hepatocytes and human liver tissues', *Drug Metabolism and Disposition*, 38(6), pp. 988-994.

Haskins, J.R., Rowse, P., Rahbari, R. and De la Iglesia, F.A. (2001) 'Thiazolidinedione toxicity to isolated hepatocytes revealed by coherent multiprobe fluorescence microscopy and correlated with multiparameter flow cytometry of peripheral leukocytes', *Archives of Toxicology*, 75(7), pp. 425-438.

Hauer, H. (2002) 'The mode of action of thiazolidinediones', *Diabetes/Metabolism Research and Reviews*, 18(SUPPL. 2).

Hewitt, N.J., Lloyd, S., Hayden, M., Butler, R., Sakai, Y., Springer, R., Fackett, A. and Li, A.P. (2002) 'Correlation between troglitazone cytotoxicity and drug metabolic enzyme activities in cryopreserved human hepatocytes', *Chemico-Biological Interactions*, 142(1-2), pp. 73-82.

Holmes, A.M., Creton, S. and Chapman, K. (2010) 'Working in partnership to advance the 3Rs in toxicity testing', *Toxicology*, 267(1-3), pp. 14-19.

Hu, D., Wu, C.Q., Li, Z.J., Liu, Y., Fan, X., Wang, Q.J. and Ding, R.G. (2015) 'Characterizing the mechanism of thiazolidinedione-induced hepatotoxicity: An in vitro model in mitochondria', *Toxicology and Applied Pharmacology*, 284(2), pp. 134-141.

- Ishibashi, H., Nakamura, M., Komori, A., Migita, K. and Shimoda, S. (2009) 'Liver architecture, cell function, and disease', *Seminars in Immunopathology*, 31(3), pp. 399-409.
- Jaeschke, H., McGill, M.R. and Ramachandran, A. (2012) 'Oxidant stress, mitochondria, and cell death mechanisms in drug-induced liver injury: Lessons learned from paracetamol hepatotoxicity', *Drug Metabolism Reviews*, 44(1), pp. 88-106.
- Kia, R., Sison, R.L.C., Heslop, J., Kitteringham, N.R., Hanley, N., Mills, J.S., Park, B.K. and Goldring, C.E.P. (2013) 'Stem cell-derived hepatocytes as a predictive model for drug-induced liver injury: Are we there yet?', *British Journal of Clinical Pharmacology*, 75(4), pp. 885-896.
- Kostrubsky, V.E., Sinclair, J.F., Ramachandran, V., Venkataramanan, R., Wen, Y.H., Kindt, E., Galchev, V., Rose, K., Sinz, M. and Strom, S.C. (2000) 'The role of conjugation in hepatotoxicity of troglitazone in human and porcine hepatocyte cultures', *Drug Metabolism and Disposition*, 28(10), pp. 1192-1197.
- Labbe, G., Pessayre, D. and Fromenty, B. (2008) 'Drug-induced liver injury through mitochondrial dysfunction: Mechanisms and detection during preclinical safety studies', *Fundamental and Clinical Pharmacology*, 22(4), pp. 335-353.
- Lancaster, E.M., Hiatt, J.R. and Zarrinpar, A. (2014) 'Paracetamol hepatotoxicity: an updated review', *Archives of Toxicology*, 89(2), pp. 193-199.
- Maes, M., Vinken, M. and Jaeschke, H. (2016) 'Experimental models of hepatotoxicity related to acute liver failure', *Toxicology and Applied Pharmacology*, 290, pp. 86-97.
- Malarkey, D.E., Johnson, K., Ryan, L., Boorman, G. and Maronpot, R.R. (2005) 'New insights into functional aspects of liver morphology', *Toxicologic Pathology*, 33(1), pp. 27-34.
- Marek, C.J., Cameron, G.A., Elrick, L.J., Hawksworth, G.M. and Wright, M.C. (2003) 'Generation of hepatocytes expressing functional cytochromes P450 from a pancreatic progenitor cell line in vitro', *Biochemical Journal*, 370(3), pp. 763-769.
- Masubuchi, Y., Kano, S. and Horie, T. (2006) 'Mitochondrial permeability transition as a potential determinant of hepatotoxicity of antidiabetic thiazolidinediones', *Toxicology*, 222(3), pp. 233-239.

- McKim Jr, J.M. (2010) 'Building a tiered approach to in vitro predictive toxicity screening: A focus on assays with in vivo relevance', *Combinatorial Chemistry and High Throughput Screening*, 13(2), pp. 188-206.
- Meyer, J.N., Leung, M.C.K., Rooney, J.P., Sendoel, A., Hengartner, M.O., Kisby, G.E. and Bess, A.S. (2013) 'Mitochondria as a target of environmental toxicants', *Toxicological Sciences*, 134(1), pp. 1-17.
- Mueller, E., Smith, M., Sarraf, P., Kroll, T., Aiyer, A., Kaufman, D.S., Oh, W., Demetri, G., Figg, W.D., Zhou, X.P., Eng, C., Spiegelman, B.M. and Kantoff, P.W. (2000) 'Effects of ligand activation of peroxisome proliferator-activated receptor γ in human prostate cancer', *Proceedings of the National Academy of Sciences of the United States of America*, 97(20), pp. 10990-10995.
- Narayanan, P.K., Hart, T., Elcock, F., Zhang, C., Hahn, L., McFarland, D., Schwartz, L., Morgan, D.G. and Bugelski, P. (2003) 'Troglitazone-Induced Intracellular Oxidative Stress in Rat Hepatoma Cells: A Flow Cytometric Assessment', *Cytometry Part A*, 52(1), pp. 28-35.
- Ogino, S., Shima, K., Baba, Y., Nosho, K., Irahara, N., Kure, S., Chen, L., Toyoda, S., Kirkner, G.J., Wang, Y.L., Giovannucci, E.L. and Fuchs, C.S. (2009) 'Colorectal Cancer Expression of Peroxisome Proliferator-Activated Receptor γ (PPARG, PPARgamma) Is Associated With Good Prognosis', *Gastroenterology*, 136(4), pp. 1242-1250.
- Ow, Y.L.P., Green, D.R., Hao, Z. and Mak, T.W. (2008) 'Cytochrome c: Functions beyond respiration', *Nature Reviews Molecular Cell Biology*, 9(7), pp. 532-542.
- Oyewole (2015) 'Mitochondrial-targeted antioxidants', *the FASEB Journal*, 29(), pp. 1-6.
- Perry, P. and Joynson, C. (2007) 'The ethics of animal research: A UK perspective', *ILAR Journal*, 48(1), pp. 42-46.
- Pessayre, D., Fromenty, B., Berson, A., Robin, M.A., Lett eron, P., Moreau, R. and Mansouri, A. (2012) 'Central role of mitochondria in drug-induced liver injury', *Drug Metabolism Reviews*, 44(1), pp. 34-87.
- Probert, P.M.E., Chung, G.W., Cockell, S.J., Agius, L., Mosesso, P., White, S.A., Oakley, F., Brown, C.D.A. and Wright, M.C. (2014) 'Utility of B-13 progenitor-derived hepatocytes in hepatotoxicity and genotoxicity studies', *Toxicological Sciences*, 137(2), pp. 350-370.

- Probert, P.M.E., Meyer, S.K., Alsaeedi, F., Axon, A.A., Fairhall, E.A., Wallace, K., Charles, M., Oakley, F., Jowsey, P.A., Blain, P.G. and Wright, M.C. (2015) 'An expandable donor-free supply of functional hepatocytes for toxicology', *Toxicology Research*, 4(2), pp. 203-222.
- Rachek, L.I., Yuzefovych, L.V., LeDoux, S.P., Julie, N.L. and Wilson, G.L. (2009) 'Troglitazone, but not rosiglitazone, damages mitochondrial DNA and induces mitochondrial dysfunction and cell death in human hepatocytes', *Toxicology and Applied Pharmacology*, 240(3), pp. 348-354.
- Ramji, D.P. and Foka, P. (2002) 'CCAAT/enhancer-binding proteins: Structure, function and regulation', *Biochemical Journal*, 365(3), pp. 561-575.
- Rodríguez-Antona, C., Donato, M.T., Boobis, A., Edwards, R.J., Watts, P.S., Castell, J.V. and Gómez-Lechón, M.J. (2002) 'Cytochrome P450 expression in human hepatocytes and hepatoma cell lines: Molecular mechanisms that determine lower expression in cultured cells', *Xenobiotica*, 32(6), pp. 505-520.
- Shen, C.N., Slack, J.M.W. and Tosh, D. (2000) 'Molecular basis of transdifferentiation of pancreas to liver', *Nature Cell Biology*, 2(12), pp. 879-887.
- Shiau, C.W., Yang, C.C., Kulp, S.K., Chen, K.F., Chen, C.S., Huang, J.W. and Chen, C.S. (2005) 'Thiazolidenediones mediate apoptosis in prostate cancer cells in part through inhibition of Bcl-xL/Bcl-2 functions independently of PPAR γ ', *Cancer Research*, 65(4), pp. 1561-1569.
- Smith, M.T. (2003) 'Mechanisms of troglitazone hepatotoxicity', *Chemical Research in Toxicology*, 16(6), pp. 679-687.
- Song, Z., Cai, J., Liu, Y., Zhao, D., Yong, J., Duo, S., Song, X., Guo, Y., Zhao, Y., Qin, H., Yin, X., Wu, C., Che, J., Lu, S., Ding, M. and Deng, H. (2009) 'Efficient generation of hepatocyte-like cells from human induced pluripotent stem cells', *Cell Research*, 19(11), pp. 1233-1242.
- Tettey, J.N., Maggs, J.L., Rapeport, W.G., Pirmohamed, M. and Park, B.K. (2001) 'Enzyme-induction dependent bioactivation of troglitazone and troglitazone quinone in vivo', *Chemical Research in Toxicology*, 14(8), pp. 965-974.
- Theocharis, S., Kanelli, H., Politi, E., Margeli, A., Karkandaris, C., Philippides, T. and Koutselinis, A. (2002) 'Expression of peroxisome proliferator activated receptor-gamma in non-small cell lung carcinoma: Correlation with histological type and grade', *Lung Cancer*, 36(3), pp. 249-255.

- Tirmenstein, M.A., Hu, C.X., Gales, T.L., Maleeff, B.E., Narayanan, P.K., Kurali, E., Hart, T.K., Thomas, H.C. and Schwartz, L.W. (2002) 'Effects of troglitazone on HepG2 viability and mitochondrial function', *Toxicological Sciences*, 69(1), pp. 131-138.
- Tosh, D., Shen, C.N. and Slack, J.M. (2002a) 'Conversion of pancreatic cells to hepatocytes', *Biochemical Society Transactions*, 30(2), pp. 51-55.
- Tosh, D., Shen, C.N. and Slack, J.M.W. (2002b) 'Differentiated properties of hepatocytes induced from pancreatic cells', *Hepatology*, 36(3), pp. 534-543.
- Valko, M., Leibfritz, D., Moncol, J., Cronin, M.T.D., Mazur, M. and Telser, J. (2007) 'Free radicals and antioxidants in normal physiological functions and human disease', *International Journal of Biochemistry and Cell Biology*, 39(1), pp. 44-84.
- Wallace, K., Fairhall, E.A., Charlton, K.A. and Wright, M.C. (2010) 'AR42J-B-13 cell: An expandable progenitor to generate an unlimited supply of functional hepatocytes', *Toxicology*, 278(3), pp. 277-287.
- Wei, S., Yang, J., Lee, S.L., Kulp, S.K. and Chen, C.S. (2009) 'PPAR γ -independent antitumor effects of thiazolidinediones', *Cancer Letters*, 276(2), pp. 119-124.
- Yamamoto, Y., Nakajima, M., Yamazaki, H. and Yokoi, T. (2001) 'Cytotoxicity and apoptosis produced by troglitazone in human hepatoma cells', *Life Sciences*, 70(4), pp. 471-482.
- Yokoi, T. 196 (2010) 'Troglitazone' *Handbook of Experimental Pharmacology* [Review]. pp. 419-435. Available at:
<https://www.scopus.com/inward/record.uri?eid=2-s2.0-77949328267&partnerID=40&md5=5250375a55482181b5d0f25500c00d23>.
- Zhang, Z., Liu, J., Liu, Y., Li, Z., Gao, W.Q. and He, Z. (2013) 'Generation, Characterization and potential therapeutic application of mature and functional hepatocytes from stem cells', *Journal of Cellular Physiology*, 228, pp. 298-305.

**Chapter 2: Simultaneous Intracellular and Extracellular ROS
Detection**

2.1 Introduction

2.1.1 Physiological ROS Production

Generation of ROS and oxidative stress is frequently associated with the cellular damage seen in the pathologies of diseases such as atherosclerosis, cancer and neurodegenerative disorders. Physiologically, the main site of ROS production is in the mitochondria as a by-product of respiration, however, exposure to exogenous drugs can also stimulate the production of ROS either directly or through metabolism. Traditionally ROS have been considered a toxic product that needed to be neutralised in order to prevent cell death. However, in recent years low level ROS production has been suggested to have a role in cell signalling, cell fate and cell proliferation (Hamanaka and Chandel, 2010). Therefore, increasing understanding of the production of ROS and their location of action in normal physiological and disease states could help in treatment of the numerous pathologies.

A role for mitochondrial ROS has been described in several cell signalling pathways. When a tissue is deficient in oxygen, cellular respiration is diminished and a state of hypoxia is induced, mitochondrial ROS production is able to stimulate the activation of signalling pathways that reduce cellular oxygen usage and decrease cellular oxygen consumption (Hamanaka and Chandel, 2010). In addition to this, mitochondrial oxidants have a role in the formation of the inflammasome, a component of the innate immune system that promotes activation of the inflammatory response by stimulating maturation of cytokines. ROS also have other, non-mitochondrial derived, functions in host defences. NOX enzymes present in neutrophils are able to generate ROS in response to inflammatory mediators and neutralise microorganisms engulfed by macrophages (Holmström and Finkel, 2014).

In the metabolism of endogenous and exogenous compounds, poor coupling of the cytochrome P450 catalytic cycle will also result in the production of ROS. P450 enzymes are heme thiolate enzymes that are involved in the monooxygenation of lipophilic compounds in preparation for phase II metabolism and excretion. Monooxygenation reactions require the input of 2 electrons, transferred to the P450 enzyme by NADPH P450 reductase. The input of electrons is required to activate oxygen and insert one oxygen atom into the substrate molecule (Zangar *et al.*, 2004). The coupling efficiency of electron transfer varies depending on the P450 isoform, however, it is usually less than 50%. In severe cases the inefficient coupling can

lead to ROS levels great enough to cause the onset of oxidative stress (Banerjee *et al.*, 2016).

The intermediate stages of metabolism of exogenous compounds usually results in a quinone metabolite capable of redox cycling and producing superoxide (O_2^-) as a by-product. The quinone is reduced via NADH to form a semi-quinone moiety. The semi-quinone is subsequently oxidised by molecular oxygen which regenerates the parent compound and forms O_2^- as a by-product. Once the parent compound is regenerated it is free to be reduced again and so a redox cycle is initiated and large amounts of O_2^- are formed (Klotz *et al.*, 2014). Menadione is a classic example of a compound that contains a quinone structure able to undergo redox cycling, while not used as a therapeutic agent in the western world, Menadione is frequently used for research purposes for causing hepatotoxicity through a redox cycling mechanism.

Doxirubicin is used as a cancer chemotherapy agent and is used to treat a wide range of solid tumour and blood cancers. It is a good example of the mechanisms by which an exogenous compound can generate ROS as it is able to drug that is able to generate ROS through more than one route. In the presence of the electron carrier, NADH, doxorubicin is able to undergo similar quinone cycling to that previously mentioned. However, if the semi-quinone moiety is not oxidised to regenerate the parent compound, the semi-quinone is able to interfere with cellular iron homeostasis, dissociating it from the ferritin that keeps it bound, and initiating the production of highly reactive hydroxyl radicals from hydrogen peroxide (Banerjee *et al.*, 2016).

While there are a whole range of ROS that can cause damage and contribute to oxidative stress, the study of O_2^- remains of particular interest as it is formed in vivo by many enzyme systems and is the progenitor to the formation of other ROS (Dikalov and Harrison, 2014).

2.1.2 Methods of ROS Detection

Due to the high inter-reactivity between ROS species and their short life span, measuring their production is extremely challenging, for example, O_2^- is notoriously difficult to measure as it is rapidly dismutated to form H_2O_2 and water by SOD. Hydrogen peroxide is not a free radical and is much more stable than O_2^- , it is also much less reactive due to being much more weakly oxidising. However, H_2O_2 has the potential, in the presence of free iron, to be broken down by Fenton's reaction

and give rise to the hydroxyl radical (OH^\cdot) which is highly toxic and indiscriminately reactive (Thannickal and Fanburg, 2000).

Traditionally, electron paramagnetic resonance (EPR) spectroscopy has been used to study materials with unpaired electrons. Electron spins are excited in a magnetic field in which they absorb and re-emit electromagnetic radiation at a specific resonance frequency depending on the compound being studied. Due to the short half-life and high reactivity of O_2^- , EPR spectroscopy can be utilised to study its production. However, O_2^- has to be immobilised using spin traps which form covalent bonds with the radical making a more stable adduct that can be measured. One of the most common spin traps is 5,5-Dimethyl-1-Pyrroline-N-Oxide (DMPO). While the technique has O_2^- specificity and can be very useful in studies of isolated enzymes in solution, where the reaction with O_2^- has a slow reaction rate, its use in biological systems is limited due to the presence of SOD which is able to outcompete the spin trap. Furthermore, intracellular reductants are able to react with the O_2^- / DMPO adducts and reduce them to a spin inactive state, severely limiting the use of the technique (Dikalov and Harrison, 2014).

Manning *et al.* described a simplified method for O_2^- detection using a functionalised gold electrode. The gold electrode surface was modified with 3,3'-Dithiobis(sulfosuccinimidylpropionate) (DTSSP) which covalently bound to the surface and acted as a linker molecule between the gold surface and the redox protein cytochrome c. O_2^- generation in a sample in liquid media caused the one electron reduction of cytochrome c^{3+} to cytochrome c^{2+} . The reduced protein was reoxidised at the electrode surface (at a potential of +100mV vs Ag/AgCl) causing a change in current that was directly proportional to the rate of O_2^- produced (figure 2.1) (Manning *et al.*, 1998).

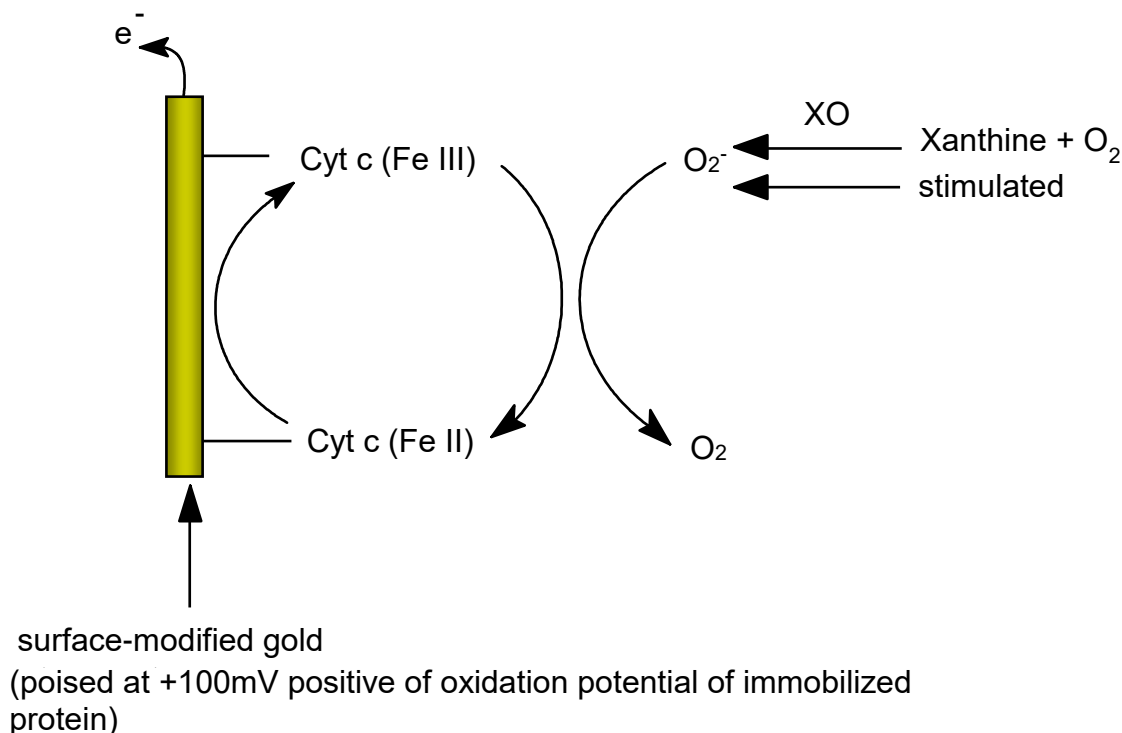


Figure 2.1: Electrochemical measures of O_2^-

Fluorescent dyes are frequently utilised in biological research for investigating cellular production of ROS as they are membrane permeable and able to diffuse into cells and therefore get closer to the site of production; a crucial feature given the transient nature of ROS (Yazdani, 2015). Most dyes for studying ROS are based on oxidation/ reduction reactions between ROS and a reduced probe (Woolley *et al.*, 2013). 2',7'-dichlorofluorescein diacetate (DCFDA) is a membrane permeable dye that passively diffuses into cells where its acetate groups are cleaved, forming 2'-7'-dichlorodihydrofluorescein. Free radicals present within cells then oxidise this molecule to form the fluorescent compound, 2'-7'-dichlorfluorescein, which can be detected using a spectrophotometer at excitation 485 nm and emission 535 nm. Similarly, dihydrorhodamine-1,2,3 is a lipophilic non-fluorescent compound that is oxidised by free radicals upon crossing the cell membrane. The oxidised product is a fluorescent probe, rhodamine-1,2,3 (excitation 507 nm and emission 529 nm) (Yazdani, 2015).

Fluorescent dyes are incredibly easy and quick to obtain results from, however, their use is fraught with problems, including auto-oxidation, phot-oxidation, photo-bleaching, photo-conversion and cytotoxicity. In addition to this, when considering O_2^- sensing, dyes also tend not to be ROS specific, despite claims, due to their

similar chemistry and reactive nature. For example, dihydroethidium can form two fluorescent products, 2-OH-E⁺ which is O₂⁻ specific and ethidium which is formed following non-specific redox reactions (Dikalov and Harrison, 2014). The fluorescent spectra of 2-OH-E⁺ and ethidium overlap, making fluorescent detection difficult. The only way to determine between the different products is to quantify 2-OH-E⁺ using high performance liquid chromatography (HPLC) which separates out products based upon molecular size. This technique, although extensively validated, is time consuming (Zielonka *et al.*, 2008).

One solution to overcome the drawbacks of free dyes is to encapsulate them in a nanosensor. PEBBLE nanosensors (Probes Encapsulated by Biologically Localised Embedding) represent a major development in sensor based technology (figure 2.2). By encapsulating free dyes in a porous polyacrylamide shell, some of the limitations inherent with free dyes are overcome. Acrylamide non-covalently traps an indicator dye inside a porous matrix. The polymer spheres are bioinert and minimally invasive to living cells due to their sub-micron size (typically 10-20nm in diameter).

Furthermore, due to their use of commercially available dyes, PEBBLES can be incredibly versatile. To date methods have been described for the detection of H⁺, Ca²⁺, K⁺, Na⁺, Mg²⁺, Zn²⁺, Cl⁻, NO₂⁻, O₂ and NO (Clark *et al.*, 1999). In addition to this, due to the simplicity of manufacture, multiple dyes can be added to the monomer mixture before polymerisation, generating a nanosensor capable of determining multiple parameters simultaneously. Alternatively, a second dye, unresponsive to the analyte of interest can be added, thus allowing for ratiometric analysis (Buck *et al.*, 2004). Ratiometric analysis is a technique that measures two different signals, one from a ROS unresponsive dye and one from a ROS responsive probe dye. This allows for a proportional rather than an absolute measure of fluorescence, the benefit of which is that the ratio between the two peaks is unaffected by the amount of PEBBLES within the cell or changes in the intensity of the excitation light.

PEBBLE nanosensors have two distinct advantages over free dyes; firstly, the polyacrylamide shell protects the surrounding cell from any inherent toxicity from the dye and secondly it protects the dye, via size exclusion, from any unwanted interactions with cellular proteins that would otherwise produce artefacts. Using nanosensors is a novel way of dynamically studying the intracellular environment. Combining this approach with the electrochemical technique for O₂⁻ detection

Chapter 2: Simultaneous Intracellular and Extracellular ROS Detection described in Section 2.1.2 would enable the simultaneous intra- and extracellular measurement of ROS production. This in turn could form the basis for a novel drug screening platform that would give unparalleled information about the effect pharmaceuticals have on the oxidative state of a cell.

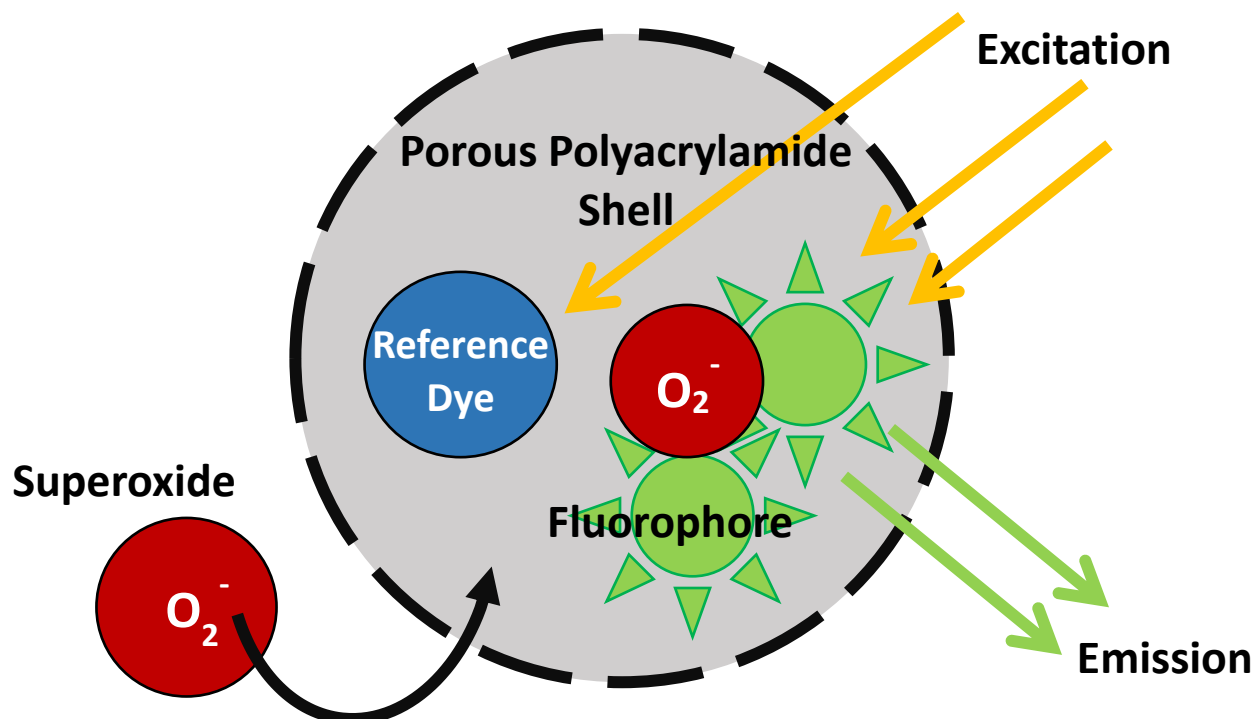


Figure 2.2: Representation of PEBBLE nanosensor

2.1.3 Aims

The aim of this chapter was to combine fluorescence-based intracellular nanosensors and extracellular electrochemical sensing technology into a system that would enable a better understanding of the role that ROS play in drug-mediated cell death. B13/H hepatocyte-like cells would be used to demonstrate the effectiveness of this combined approach in understanding the importance of drug-induced changes to oxidative metabolism.

Key objectives were:

- To develop and characterise fluorescent nanosensors suitable for real-time intracellular ROS sensing.
- To characterise an electrochemical system for the direct, real-time extracellular detection of $O_2^{\cdot -}$.
- To combine the intracellular ROS nanosensors with extracellular electrochemical $O_2^{\cdot -}$ detection. This combination could ultimately lead to the development of a novel platform for drug screening.

Chapter 2: Simultaneous Intracellular and Extracellular ROS Detection

- To validate this system using B13 (pancreatic, control cells) and B13/H (hepatocyte-like, test cells) exposed to a range of hepatotoxins.

2.2 Methods

2.2.1 Materials

Superoxide Detection: A Uniscan Bi Stat 3200 potentiostat with proprietary software and gold working electrodes (2mm O.D.) were supplied by Alvatek (Gloucestershire, UK). Ag/AgCl reference electrodes were supplied by Harvard Apparatus Ltd (Cambridge, UK), DTSSP was supplied by Thermofischer (Loughborough, Leicestershire, UK). Cytochrome c (from horses' heart) was supplied by Sigma Aldrich (Poole, Dorset, UK). Electrodes were prepared prior to surface modification by using a BASi® PK-4 electrode polishing kit (Alvatek, Gloucestershire, UK). The electrodes were calibrated using xanthine (sodium salt) and xanthine oxidase (from buttermilk) which were both supplied by Sigma Aldrich (Poole, Dorset, UK).

PEBBLE manufacture: TAMRA, FAM, Oregon Green, DCFDA were supplied by Life technologies (Glasgow UK). All other materials were supplied by Sigma-Aldrich (Poole, UK) unless otherwise stated.

2.2.2 Cell Culture

B-13 cells were a gift from Prof. Matthew Wright (Newcastle University). Cells were routinely cultured in low glucose (1000 mg/l) DMEM which was supplemented with 10% FBS, 500 U/ml penicillin and streptomycin, 2 mM L-Glutamine and 1% amphotericin B. Cells were incubated at 37°C in a humidified environment containing 5% CO₂. The medium was changed every 2-3 days.

When cells reached 70-90% confluence, the cells were passaged. The medium was removed from the flask and the cell layer was washed once with pre-warmed PBS to remove traces of media. As cells were adherent, 2 ml of 10x trypsin in EDTA was added to the flask. The flask was gently tilted back and forth and then tapped gently to encourage the detachment of the cell layer from the surface. Culture medium (~8 ml) was then added to the flask to inhibit the action of the trypsin and the full 10 ml was then transferred to a 15ml falcon tube which was then centrifuged at 720G for 5 minutes. Supernatant was subsequently removed and the cell pellet was re-suspended in fresh medium for counting using a haemocytometer. Finally, cells were seeded as required, either into a fresh t75 culture flask for maintenance of the stock or for a specific experiment.

For B-13/H cells, B-13 cells were routinely cultured before being seeded at the relevant density; 1×10^5 for electrochemistry into a 24 well plate and 1×10^4 into a 96

well plate for cell viability assays. B-13 cells were incubated overnight to attach and B-13/H cells were incubated for 5-10 days in media containing 10 nM dexamethasone made from a serial dilution of a 100 μ M stock in ethanol to allow for an optimal response to be determined.

2.2.3 Long Term Cell Storage

For long term storage, cells were placed in liquid nitrogen. Cells were detached from the culture vessel as previously described. After the supernatant was removed the cell pellet was resuspended in a freezing mixture of 10% DMSO and 90% FBS. This was aliquoted into sterile cryovials at 1 ml per tube. Cryovials were placed in a -80 °C freezer overnight before being transferred to liquid nitrogen for long-term storage.

2.2.4 Cell Stock Revival

Cryovials were removed from the liquid nitrogen and placed in a pre-warmed water bath at 37 °C. Once thawed, cells were transferred to a 15 ml centrifuge tube and made up to 10 ml with fresh media. Cells were centrifuged at 2000 rpm for 5 minutes, supernatant was removed and cells were resuspended in fresh media and transferred to a culture flask.

2.2.5 Electrode Preparation

The working electrode consisted of a 2mm OD solid gold electrode encased in a chemically inert plastic (KEL-F). The gold electrode was prepared by first polishing on a micro-cloth pad containing aluminium oxide slurry followed by sonication for 5 minutes in distilled water to remove any residue. The electrode was then carefully dried and clamped upside down before a bead of DTSSP (50 mM in PBS) was dropped onto the gold surface. The surface modification reaction was allowed to proceed for 1 minute at room temperature. Excess DTSSP was removed and the electrode placed in 2mM cytochrome c in PBS solution overnight at 4°C.

2.2.6 Electrode Calibration

The modified electrode was rinsed in DI water immediately before use and the electrode was then calibrated using the reaction between xanthine/ xanthine oxidase (XOD) to generate O_2^- as previously described by Cooper 1992 and Manning 1998 (McNeil et al., 1992; Manning et al., 1998). The gold working electrode was poised at +100mV vs an Ag/AgCl reference electrode that also secondarily acted as a counter electrode. Both were placed in the well of a 24 well plate containing 1.5 mM xanthine (an excess) in PBS. Upon achieving a stable baseline reading varying

concentrations of XOD were added and the corresponding change in current was observed. The system was stirred to enable even and rapid distribution of reagents within the well. To test the specificity of the electrode for O_2^- over other reactive oxygen species the ability of SOD to quench current responses was assessed at concentrations ranging from 0.005 U/ml - 0.5 U/ml.

2.2.7 Cellular Superoxide Measurement in B-13 and B-13/H Cells

B-13 cells were left to attach to the well surface overnight, B-13/H cells were left for between 3-10 days to determine at what stage optimal response could be obtained. Cells were tested for their ability to produce O_2^- using the electrode system. A variety of chemical stimulants including phorbol 12-myristate 13-acetate (PMA) (0.25 μ M- 1.00 μ M), menadione (5 μ M- 100 μ M) and ethanol (1.7 M- 8.6M) were used to try and induce the production of O_2^- radicals which would in turn alter the current at the electrode and produce a measurable response that was recorded using Uiscan software. Ethanol was chosen as an initial extreme insult in order to prove the concept before more physiologically relevant compounds were tested; menadione, a known redox cycler and PMA, a tumour promoter known to stimulate O_2^- production. In all cases unless otherwise stated cells were seeded at a density of 1×10^5 cells per well. The stimulants used to try and generate O_2^- production included menadione used at concentrations ranging from 1 μ M- 100 μ M. Stimulants were added to the wells without disturbing the probes and gently pipetted up and down to cause diffusion across the bottom of the well. Between each measurement the electrodes were rinsed with deionised water. Unlike the stirred system of the calibration experiment, the electrodes had to be placed as close to the cell layer as possible without contact as a magnetic stirrer would have disturbed the cell layer. In addition to this the electrodes were placed over the region of the well where there was greatest cell coverage in order to maximise the response obtained.

2.2.8 Nanosensor Production

The PEBBLE nanosensors were synthesised in a multi-stage process adapted from Chauhan et al (2011). Briefly, Acrylamide (7.6 mM) and N,N methylene bisacrylamide (1.3 mM) were dissolved in 1.5 ml of deionised water by sonication to create a monomer solution. To the monomer solution, 5mg/ml of the reference dye, 5-Carboxytetramethylrhodamine (TAMRA), and 10 mg/ml of the indicator dyes, (FIT-C and Oregon Green or pH nanosensors, DCFDA for ROS nanosensors) were added

and covered to avoid exposure to light as the dyes are photosensitive. A surfactant mixture was prepared of Dioctyl sulphosuccinate (3.6 mM) and Brij30 (8.5 mM) and deoxygenated before being added to 42ml of deoxygenated hexane to form a micro-emulsion. The monomer/ fluorophore solution was added to the surfactant mixture and left for 10 minutes. Following this the polymerisation process was initiated by immediate addition of 30 μ l of ammonium persulfate (10% w/v) and 15 μ l of N,N,N',N'-tetramethylethylenediamine. After 2 hours' polymerisation in the absence of oxygen, hexane was removed by rotary evaporation and the remaining nanosensors washed 5 times in absolute ethanol with the ethanol being removed by rotary evaporation after the last wash. The remaining sensors were stored in a covered airtight container in the refrigerator.

2.2.9 pH Nanosensor Calibration

Stock solutions of 0.2 M sodium phosphate dibasic and 0.1 M citric acid monohydrate were used to make buffer solutions between pH 4 and 8. Nanosensors were dissolved in the buffer solutions for a final concentration of 5 mg/ml. The PEBBLE nanosensors contained 3 dye probes: Oregon Green, FIT-C and TAMRA. As TAMRA is not pH sensitive it acted as a reference probe to allow for ratiometric analysis of the fluorescent signals obtained from Oregon Green and FIT-C. Buffer/ nanosensor mix (200 μ l) was added in triplicate to the wells of a 96 well plate along with a blank that contained buffer alone to ensure that any background fluorescence did not interfere or overlap with the response achieved from the dye sensors. Fluorescence intensity measures were taken using a Tecan Infinite M200 spectrophotometer (Tecan, Austria).

2.2.10 Free Dye ROS Assay

A free dye assay was performed as a comparison to the nanosensor platform as it is a widely-accepted technique in its own right for the study of ROS production in cells. Cells were routinely cultured and seeded at 2.5×10^4 cells per well. For B-13 cells, plates were left overnight for cell attachment to the well surface, for B-13/H cells, plates were left in DEX media for 7 days to allow for trans-differentiation. Media was changed every 2-3 days. The rest of the experiment was carried out as per the manufacturer's instructions. On the day of the experiment DCFDA dye solution was made to a concentration of 30 μ M in buffer solution. The cells were removed from the incubator and the media was removed. The cell layer was washed with buffer before being replaced with 100 μ l DCFDA solution. Plates were then incubated at 37

°C for 45 minutes. Menadione concentrations were made separately at 10x desired concentration in unsupplemented, phenol red free DMEM. DCFDA was removed from the cells and replaced with unsupplemented media and a 1 in 10 dilution of Menadione for final concentrations between 1 µM and 50 µM. Plates were incubated for 3 hours at 37 °C. Plate fluorescence was measured at 485 nm excitation and 535 nm emission.

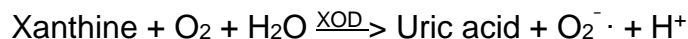
2.2.11 Resazurin Cell Viability Assay

B-13 and B-13/H cells were routinely cultured and seeded into 96 wells plates at a seeding density of 1×10^4 cells per well. B-13 cells were incubated overnight to allow for cell attachment whereas B-13/H cells were left for 7 days in DEX media to allow for transdifferentiation. On the day of the experiment, the media was removed and cells were washed with PBS, media was replaced with unsupplemented DMEM containing a range of concentrations of blank nanosensors (containing no DCFDA) or a range of concentrations of DCFDA. Cells were incubated at 37 °C for 3, 6 and 24 hours. Cell viability was measured by adding resazurin (0.03% w/v) to each well. Resorufin, produced as a result of bio-reduction of resazurin was measured fluorometrically at excitation 530nm and emission 590 nm using the Tecan-I plate reader.

2.3 Results

2.3.1 Calibration of Superoxide response using Electrochemistry

The gold electrode was calibrated using the generation of superoxide from the reaction of xanthine in water catalysed by xanthine oxidase (*Equation 2.1*).



Equation 2.1: Production of superoxide from xanthine catalysed by xanthine oxidase

Figure 2.3 showed that as there was a linear relationship between superoxide production and the current response. A strong response was obtained with a maximum current of 50 nA seen with 1 μM xanthine oxidase.

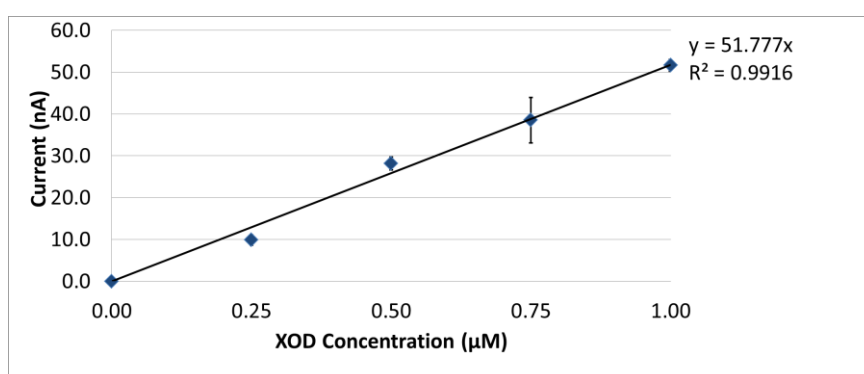


Figure 2.3: Calibration of the gold electrode to superoxide in a stirred system. The superoxide radical was produced during the reaction of xanthine with water. The reaction was catalysed by Xanthine Oxidase. As the concentration of XOD increased, there was an increase in current production. The response was concentration dependent. Data presented as mean of 3 replicates \pm S.D. $R^2 = 0.99$.

2.3.2 Stimulated Extracellular O_2^- Production in B-13 and B13/H Cells

2.3.2.1: Ethanol

Measuring O_2^- in a cell based system presented challenges as the system was unstirred so as not to disturb the cell layer attached on the well surface. However, it was shown that with an increasing concentration of ethanol there was a linear increase in the current produced. To characterise the specificity of the electrode response to O_2^- the effect of a highly specific O_2^- scavenger, SOD (500 U/mL, an excess) on recorded current values was assessed. Figure 2.4 showed that the response was completely abolished upon addition of SOD. The maximum response attained, however, was approximately 25 times smaller than that observed in the xanthine/ XOD calibration system. In addition to this, a linear response to ethanol was only observed in B-13/H cells and no response could be obtained from B-13

cells under equivalent conditions; B-13 cells were unresponsive to ethanol stimulation.

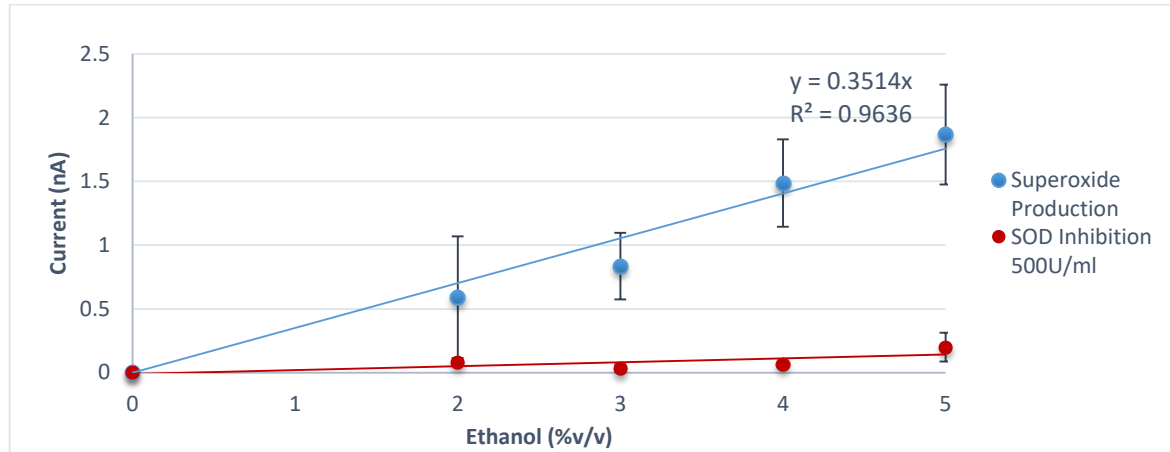


Figure 2.4: Response of B-13/H cells to ethanol. There was a linear relationship between ethanol concentration and current produced over concentration range tested ($R^2=0.96$). As the total well percentage of ethanol increased the current generated increased in a dose dependent manner. The responses were quenched at all ethanol concentrations by the addition of 500 U/ml SOD. This was a novel finding in this cell line and suggests that B-13/H cells are capable of responding to a toxin such as ethanol with the generation of O_2^- , a response that was not seen prior to differentiation in pancreatic B-13 cells. Data presented as mean of 3 replicates \pm S.D.

Figure 2.5 showed that a response to ethanol was only observed in B-13/H cells treated for 5 days with DEX. Ethanol was not seen to produce a consistent response in B-13 cells (0 days) or at 7 or 10 days (data not shown).

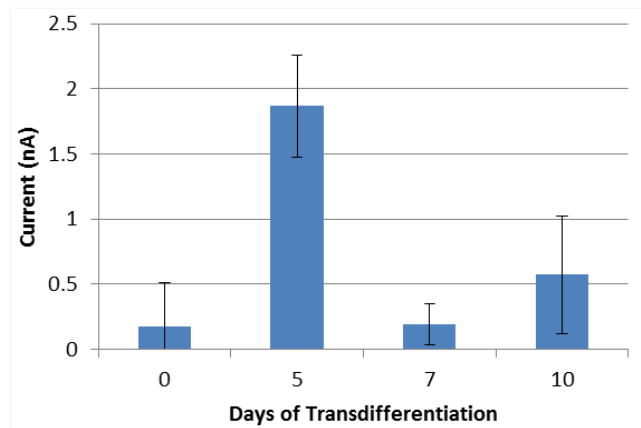


Figure 2.5: O_2^- production by B-13 and B-13/H cells during the transdifferentiation process following stimulation with 5% v/v ethanol. Data presented \pm SD, $n=3$.

2.3.2.2: Menadione

The extracellular O_2^- response of B-13 and B-13/H cells to known hepatotoxin, Menadione, was assessed. Menadione was shown in figure 2.6A to have a mild stimulatory effect in B-13/H cells but not at all in B-13 cells (figure 2.6B). The

response of the B-13/H cells was concentration dependent up to 50 μM . At 100 μM the response was completely abolished. Again, even at peak response, the maximum current achieved was still only about 0.5 nA. Figure 2.7 shows a typical trace containing the raw data from a single electrochemistry experiment, specifically, B-13/H cell response to stimulation with 10 μM menadione.

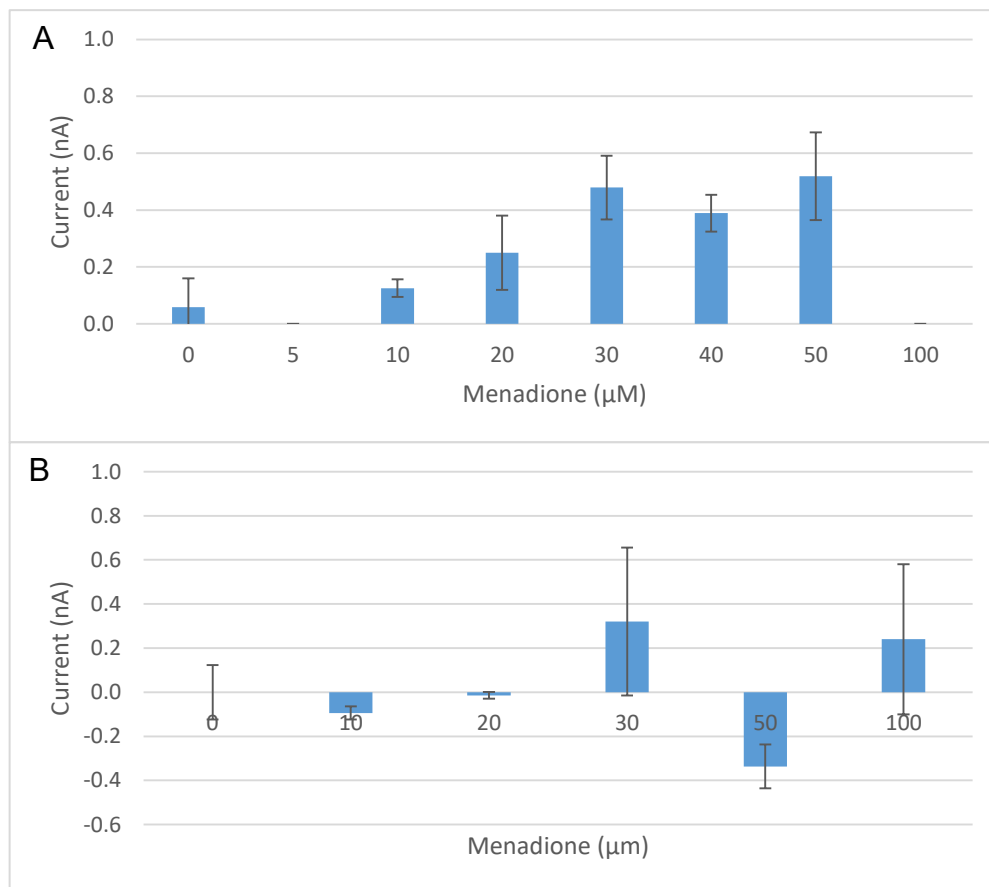


Figure 2.6: Current production from B-13 and B-13/H cells treated with menadione (A) Response of B-13/H cells following a 5 day transdifferentiation period to varying concentrations of menadione. Increasing concentrations of menadione appeared to cause an increase in the production of superoxide until 100 μM when the effect was completely abolished ($R^2=0.91$). Data presented as mean of 3 replicates \pm S.D. (B) Response of B-13 cells to Menadione. There was no response seen in B-13 cells to Menadione treatment. Data is presented as mean of 3 replicates \pm S.D.

2.3.2.3 PMA

PMA was unable to elicit a response at the electrode when tested with B-13 and B-13/H cells.

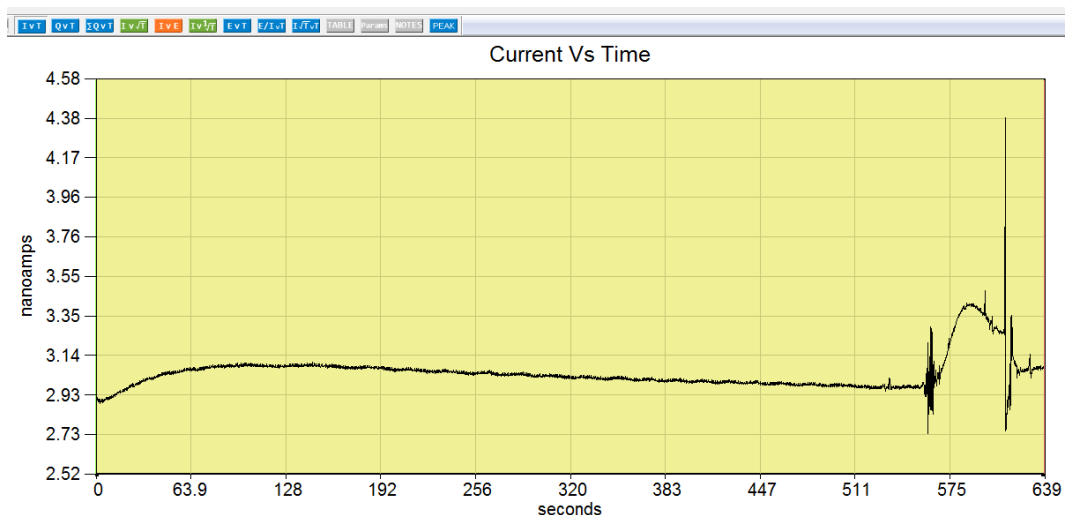


Figure 2.7: Example electrochemistry trace showing 5-day B-13/H cell response to 10 μ M menadione

2.3.3 Development of PEBBLE nanosensors for the detection of intracellular ROS based on a pH sensor proof of concept.

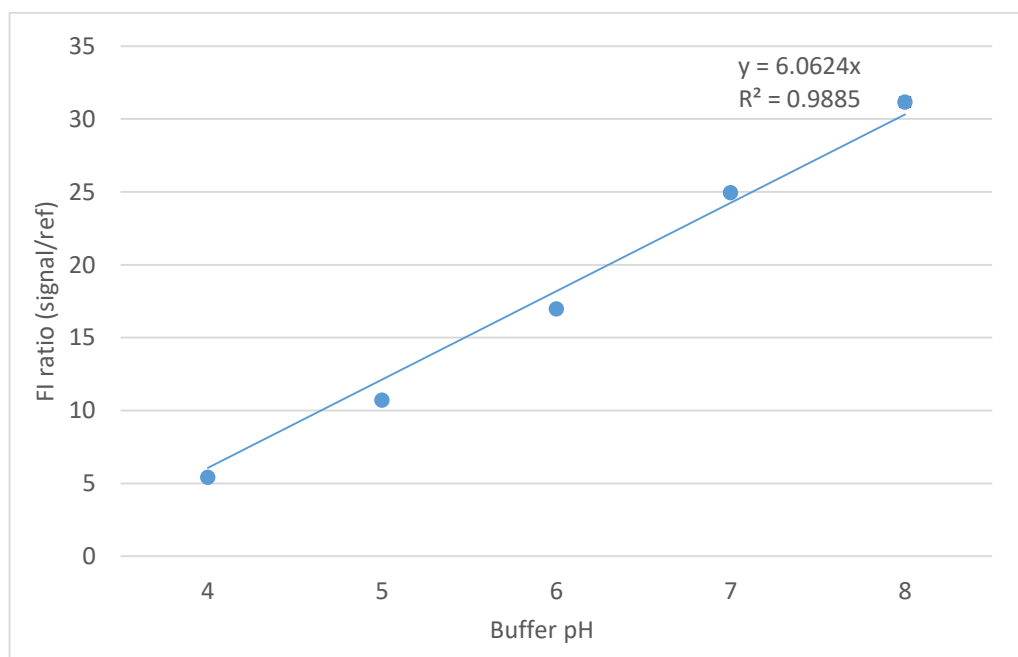


Figure 2.8: Calibration of pH sensitive nanosensors FAM and Oregon green. Fluorescent ratio was shown to be linearly dependent upon pH. The data is presented as mean \pm S.D, $n=5$, $R^2=0.99$

pH nanosensors have been previously described and were used as a template for the development of ROS responsive sensors (Clark *et al.*, 1999). The synthesised pH responsive sensors (25 mg/ml) responded linearly to pH values as seen in figure 2.8. The nanosensors contained two pH responsive dyes in order to increase the dynamic range of the sensors (fluorescent response from Oregon green / 5(6)-

Carboxyfluorescein N-hydroxysuccinimide ester (FAM)) and a pH unresponsive dye, TAMRA, that was used as a reference dye and allowed ratiometric analysis. The response obtained is presented as the ratio of fluorescent response from Oregon green / 5(6)-Carboxyfluorescein N-hydroxysuccinimide ester (FAM) to the response from TAMRA. As the pH increased the fluorescent signal increased linearly, the PEBBLE nanosensors were sensitive to pH levels between pH4 and pH8. The successful production and calibration of pH nanosensors provided the rationale to develop a similar nanosensor for detection of intracellular ROS production.

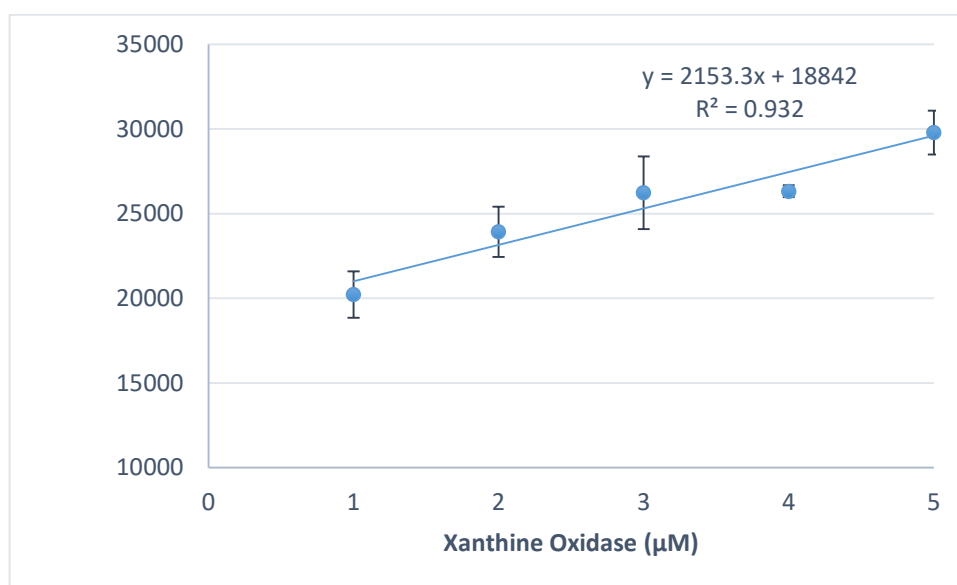


Figure 2.9: Calibration curve of DCFDA in response to the catalysis of Xanthine by Xanthine Oxidase to produce Superoxide in a cell free system. At a concentration of 25μg/ml DCFDA and an excess of xanthine there is a linear increase in the fluorescent signal with an increase in xanthine oxidase ($R^2=0.93$) ($n=3 \pm S.D.$)

The ROS responsive dye, DCFDA was calibrated in its free state, DCFDA, although not O_2^- specific, was responsive to O_2^- production. Albeit over a narrow range, figure 2.9 showed that there was a concentration dependent linear response. Nanosensors, when calibrated for response to ROS in a system similar to that used for the free dye, showed no response. There was no relationship observed between increasing O_2^- concentration and fluorescent response, in fact, at all concentrations; the response was equivalent to that seen in the untreated controls (figure 2.10).

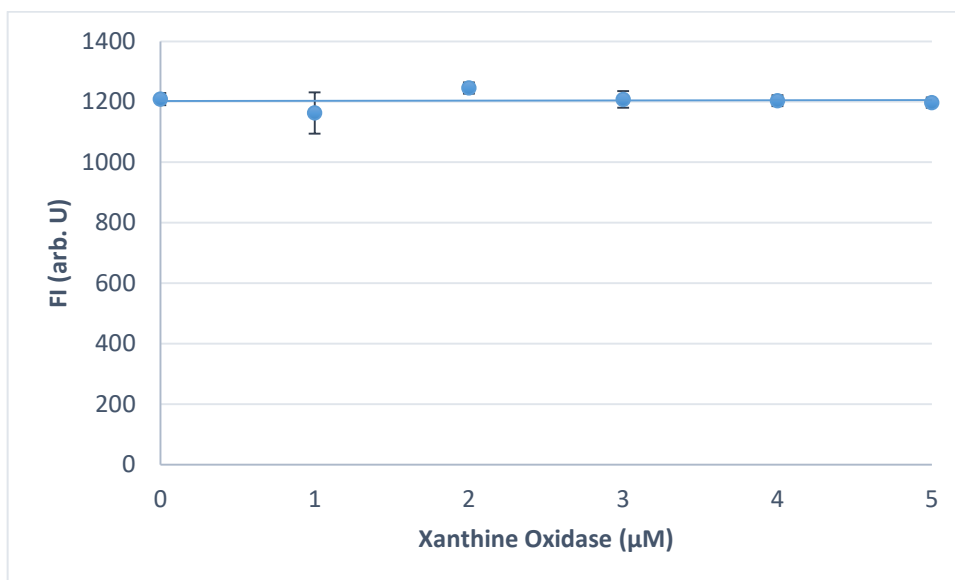


Figure 2.10: Calibration curve of DCFDA PEBBLE nanosensors. No response was seen to Xanthine Oxidase ($n=3 \pm S.D.$)

2.3.4 Toxicity of PEBBLE nanosensors

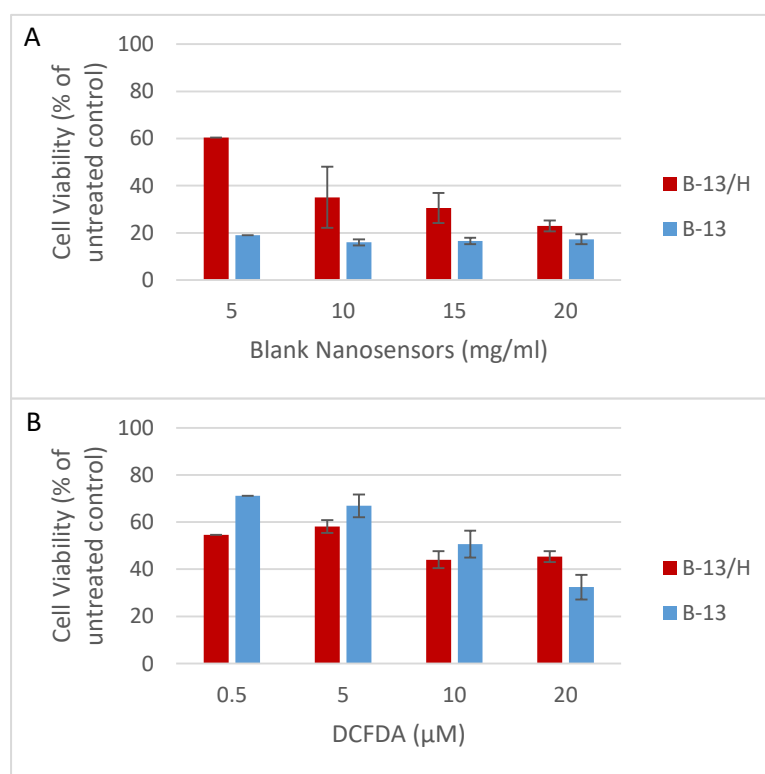


Figure 2.11: (A) Cell viability following 3-hour exposure to blank nanosensors. PEBBLES were manufactured to contain no active dye, just polyacrylamide matrix. B-13 cells were more susceptible than B-13/H cells and all concentrations reduced viability to below 20%. B-13/H cells showed a concentration dependent decrease in viability. (B) Cell viability following 3-hour exposure to DCFDA free dye. Concentration dependent decrease was seen in B-13 cells which were less susceptible to lower concentrations of DCFDA than B-13/H cells, at 20 µM DCFDA B-13 cells were more susceptible. In B-13/H cells there was very little variability in viability. Cell death was between 40% and 55%. ($n=3 \pm S.D.$)

PEBBLE nanosensors were designed to be biologically inert. The polyacrylamide matrix should provide a way of trapping the dye without participating in the reaction, in addition to this, free dyes also have an inherent toxicity that the polyacrylamide shell was designed to prevent.

However, figure 2.11B showed that DCFDA was toxic on both B-13 and B-13/H cells. When using DCFDA free dye, it is recommended that cells are not incubated with the dye for longer than 3-4 hours. At 3 hours there was a concentration dependent decrease in viability observed in B-13 cells, in B-13/H cells viability was reduced below 50% at concentrations of 10 μ M and above. In contrast, when cells were exposed to blank nanosensors i.e. nanosensors made via the same process but without the addition of reactive probes, it was observed that following 3 hours exposure, cell viability was less than 20% in B-13 cells at all concentrations. B-13/H cells were less susceptible but a concentration dependent decrease in viability was observed, at concentrations of 10 mg/ml and above, cell viability was less than 50%. The data presented, suggested that the PEBBLE nanosensors were more toxic than the free dye and were more toxic to the B-13 cells than the B-13/H cells. Following 24 hours' exposure, cell viability in both cells lines was negligible at all nanosensor concentrations.

2.3.5 ROS measures using DCFDA Free Dye

Menadione is a known hepatotoxin that elicits damage through excess superoxide production via redox cycling. It was shown that there was a greater level of ROS produced in B-13/H cells compared to B-13 cells where there was no apparent ROS production greater than that seen in untreated control cells. However, the levels of ROS production seen in B-13/H cells was not significantly greater than that seen in untreated cells (figure 2.12).

2.3.6 ROS measures using PEBBLES in Ethanol Treated Cells

No response was elicited from the use of PEBBLE nanosensors in B-13 or B-13/H cells treated with ethanol.

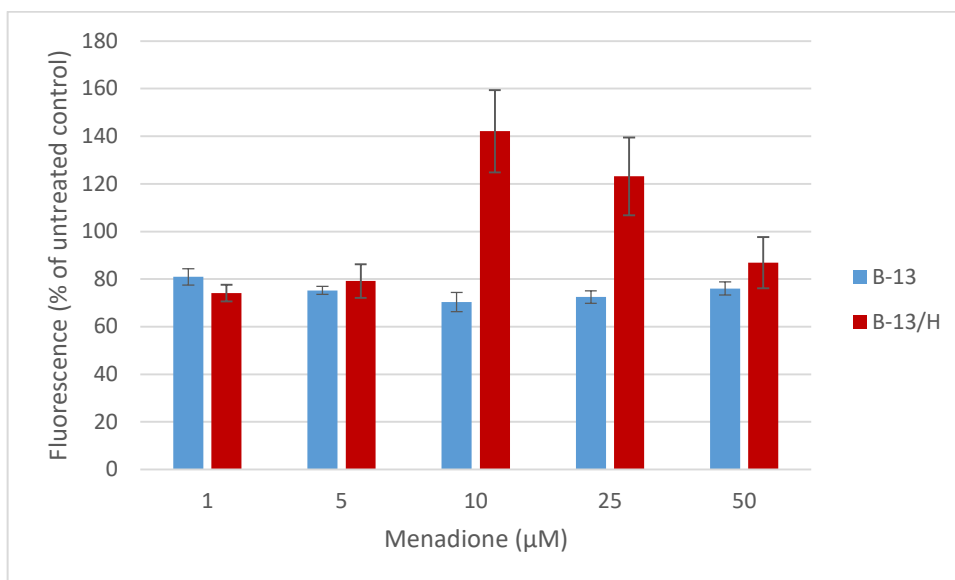


Figure 2.12: ROS production in response to treatment with redox cyclers, menadione. Cells were pre-treated with ROS responsive dye, DCFDA for 45 minutes before being incubated with menadione for 3 hours. A response above untreated controls was only observed in B-13/H cells at concentrations of 10 μM and 25 μM . In B-13 cells response remained consistently around 80% of untreated cells. Data is presented as mean of 3 replicates \pm S.D.

2.4 Discussion

Many challenges still exist in the detection of reactive oxygen species due to the speed at which they react and, particularly in whole cell experiments where there is, competition with antioxidants. Furthermore, O_2^- specificity is often difficult to achieve due to the similarity of the chemistry of reactive oxygen species.

Electrochemistry offers a technique that is able to selectively measure O_2^- owing to a low operating potential (Manning and McNeil, 2011). When the functionalised gold probe was calibrated in a xanthine/ xanthine oxidase system, it was seen that there was a XOD concentration dependent increase in current produced. The response was also shown to be O_2^- specific in the cell system, as when the antioxidant SOD was added to wells, the signal was completely abolished. Although a strong response was observed in a stirred system, when the probe was used over a cell layer the response was significantly diminished. Never-the-less, ethanol was still able to stimulate a concentration dependent response in B-13/H cells, albeit at incredibly high concentrations that would not be physiologically relevant. It is thought that ethanol is able to generate ROS during metabolism via CYP 2E1. CYP 2E1 forms part of a minor pathway through which ethanol is broken down to acetaldehyde, using NADPH, two electrons are transferred to ethanol, however, due to poor coupling of this reaction often electrons leak and form O_2^- (Diesen and Kuo, 2010).

In order to try and obtain a physiologically relevant response, the next step was to investigate the effects of a known hepatotoxin on the cells. Menadione is known to be toxic via a redox cycling mechanism that can stimulate the production of oxidative stress through over production of O_2^- . Menadione was shown to increase O_2^- production in B-13/H cells up to a concentration of 50 μ M. The effect was abolished at 100 μ M. In contrast, there was no observed effect in the B-13 cells at any concentration. This would be the expected result as menadione is a hepatotoxin, suggesting that the B-13/H cells had transdifferentiated into hepatocyte like cells that were responsive to toxins in a similar way to hepatocytes. However, these results were observed after only 5 days transdifferentiation and all further experiments described here using B-13/H cells were used at (and showed an optimal response at) a 7-day time point as shown in chapter 3, section 3.3.2, figure 3.7. It was observed in the preliminary experiments with ethanol that a response could only be found at early in the transdifferentiation process and at 7 and 10 days no response could be

obtained from the electrode (figure 2.5). The transdifferentiation process is only partially complete after 5 days and as all further work was conducted at a later stage it would seem likely that the cells were not fully differentiated and the response seen was from an intermediate cell type (Marek *et al.*, 2003). When B-13/H cells were tested later in the differentiation process, however, a stable and consistent response was not observed.

The responses obtained from electrochemical detection of O_2^- in a non-cell system were much larger than those in a cell system. This could be because when the electrode is placed in a well with a cell layer attached, it is not possible to stir the system with a magnetic flea, thus, the system relies upon diffusion of the analyte thorough the surrounding media and as O_2^- is rapidly neutralised by antioxidants present in the cells or even spontaneously to H_2O_2 and water. Therefore, it is possible that the O_2^- was not present for long enough in the media to be reactive at the probe surface. In order to minimise this effect, the probe was placed as close to the cell layer as possible. This also introduces a further variable in the technique as there is no set way of ensuring that the probe remained at a constant distance from the cell layer between experiments and could have impinged upon the strength of the signal obtained and contributed to the variation in the results obtained. It is possible that the technique was not sensitive enough to accurately detect O_2^- at the low levels produced by the cells. Figure 2.7 showed raw data from a typical electrochemistry trace before normalising for blank values. Peak response to menadione was only 1.2x greater than the response from the blank value suggesting that the minimum detection level was not obtained and could account for variable and inconsistent results. The limit of detection should be 3x that seen in blank controls. When using whole cells it is also important not to stress the cells in the well and generate unwanted artefacts. This means working as quickly as possible so that when the cells were removed from the incubator there was as little time as possible for the media to cool down but also meant that the cells remained in media while being tested, however, there is also a complex mix of substrates within the media that could also react with the O_2^- generated and reduce the O_2^- present at the electrode surface. In addition to these factors it is likely that the concentration of O_2^- producing XOD was far in excess of any physiological relevant model when calibrating the electrode. Since the aim of electrode calibration was to establish responsiveness and

not to quantify the amount of O_2^- being produced by the cells this was not considered to be a significant issue.

Nanosensors have already been shown to be a useful way of measuring intracellular analytes (Clark *et al.*, 1999). As a proof of concept, pH nanosensors made with the responsive dyes, FAM and Oregon green and the unresponsive dye, TAMRA were calibrated. Combining both FAM and Oregon green fluorophores extended the dynamic range of pH measurements. The ratio of response from the active dyes was calculated in a range of pH solutions. Ratiometric methods are based on the ratio of 2 fluorescent indicators allowing for correction for artefacts, photo-bleaching and uneven dye loading. As can be seen in figure 2.8, as pH became more basic the fluorescent response increased. pH nanosensors were also a good example of how multiple active dyes can be added to a sensor to maximise sensitivity. In this case Oregon Green is responsive at the acidic end of the pH range and FAM is responsive closer to the neutral end. Recently a method has been described for a nanosensor containing 4 fluorophores; difluoro-oregon green, Oregon green 488, fluorescein and non-responsive dye, Alexa 568, for an even broader measurement range between pH 1.4 and pH 7.0. In doing so, the pH of acidic compartments including lysosomal fluctuations was able to be measured (Zhang *et al.*, 2015). pH nanosensors have also been successfully utilised for measuring the pH of whole organisms. Using nanosensors containing Oregon green and FAM, the full physiological pH range of *C. elegans* was visualised. As whole organisms were being used the nanosensors were internalised by ingestion, the *C. elegans* worms were then imaged under a microscope, a pH range from pH 5.96 in the anterior pharynx to pH 3.59 in the posterior intestine was observed (Chauhan *et al.*, 2013).

Nanosensors have wide ranging potential for sensing of intracellular analytes. The ability to sense intracellular ROS production would provide information on the source of ROS in relation to the pathology of disease but also possible information on ROS production in response to drug treatment. For example, in research and development of new compounds, if ROS production is witnessed it may be indicative of a potential to cause oxidative damage.

A ROS nanosensor has been described previously in the literature, this project aimed to replicate the results and develop a sensor for ROS detection within hepatocytes (Henderson *et al.*, 2009). The first step was to calibrate the PEBBLE nanosensors in a system known to generate O_2^- in a similar manner to the electrochemistry

experiments. The DCFDA was calibrated first, in a xanthine/ xanthine oxidase system and, although it has a narrow functional range, showed that an increase in O_2^- resulted in a linear increase in fluorescent response, thus demonstrating that the dye is suitable for the detection of ROS. When PEBBLES, containing DCFDA, were calibrated in the same process there was no resultant fluorescence. As the concentration of O_2^- in the solution increased there was no change in fluorescence above control levels. There are several explanations for the unresponsiveness observed. As ROS are so transient, it is possible that with the polyacrylamide matrix adding an extra barrier between the analyte and probe the dye was unable to interact with the ROS as quickly and subsequently it is possible that the ROS had already been neutralised. A nanosensor described for the detection of the hydroxyl radical (OH^\cdot), was also found to only sense OH^\cdot on the surface of the sensor due to high reactivity (King and Kopelman, 2003). However, it is more likely that the small size of the fluorescent molecules resulted in leaching from within the matrix with the result that most of the dye was lost during ethanol washing stages in the PEBBLE manufacturing process. This was evidenced by the colouration of the ethanol wash effluent. It has previously been found that fluorophores can leach from nanosensors once internalised and form fluorescent artefacts within the cells (Chauhan *et al.*, 2013). It was hypothesised, therefore, that had the nanosensors been washed fewer times some of the dye might have been retained and produced a higher fluorescent signal. The method for PEBBLE manufacture states that the sensor mix should be washed between 7 and 12 times to ensure that all the surfactant is washed away. It was found that fewer than 7 washes left behind surfactant that created a waxy layer to the nanosensors that also caused aggregation and as a consequence was insoluble in PBS and therefore not possible to test.

It is possible to enlarge the size of the DCFDA molecules without altering their reactivity to the analyte of interest. Dextran is a long inert carbohydrate chain structure that can be covalently bound to the DCFDA structure making a physically larger molecule that should not be able to leach from the pores of the polyacrylamide matrix. While some dyes can be purchased already dextran linked, ROS sensing dyes with dextran are not commercially available. Methods have been described for in-house dextran linking and this is something to be considered in the future for developing a ROS nanosensor. This concept has been previously demonstrated by Henderson *et al* in macrophage cells stimulated with PMA. An OH^\cdot nanosensor has

been described, using the fluorophore, coumarin-3-carboxylic acid. The nanosensor was calibrated using the photolysis of H_2O_2 which generates OH^\cdot , this, however, was only a proof of concept study and the cells have not been used in vitro (King and Kopelman, 2003). Similarly, a H_2O_2 nanosensor has also been described, but this utilised the dye DCFDA, so it has questionable specificity (Oh *et al.*, 2012). There is definite potential for development in this area but as of yet, ROS nanosensors have not progressed beyond the development stage and into common practise.

Furthermore, free dye experiments may still be preferential to the use of PEBBLE nanosensors as it is not possible to quantify the concentration of dye within the nanosensor, this made calibration comparisons between PEBBLEs and free dye difficult as an absolute comparison of equivalent dye concentrations is not possible.

Finally, one of the biggest advantages of the PEBBLE nanosensors over free dye based assays is, purportedly, their ability to protect cells from the inherent toxicity of free dyes. However, the data presented here showed that over a 3-hour time period, the blank nanosensors were far more toxic to B-13 and B-13/H cells than the DCFDA free dye counterpart. It is likely that residual surfactant may have resulted in cell membrane damage and ultimately cell lysis. Additionally, this could, in part, be due to bacterial infection of the cells that occurred when introduced to the nanosensors which are not sterile. Autoclaving of the nanosensors was considered but the dye integrity would have been lost at high temperatures. Chauhan *et al.* also found toxicity in *C. elegans* with the use of nanosensors that could only be compensated for by reducing exposure time to the nanosensors (Chauhan *et al.*, 2013).

The use of free dye based assays is not without problems. As a means of comparison to the PEBBLEs, an equivalent ROS detection assay was performed using menadione and free dye to detect ROS in B-13 and B-13/H cells. No response was seen in B-13 cells and only the higher concentrations of menadione elicited a response in the B-13/H cells, however this response was not significantly different to that seen in untreated cells and therefore is itself not a necessarily a reliable technique in its own right.

While there is great potential for the development of a PEBBLE nanosensor for intracellular ROS detection, there are many issues with the development that are still to be addressed to make them a more attractive alternative to free dye based assays. Similarly, with the electrochemistry, a method for continuous stirring of the system and closer proximity of the probe to the cell layer is required before

Chapter 2: Simultaneous Intracellular and Extracellular ROS Detection

meaningful data can be obtained. Unfortunately, the work that was needed to solve these problems was beyond the scope and time frame of this project and as such alternative methods for the detection of drug induced damage were sought.

Subsequent chapters will discuss the use of known hepatotoxins to cause cellular death and damage and assess the role of mitochondria, one of the largest physiological sources of O_2^- in drug damage to B-13 and B-13/H cells.

2.5 References

Banerjee, S., Ghosh, J. and Sil, C.P. (2016) 'Drug Metabolism and Oxidative Stress: Cellular Mechanism and New Therapeutic Insights', *Biochemistry & Analytical Biochemistry*, 5(255).

Buck, S.M., Xu, H., Brasuel, M., Philbert, M.A. and Kopelman, R. (2004) 'Nanoscale probes encapsulated by biologically localized embedding (PEBBLEs) for ion sensing and imaging in live cells', *Talanta*, 63(1), pp. 41-59.

Chauhan, V.M., Orsi, G., Brown, A., Pritchard, D.I. and Aylott, J.W. (2013) 'Mapping the pharyngeal and intestinal pH of *Caenorhabditis elegans* and real-time luminal pH oscillations using extended dynamic range pH-sensitive nanosensors', *ACS Nano*, 7(6), pp. 5577-5587.

Clark, H.A., Kopelman, R., Tjalkens, R. and Philbert, M.A. (1999) 'Optical nanosensors for chemical analysis inside single living cells. 2. Sensors for pH and calcium and the intracellular application of PEBBLE sensors', *Analytical Chemistry*, 71(21), pp. 4837-4843.

Diesen, D.L. and Kuo, P.C. (2010) 'Nitric Oxide and Redox Regulation in the Liver: Part I. General Considerations and Redox Biology in Hepatitis', *Journal of Surgical Research*, 162(1), pp. 95-109.

Dikalov, S.I. and Harrison, D.G. (2014) 'Methods for detection of mitochondrial and cellular reactive oxygen species', *Antioxidants and Redox Signaling*, 20(2), pp. 372-382.

Hamanaka, R.B. and Chandel, N.S. (2010) 'Mitochondrial reactive oxygen species regulate cellular signaling and dictate biological outcomes', *Trends in Biochemical Sciences*, 35(9), pp. 505-513.

Henderson, J.R., Fulton, D.A., McNeil, C.J. and Manning, P. (2009) 'The development and in vitro characterisation of an intracellular nanosensor responsive to reactive oxygen species', *Biosensors and Bioelectronics*, 24(12), pp. 3608-3614.

Holmström, K.M. and Finkel, T. (2014) 'Cellular mechanisms and physiological consequences of redox-dependent signalling', *Nature Reviews Molecular Cell Biology*, 15(6), pp. 411-421.

King, M. and Kopelman, R. (2003) 'Development of a hydroxyl radical ratiometric nanoprobe', *Sensors and Actuators, B: Chemical*, 90(1-3), pp. 76-81.

Klotz, L.O., Hou, X. and Jacob, C. (2014) '1,4-naphthoquinones: From oxidative damage to cellular and inter-cellular signaling', *Molecules*, 19(9), pp. 14902-14918.

- Manning, P. and McNeil, C.J. (2011) 'Electrochemical and optical sensing of reactive oxygen species: Pathway to an integrated intracellular and extracellular measurement platform', *Biochemical Society Transactions*, 39(5), pp. 1288-1292.
- Manning, P., McNeil, C.J., Cooper, J.M. and Hillhouse, E.W. (1998) 'Direct, real-time sensing of free radical production by activated human glioblastoma cells', *Free Radical Biology and Medicine*, 24(7-8), pp. 1304-1309.
- Marek, C.J., Cameron, G.A., Elrick, L.J., Hawksworth, G.M. and Wright, M.C. (2003) 'Generation of hepatocytes expressing functional cytochromes P450 from a pancreatic progenitor cell line in vitro', *Biochemical Journal*, 370(3), pp. 763-769.
- McNeil, C.J., Greenough, K.R., Weeks, P.A., Self, C.H. and Cooper, J.M. (1992) 'Electrochemical sensors for direct reagentless measurement of superoxide production by human neutrophils', *Free Radical Research*, 17(6), pp. 399-406.
- Oh, W.K., Jeong, Y.S., Kim, S. and Jang, J. (2012) 'Fluorescent polymer nanoparticle for selective sensing of intracellular hydrogen peroxide', *ACS Nano*, 6(10), pp. 8516-8524.
- Thannickal, V.J. and Fanburg, B.L. (2000) 'Reactive oxygen species in cell signaling', *American Journal of Physiology - Lung Cellular and Molecular Physiology*, 279(6 23-6), pp. L1005-L1028.
- Woolley, J.F., Stanicka, J. and Cotter, T.G. (2013) 'Recent advances in reactive oxygen species measurement in biological systems', *Trends in Biochemical Sciences*, 38(11), pp. 556-565.
- Yazdani, M. (2015) 'Concerns in the application of fluorescent probes DCDHF-DA, DHR 123 and DHE to measure reactive oxygen species in vitro', *Toxicology in Vitro*, 30(1), pp. 578-582.
- Zangar, R.C., Davydov, D.R. and Verma, S. (2004) 'Mechanisms that regulate production of reactive oxygen species by cytochrome P450', *Toxicology and Applied Pharmacology*, 199(3), pp. 316-331.
- Zhang, M., Søndergaard, R.V., Kumar, E.K.P., Henriksen, J.R., Cui, D., Hammershøj, P., Clausen, M.H. and Andresen, T.L. (2015) 'A hydrogel based nanosensor with an unprecedented broad sensitivity range for pH measurements in cellular compartments', *Analyst*, 140(21), pp. 7246-7253.
- Zielonka, J., Vasquez-Vivar, J. and Kalyanaraman, B. (2008) 'Detection of 2-hydroxyethidium in cellular systems: A unique marker product of superoxide and hydroethidine', *Nature Protocols*, 3(1), pp. 8-21.

Chapter 3: Drug Induced Cytotoxicity and Antioxidant Treatment

3.1 Introduction

3.1.1 *Thiazolidinediones*

As shown in Chapter 2, many challenges still exist with the direct measurement of reactive oxygen species (ROS), including substrate specificity. An alternative technique for the detection of ROS is the addition of antioxidants to measure the quenching of a signal. While not quantitative, it is possible to get an idea of ROS production by a change in response of cells in the presence of an antioxidant. For example, if antioxidants can be used during a resazurin cell viability assay and maintain cell viability in the presence of a toxic drug it is indicative of the drug causing ROS induced damage. In addition to this, as antioxidants can be specific to particular ROS, experiments can be designed to discover which species are causing damage and build a detailed picture of ROS generation. Furthermore, if it is observed that antioxidants can preserve cellular viability this could provide a rationale for a possible preventative treatment options for oxidative cell damage.

Troglitazone is a drug that is part of a wider group of drugs known as the thiazolidinediones (TZDs) which were used in the treatment of type 2 diabetes. The TZDs were first discovered as part of a screen to search for compounds with lipid lowering properties (Sarafidis, 2008). The prototype drug, ciglitazone, was discovered in 1982, but due to a lack of efficacy it never made it into clinical use. Troglitazone was the first TZD to be approved for clinical use in 1997, closely followed by pioglitazone and rosiglitazone. Like ciglitazone, all clinically used TZDs have the same pharmacologically active core, a thiazolidine-2-4-dione structure with the addition of different side chains (figure 3.1). It is the addition of an α -tocopherol side chain that is thought to be a potential cause of the hepatotoxicity that saw the drug withdrawn from the market in 2000 after reports of severe liver injury (Rachek *et al.*, 2009). Rosiglitazone and pioglitazone were adapted from the troglitazone structure by replacement of the α -tocopherol side chain with an aminopyridyl and a pyridine side chain respectively (Sarafidis, 2008). Rosiglitazone stayed on the market longer than troglitazone but was similarly removed in 2010 and the use of pioglitazone has been greatly restricted due to a potential increased risk of bladder cancer (Fröhlich and Wahl, 2015).

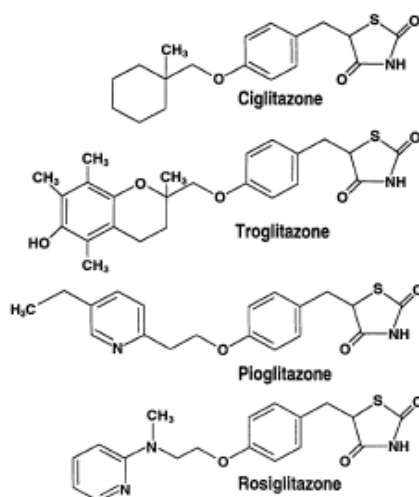


Figure 3.1: The structure of thiazolidinediones (adapted from (Day, 1999))

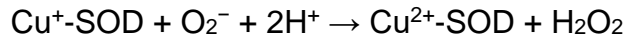
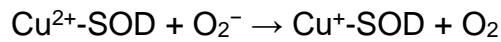
TZDs act through a novel mechanism to reduce insulin resistance. In healthy individuals, insulin acts to suppress glucose production in hepatocytes and stimulates the uptake of glucose instead (Owens, 2002). In type 2 diabetes a state of hyperglycaemia develops due to peripheral insulin resistance in the muscles and the liver, causing pancreatic β cells to compensate and secrete increased levels of glucose (Owens, 2002). This continues until the β cells begin to fail to compensate and insulin deficiency develops, insulin levels fall and fasting levels of glucose increase (Sarafidis, 2008). TZDs act through a novel mechanism to reduce insulin resistance, involving activation of the nuclear receptor, PPAR γ . Troglitazone acts as a ligand at the PPAR γ receptor and binding initiates heterodimer formation with the retinoid X receptor (RXR). The PPAR γ -RXR complex then stimulates the binding of the complex to PPAR γ response elements (PPREs). PPREs are found in numerous genes involved with lipid metabolism, including those involved in fatty acid transport and acetyl co-A synthesis, and is thus able to mimic the action of insulin (Hauner, 2002). A few months after approval there were reports of hepatotoxicity that were associated with liver failure, and even death in some cases. Thus, in 2000, troglitazone was withdrawn from the market. Toxicity of this scale had not been observed in clinical trials. Increased levels of ALT were noted in 1.9% of patients and 0.6% of controls, however, as levels returned to normal, even in those that did not discontinue treatment, it was difficult to attribute these effects of troglitazone toxicity (Sarafidis, 2008). It was later found that of the reported cases of hepatotoxicity 80-90% of those patients ultimately developed acute liver failure (Gitlin *et al.*, 1998).

Interestingly, troglitazone was found to have the lowest affinity for the PPAR γ receptor of the 3 clinically approved TZDs, 10 times lower than pioglitazone which in turn has 10 times lower affinity than rosiglitazone. Since troglitazone was found to be the most hepatotoxic drug in the TZD family this finding suggested that toxicity was not PPAR γ mediated (Hauner, 2002). It has instead been suggested that it is the side chain of troglitazone that mediates the observed hepatotoxicity; a chroman ring containing an α -tocopherol group is attached to the thiazolidone-2-4-dione core which is able to be metabolised to a quinone that is subsequently able to undergo redox cycling (Rachek *et al.*, 2009). The generation of ROS and subsequent oxidative stress is one possible explanation for the toxicity observed with troglitazone. By using specific antioxidants to try and prevent a loss of cellular viability, it would pave the way to a better understanding of the mechanism of troglitazone toxicity. Understanding this mechanism is of great importance because despite troglitazone having being withdrawn from the market, there has recently been a growing interest in repurposing the drug for other clinical uses, particularly as an anti-cancer treatment. The first trial of anti-tumour effects was conducted in 3 liposarcoma patients and it found that troglitazone caused a decrease in proliferation of tumour cells (Fröhlich and Wahl, 2015). Experimentally, troglitazone has also been found to have positive effects in rodent models of colon and oral cancer (Kohno *et al.*, 2001; Yoshida *et al.*, 2003). Therefore, if there is a central role for the production of ROS in troglitazone toxicity, prevention via co-administration of an antioxidant could allow it to be reused in the clinic.

3.1.2 Antioxidants

Antioxidants can broadly be divided into two categories, enzymatic and non-enzymatic; their main function is to inhibit oxidising molecules by neutralising their activity, usually through reduction reactions (Oyewole, 2015). Antioxidants are widely distributed throughout the body, however, they have different localisations and methods of action depending on the nature of the ROS. ROS are not only produced as a toxic by-product of drug metabolism but also during endogenous metabolic reactions. Most antioxidants are located within the cytosol of cells with a small number being specific to the mitochondria.

Superoxide dismutase is an antioxidant that catalyses the near diffusion limited conversion of superoxide into molecular oxygen and hydrogen peroxide (*Equation 3.2*) (Pisoschi and Pop, 2015):



Equation 3.2: The dismutation of O₂⁻ by SOD

It has 3 main isoforms: CuZn SOD (SOD1) which is localised in the cytosol, MnSOD (SOD2) which is localised within the mitochondrial matrix and ECSOD (SOD3) which is found in the extracellular matrix and is the only isoform expressed extracellularly (Pisoschi and Pop, 2015). SOD is one of the most important antioxidants due to the fact that superoxide is produced as a by-product of many biological metabolic reactions. Although there are 3 isoforms, 90% of SOD activity is via SOD1 (Weydert and Cullen, 2010).

The dismutation of superoxide leads to the formation of H₂O₂, which, while not a radical itself, is still classed as a reactive species owing to its ability to form hydroxyl radicals (OH[•]) (*Equation 3.3*). H₂O₂ can diffuse out of the mitochondria where it is produced and into the cytoplasm. In the presence of high iron concentrations H₂O₂ can form OH[•] via Fenton's reaction:



Equation 3.3: Fenton's reaction

OH[•] is the most powerful oxidising agent, however, due to instability at physiological pH, it only reacts at the site of production. This can, however, still cause damage including lipid peroxidation (figure 3.2) (Pisoschi and Pop, 2015). Lipid peroxidation is the process under which oxidants attack the carbon/ carbon double bond of lipids, particularly polyunsaturated fatty acids. Lipid peroxidation is a chain reaction that produces breakdown molecules that contain aldehyde structures which can form DNA adducts and protein molecules and initiate intra and intermolecular cross-linking which can lead to profound alterations in biological function and biochemical properties (Ayala *et al.*, 2014).

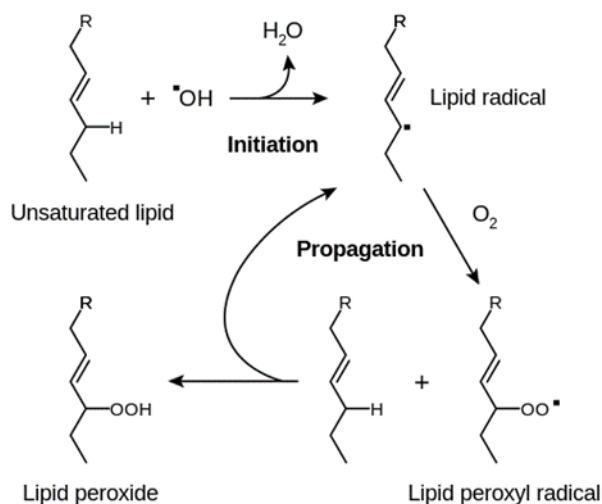
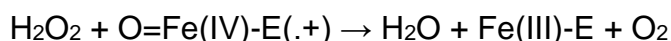
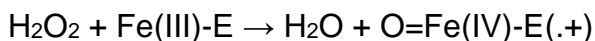


Figure 3.2: Schematic representation of lipid peroxidation (McEneny, 2001).

Catalase is an enzyme antioxidant that detoxifies H_2O_2 , it is found in all major organs of the body, in particular, the liver, kidneys and erythrocytes (Glorieux *et al.*, 2015). Catalase is not found in mitochondria in humans and is confined to the peroxisome. Interestingly, however, a functional catalase located in the mitochondrial cytoplasm of rat cardiomyocytes has been discovered (Radi *et al.*, 1991). Catalase exists as a tetramer of 4 identical monomers that contain heme groups at the active site which are sequentially oxidised and reduced by H_2O_2 yielding H_2O and O_2 (Equation 3.4) (Birben *et al.*, 2012).



Equation 3.4: Action of catalase

Glutathione (GSH) is a non-enzymatic antioxidant that also neutralises H_2O_2 , albeit that it does require the enzyme glutathione peroxidase to function. Due to its highly abundant nature in all cell compartments it is the major soluble antioxidant and the ratio of reduced to oxidised glutathione is often a determinant in the development of oxidative stress. GSH detoxifies H_2O_2 by reducing it to H_2O and O_2 , in the process GSH becomes oxidised to glutathione disulphide which is subsequently returned to its reduced GSH state by GSH reductase and NADPH as an electron donor (Birben *et al.*, 2012).

Co-enzyme Q10 (CoQ10), also known as ubiquinone, is an electron carrier in the mitochondrial respiratory chain but it also has a secondary role in its free enzyme form as a lipid soluble antioxidant (Hargreaves, 2014). CoQ10 is the only lipid

soluble antioxidant that is produced endogenously (Littarru and Tiano, 2007). It has a protective role towards cell membranes. In its reduced form CoQ10 is able to quench carbon centred lipid radicals and lipid peroxyradicals, furthermore CoQ10 is also able to regenerate the antioxidant properties of vitamin E to prevent it from becoming a free radical itself (Pisoschi and Pop, 2015). There is currently a lot of research looking into CoQ10 as a potential therapy for mitochondrial disease due to its lipid soluble properties.

Non-enzymatic antioxidants can also be obtained exogenously from the diet, including vitamin C (ascorbic acid) and vitamin E (α -tocopherol). Vitamin E is hydrophobic, it is found concentrated in the interior area of cell membranes and acts as a key defence against oxidant induced membrane injury. Vitamin E works via the donation of an electron to peroxy radicals, thus stopping a radical chain reaction (Birben *et al.*, 2012). In contrast, vitamin C is water soluble and therefore is restricted to the cellular aqueous phase. Vitamin C is a general antioxidant and is able to quench hydroxyl, alkoxyl and superoxide radicals by forming semihydroascorbic acid which is then subsequently reduced back to ascorbic acid by glutathione (Birben *et al.*, 2012).

Recent antioxidant research has focussed on the development of an antioxidant that can be localised to the mitochondria as this is the main physiological source of ROS production, a lipophilic antioxidant that could be targeted to the mitochondria by crossing the phospholipid bilayer would be able to quench ROS at their site of production before they have a chance to cause cellular damage (Oyewole, 2015). CoQ10, as mentioned, is the only endogenously produced lipophilic antioxidant, much work has been done to develop a similar synthetic analogue that will act in a similar way. This has led to the production of MitoQ, a ubiquinone derivative that is attached to a lipophilic cation in order to make it membrane permeable and able to accumulate in mitochondria. Development has so far been successful and it has already been tested in clinical trials for the treatment of Parkinson's and liver damage (Gane *et al.*, 2010; Snow *et al.*, 2010). Furthermore, there is also research currently underway looking into using existing antioxidants and targeting them directly to the mitochondria. This has shown some success in mice with induced over expression of human catalase (Rehman *et al.*, 2016).

Troglitazone, unlike other TZDs is able to undergo redox cycling due to a quinone structure, however, this quinone structure is part of the α -tocopherol side group

attached to the core glitazone structure and originally designed to have anti-lipidemic effects. This consequently means that troglitazone can also act as an antioxidant in the presence of low level ROS, making the measurement of ROS production quite difficult. It is thought, however, that the antioxidant effects can eventually be exhausted and it is at this point that ROS production can be toxic (Masubuchi *et al.*, 2006)

A resazurin assay is able to assess the ability of mitochondria to metabolise a non-fluorescent dye, resazurin, to a fluorescent product, resorufin. When mitochondria are functional and active, more fluorescence is measured. If mitochondria are no longer functional it is also a reporter of cell health in general and therefore acts as a proxy for measurement of cell viability. The quantity of resorufin produced is proportional to the number of viable cells.

3.1.3 Aims

- To investigate the toxic effect of known hepatotoxins, menadione and troglitazone, on B-13 cells and B-13/H cells.
- To study the differences between pre and post differentiated cells in order to understand whether cells had a hepatic behaviour following DEX treatment.
- To understand whether there was a role for ROS in any cytotoxicity observed by the addition of antioxidants to viability assays and to determine whether antioxidants have a protective effect on cell viability.

3.2 Methods

3.2.1 Materials

Unless otherwise stated all materials were supplied by Sigma Aldrich (Poole, UK).

3.2.2 Cell Culture

B-13 and B-13/H cells were cultured as previously described in section 2.2.2.

3.2.3 Resazurin Cell Viability Assay

B-13 and B-13/H cells were routinely cultured and seeded into 96 wells plates at a seeding density of 1×10^4 cells per well. B-13 cells were incubated overnight to allow for cell attachment whereas B-13/H cells were left for 7 days in DEX media to allow for trans-differentiation. On the day of the experiment, the media was removed and cells were washed with PBS. Media was replaced with unsupplemented DMEM containing a range of concentrations of menadione or troglitazone (1 μ M-500 μ M). Cells were incubated at 37 °C for 3, 6 and 24 hours. Cell viability was measured by adding resazurin (0.03% w/v) to each well. Resorufin, produced as a result of bioreduction of resazurin was measured fluorometrically at excitation 530 nm and emission 590 nm using the Tecan-I plate reader.

3.2.4 Antioxidant Effect on Cell Viability

B-13 and B-13/H cells were seeded into 96 well plates and incubated as previously described. Cells were simultaneously treated with troglitazone at 100 μ M, a concentration known to cause significant cytotoxicity, and then a range of concentrations of antioxidants- CoQ10, SOD or catalase. Cells were then incubated at 37 °C for 3, 6 and 24 hours. Cell viability was measured by adding resazurin (0.03% w/v) to each well. Resorufin, produced as a result of bioreduction of resazurin was measured fluorometrically at excitation 530 nm and emission 590 nm using the Tecan-I plate reader.

3.3 Results

3.3.1 Menadione Cytotoxicity and antioxidant effects in B-13 and B-13/H cells

Menadione is a hepatotoxin, known for being metabolised to quinone that elicits toxic effects through redox cycling. It was found to be mildly toxic to the B-13 cells with a reduction in viability of no more than 20% even at high concentrations. Similarly, there was no time-dependent effect as toxicity did not increase with increased incubation time. Conversely, the B-13/H viable was drastically reduced by menadione. This effect was found to be both concentration and time dependent, as shown in figure 3.3.

There was an acute effect seen with menadione. At a 3-hour time point concentrations as low as 10 μM were shown to decrease viability by 40% and at concentrations of 50 μM and above the viable population dropped to less than half that seen for untreated cells. The longer the cells were incubated with menadione the greater the reduction in viability. At 24 hours, 80% of cells were no longer viable at all concentrations and there was a plateau in response.

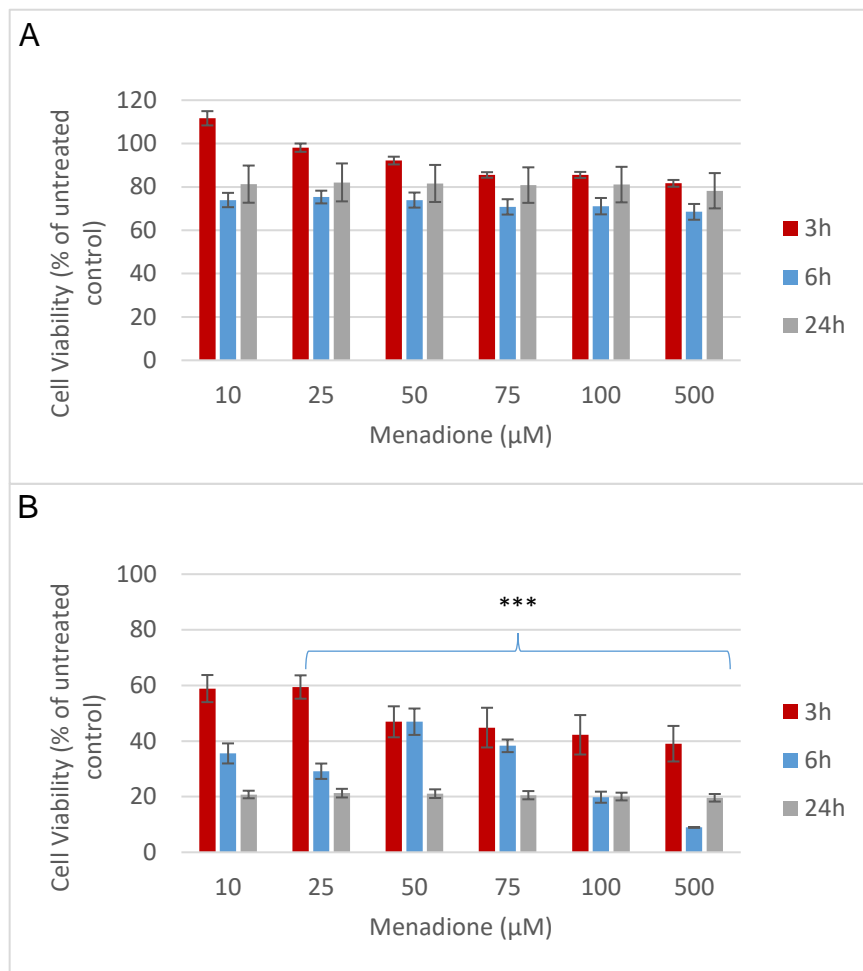


Figure 3.3: (A) B-13 at a 3-hour time point there was a concentration dependent decrease in viability of B-13 cells up to 75 μM, viability plateaued above this at approximately 80%. (B) B-13/H at a 3-hour time point there was a concentration effect of menadione, this was not seen at 6 hours and 24 hours. There was a time effect of menadione. At 6 hours all concentrations of menadione reduced viability to less than 50%. At 24 hours, all concentrations of menadione reduced viability to less than 20%. Data presented as mean of 3 replicates \pm SD, (***) $P < 0.001$.

B-13 and B-13/H cells were subsequently exposed to a co-treatment of menadione plus antioxidant. As shown in figure 3.4, It was found that there was no effect of either catalase or SOD in the B-13 cells. Results seen were equivalent to those obtained from cells treated with menadione only. However, following 7 days' treatment of DEX it was observed that there were differences in the response of the cells following antioxidant treatment. While SOD still showed no discernible effect, Figure 3.5 showed that catalase did cause a concentration dependent increase in cell viability that was significantly greater than viability of cells treated with menadione only at the higher concentrations of 500 U/ml and 1000 U/ml. At the highest concentration of catalase used (1000 U/mL) cellular viability had increased by approximately 25%. Despite initial promising results, this effect was not seen at later time points.

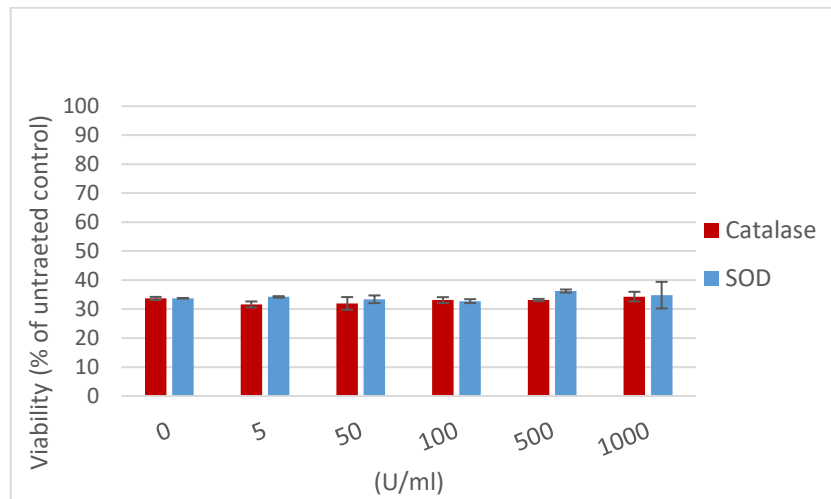


Figure 3.4: Antioxidant effects of catalase and SOD on B-13 cells following 3 hours' exposure to menadione at a concentration of 100 μ M. Without antioxidant treatment, 100 μ M menadione reduced B-13 cells viability to approximately 30%. Treatment with either catalase or SOD did not increase viability above this level. Data presented as mean of 3 replicates \pm SD.

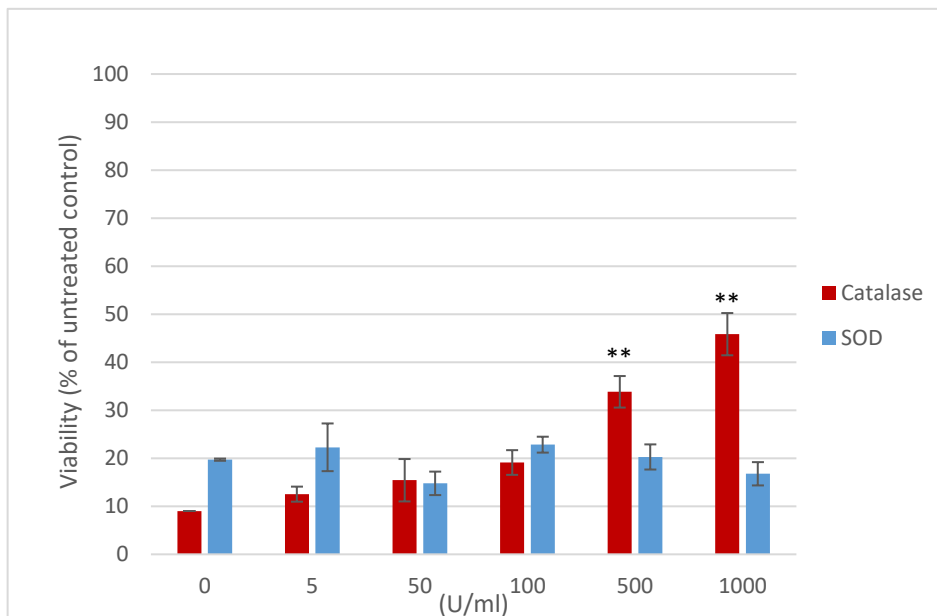


Figure 3.5: Antioxidant effects of catalase and SOD on B-13/H cells following 3 hours' exposure to menadione at a concentration of 100 μ M. The SOD has no significant effect at any concentration on viability. Catalase showed a concentration dependent increase in cell viability, at the higher end of the concentration range (500 U/ml- 1000 U/ml). Viability was significantly greater than control cells which had only been exposed to menadione. Data presented as mean of 3 replicates \pm SD, (** $P < 0.01$)

3.3.2 Troglitazone Cytotoxicity and Antioxidant effects in B-13 and B-13/H cells

Troglitazone is known to cause hepatic injury and while a mechanism of toxicity is yet to be elucidated it is thought that due to a quinone moiety in its structure it could be able to generate ROS which could lead to damaging levels of oxidative stress and subsequent cell death. When the B-13 and B-13/ cells were exposed to a range of

concentrations of troglitazone over a range of time points, it was observed that the toxic effects were much more evident in the B-13/H cells than the B-13 cells.

Interestingly, in the B-13 cells there appeared to be a plateau in cell viability, beyond which toxicity did not worsen. Figure 3.6 showed that at concentrations of $\geq 50 \mu\text{M}$ and ≥ 6 hours there was no further loss in viability below 60%. At a 24-hour time point there was a concentration dependent decrease in cellular viability, all concentrations of troglitazone above $1 \mu\text{M}$ had reduced the viable B-13/H cell population by half.

To see if there was an effect from the stage of differentiation on the response to troglitazone cells were tested at an intermediate stage. Results in figure 3.7 showed that following DEX treatment for 5 days there was a response to troglitazone that was similar to that seen at 7 days but was less pronounced, unlike the B-13 cells there was no plateau in viability. At a 24-hour time point there was a concentration dependent response to troglitazone treatment, as the concentration increased, there was a decrease in viability.

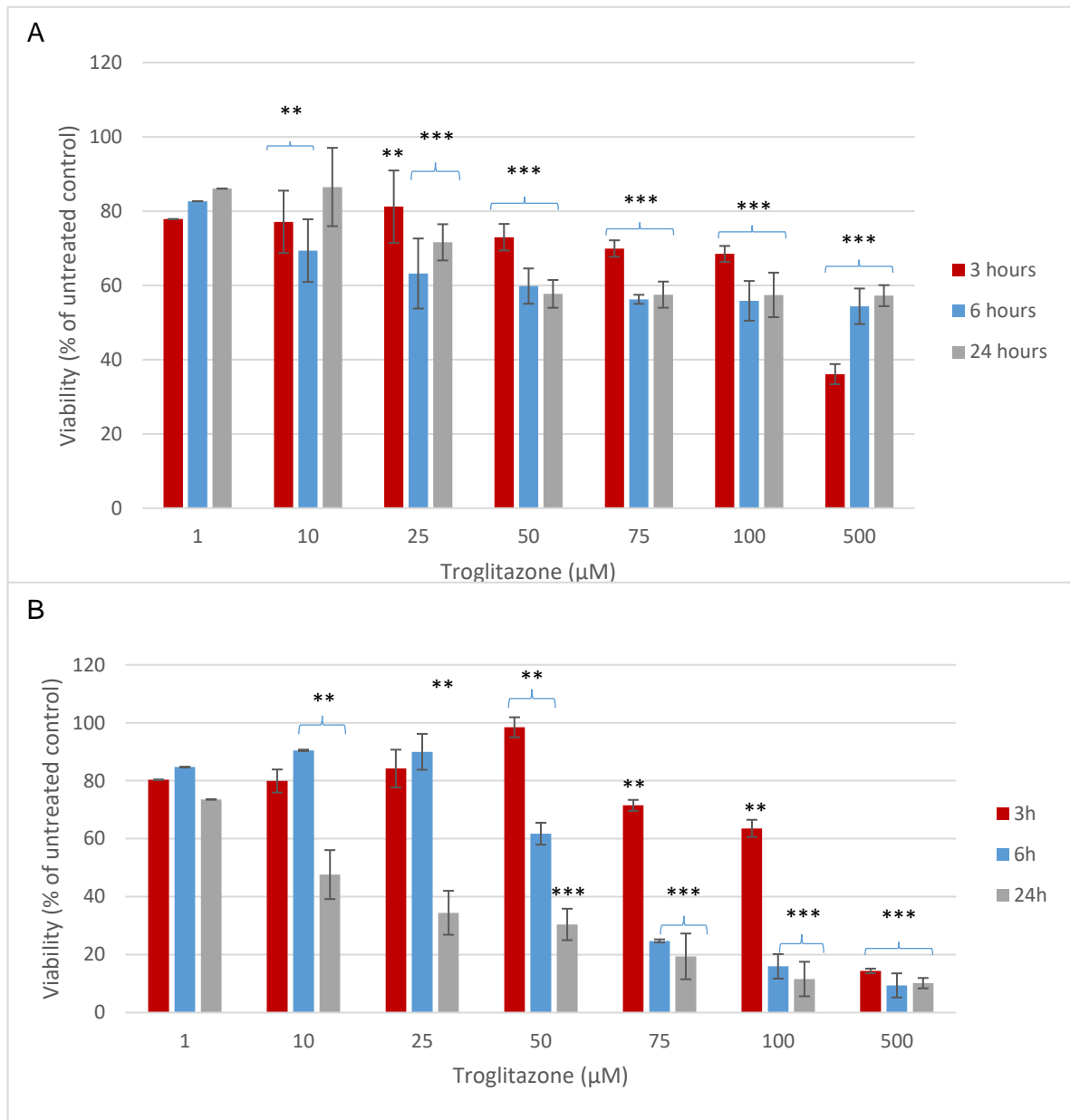


Figure 3.6: (A) Following 3- hours treatment in B-13 cells there was a gradual decline from 80% to 70% viability up to 100 µM, beyond which there was a drop to approximately 40%. At 6 hours and 24 hours a plateau was observed at concentrations ≥ 50 µM. Troglitazone was similarly toxic at 6 hours and 24 hours. (B) B-13/H cells showed an initial plateau in cell viability at 3 hours and 6 hours up to concentrations of 50 µM and 25 µM respectively, beyond which there was a concentration dependent decrease in viability. At 24 hours a concentration dependent decrease in cell viability was seen to a minimum level of approximately 10% of untreated control cells at 500 µM. Data presented as mean of 3 replicates \pm SD, (**P<0.01, ***P<0.001).

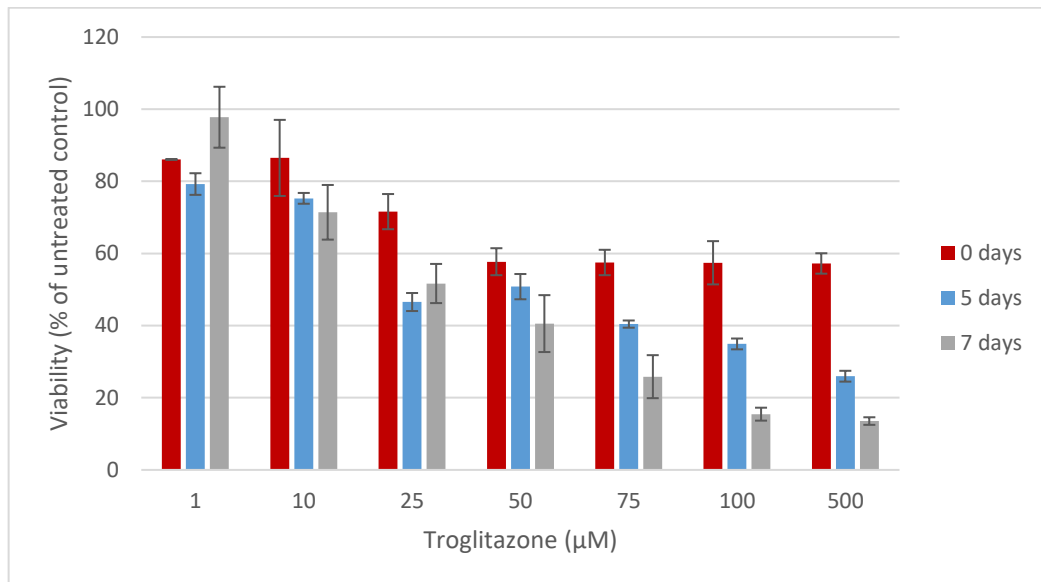


Figure 3.7: The effect of stage of differentiation on susceptibility to troglitazone. Cells were exposed for 24 hours to a range of concentrations of troglitazone at 0, 5 and 7 days transdifferentiation. When the experiment was repeated at an intermediate time point in differentiation there was an intermediate response. At 5 days transdifferentiation, there was a concentration dependent effect of troglitazone on cell viability. The effect was not as pronounced as that seen at 7 days transdifferentiation. Data presented as mean of 3 replicates \pm SD.

Following promising results from co-treatment of catalase with menadione at a 3-hour time point, it was hypothesised that if troglitazone elicited toxicity in a similar way to menadione that catalase might act in a similar way. B-13/H cells were treated with 100 μ M troglitazone and a range of concentrations of catalase. While a small increase in viability was observed, this was not significantly different from cells that had been treated with troglitazone only and catalase was not shown to prevent a loss in viability (figure 3.8).

CoQ10 is a mitochondrial permeable antioxidant that should be able to scavenge ROS close to their site of damage. Figure 3.9 showed what happens when B-13 and B-13/H cells were exposed to a co-treatment of 100 μ M troglitazone and a range of concentration of CoQ10. It was found that levels of viability did not increase above control levels in which no antioxidant was present. There was no difference found between pancreatic B-13 cells and hepatic-like B-13/H cells.

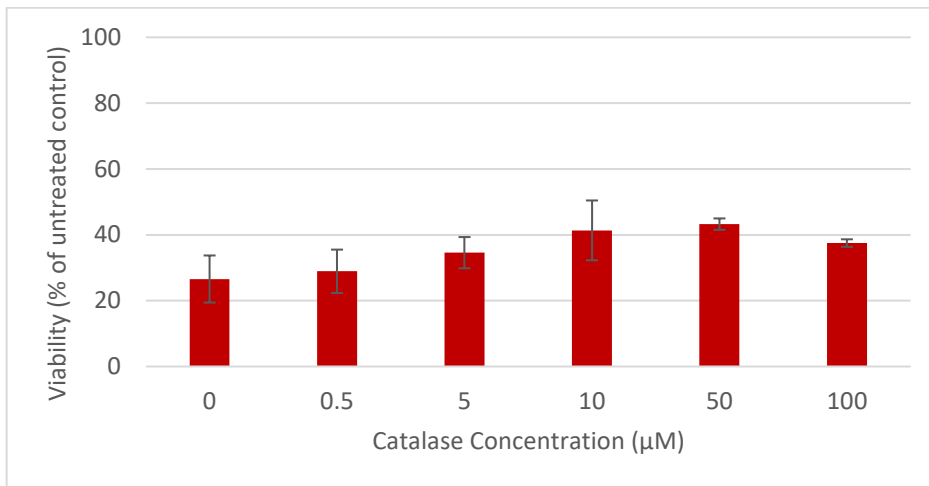


Figure 3.8: Effect of a range of concentrations of catalase on the viability of B-13/H cells following exposure to 100 µM troglitazone. Control cells were treated with troglitazone but not catalase, representing maximal death levels. No response was seen from cells at any concentration of catalase. Data presented as mean of 3 replicates \pm SD.

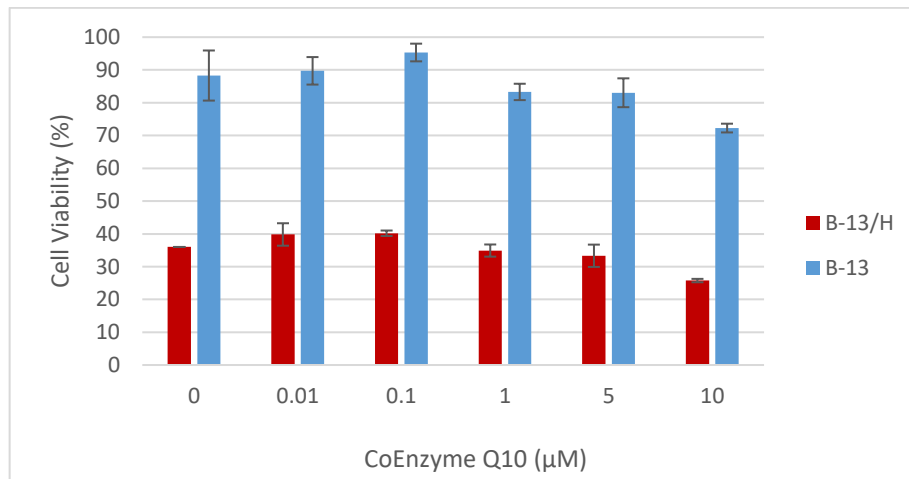


Figure 3.9: Effect of a range of concentrations of Co-enzyme Q10 on the viability of cells following exposure to 100 µM troglitazone. Control cells were treated with troglitazone but not Co-enzyme Q10, representing maximal death levels. No response was seen from either B-13 or B-13/H cells at any concentration of Co-enzyme Q10. Data presented as mean of 3 replicates \pm SD.

3.4 Discussion

Menadione is a known hepatotoxin and has been used as a model for ROS production in hepatocytes for a number of years. Therefore, it was expected that if B-13/H cells had become more hepatic they would be more susceptible to menadione treatment than B-13 cells.

It was shown that menadione was not significantly toxic to B-13 cells at any concentration tested or any duration of time up to 24 hours. Conversely there was a time and concentration dependent effect in the B-13/H cells. As the concentration of menadione increased the viability of cells decreased. Similarly, this effect was more pronounced the longer the cells were exposed to menadione. This shows hepatic behaviour in the B-13/H cells, suggesting a more hepatic phenotype in B-13/H cells than B-13 cells.

Troglitazone showed both time and concentration dependent effects on B-13/H cells. Toxicity was greater the higher the concentration of troglitazone, similarly, concentrations of troglitazone became more toxic as time progressed. This pattern of toxicity was not, however, observed in the B-13 cells. B-13 cells were much more resistant to the toxic effects of troglitazone. The plateau in viability observed in Figure 3.6 was seen up to at least 24 hours suggesting that acute toxicity was better tolerated in B-13 cells than in B-13/H cells. Similar levels of toxicity to those observed in the B-13/H cells have been reported in multiple hepatocyte cell lines including HepaRG, HepG2, primary human hepatocytes (Bova *et al.*, 2005; Rachek *et al.*, 2009; Hu *et al.*, 2015). Testing the cells over longer periods of time would be useful to understand if the plateau remains or if cells eventually become susceptible. B-13/H cells were highly susceptible to the toxic effects of troglitazone, at 3 hours there was not a significant drop in the viable population until the concentration was 75 μM and above, at 6 hours this was 50 μM and above. At 24 hours there was a concentration dependent decrease in the viable population suggesting that any compensatory mechanisms had been overcome by this point. Any concentration of 10 μM and above was significantly toxic at 24 hours. Toxicity in B-13 cells did not drop below 60% whereas, at high concentrations of 100 μM and 500 μM , the viable population of B-13/H cells was almost completely abolished. This indicated that at 7 days transdifferentiation the cells were responding differently to a drug that is a known hepatotoxin, suggesting that cells were more hepatic in nature than pancreatic cells. It has been reported that 10-14 days in DEX media was optimal for

transdifferentiation (Marek *et al.*, 2003; Probert *et al.*, 2014). However, in the experiments described here, when the cells were grown in the confined space of a 96 wells plate, 10 days was too long, even with media changes, as cell health declined. This was probably due to the overgrowth of a small population of undifferentiated cells. Probert *et al.* also reported that conversion was approximately 80%, converted cells do not proliferate, however, the remaining 20% form a subpopulation of cells that maintain their pancreatic phenotype and therefore continue to proliferate.

To further investigate the cell differences, a midpoint in the differentiation process was chosen and cells tested again under identical treatment conditions to see if cells became gradually more hepatic over time or whether there was a determining change over point. It was found that when cells were treated with DEX for 5 days and had subsequent 24 hours troglitazone treatment, the pattern of viability observed matched that in the 7d treated cells but was less pronounced. This suggested that at 5 days' transdifferentiation cells are starting to take on a more hepatic phenotype and that while the process happens gradually cells become more hepatic than pancreatic very quickly after DEX treatment.

It is likely that troglitazone is more toxic to B-13/H cells than B-13 cells because of a change in metabolic profile of the cells following trans-differentiation. Hepatocytes have a repertoire of drug metabolising enzymes that are not found in pancreatic cells. This is because the liver is the main site of drug detoxification and receives blood directly from the gut following ingestion, thus the liver acts as the first line of defence. This subsequently means that hepatocytes are more susceptible to the by-products or reactive intermediates of drug metabolism. While there is much dispute over whether it is troglitazone itself or a metabolite that results in cytotoxicity, the data here suggest that there is a potential role for a combination of effects as some toxicity was observed in B-13 cells with a maximum loss in viable population of 40% at high concentrations. However, the toxicity was much greater in B-13/H cells with the population almost eradicated at higher concentrations. It is therefore possible that there is secondary toxicity in the B-13/H cells caused by a metabolite that is not produced in the B-13 cells. Previous research has suggested that troglitazone sulphate is partially to blame, although this remains controversial (Funk *et al.*, 2001; Hewitt *et al.*, 2002). It is known that troglitazone is also able to be metabolised to a quinone by-product which are known to take part in redox cycling, subsequent ROS production following troglitazone treatment is widely reported (Narayanan *et al.*,

2003; Masubuchi *et al.*, 2006). The evidence supporting quinone metabolite toxicity is confounding as at low levels it can act as an antioxidant. One potential method of determining whether ROS production from troglitazone is toxic is the addition of antioxidants to drug toxicity studies. If viability can be retained in the cell population it would suggest that ROS was a cause of cytotoxicity. Furthermore, by specific tailoring of antioxidants it also becomes possible to suggest the toxic oxidant species as some antioxidants are radical specific. Troglitazone and menadione toxicity was subsequently assessed in the presence of a range of different antioxidants.

It was observed that catalase but not SOD could maintain some cell viability in B-13/H cells treated with menadione. This indicated that that H_2O_2 rather than O_2^- was responsible for subsequent damage in cells. It is possible that endogenous antioxidant SOD dismutated the O_2^- produced more successfully than endogenous antioxidants for H_2O_2 and subsequently, as a by-product of dismutation, H_2O_2 was produced. H_2O_2 , as previously mentioned, can have a whole range of toxic effects, especially when further metabolised to OH^\cdot via the Fenton reaction. There was no effect of catalase or SOD observed in B-13 cells, however, as there was no significant loss in viability with menadione exposure it is unlikely that ROS production is a significant feature of metabolism in B-13 cells. Similarly, no effect on viability was observed in B-13/H cells exposed to troglitazone with subsequent catalase or SOD treatment. It is known that troglitazone can produce ROS and ROS have been identified as one possible cause of hepatotoxicity. However, neither catalase or SOD appeared to retain viability in cells. It is possible that other mechanisms of toxicity are present, reports of mitochondrial damage caused by mitochondrial permeability pore opening and loss of mitochondrial membrane potential are gaining momentum and ROS may be a secondary mechanism of damage (Masubuchi *et al.*, 2006). It would therefore be of interest to extend the period of incubation of both drug and antioxidant in order to establish whether secondary ROS is produced that could be quenched, alternatively, the antioxidants may not have been able to get close enough to the source of ROS to elicit a beneficial effect.

Troglitazone has been reported as causing mitochondrial damage, therefore, a mitochondrial membrane permeable antioxidant, CoQ10 was chosen in order to establish if an antioxidant that was able to enter the mitochondria could help to prevent loss of cell viability. Both B-13 and B-13/H cells treated with troglitazone and CoQ10 did not show any significant changes. Interestingly, mitochondrial targeted

analogues of CoQ10 have been shown to reduce ROS in liver patients subsequently preventing the onset of inflammation induced fibrosis. It is known that in individuals with hepatitis C infection (HCV) there is evidence of the presence of mitochondrial oxidative stress concomitant with an increase in cell death and the development of liver tissue fibrosis. Historically, antioxidant treatment has been largely unsuccessful in the treatment of mitochondrial oxidative stress and this has been attributed to the inability of mitochondria to take up the antioxidants. The development of MitoQ, a ubiquinone analogue with a mitochondrial membrane permeable moiety attached has shown promising results in clinical trials and possibly represents a potential antioxidant therapy in the treatment of HCV. The presence of a lipophilic cation attached to the structure allows for the antioxidant to accumulate several hundred fold in the mitochondria. In clinical trials, doses of 40-80mg a day for 28 days in patients with chronic HCV infection showed improvement in symptoms with reduced necroinflammation reported and decreased ALT and AST levels (Gane *et al.*, 2010). More recently it has been found that in addition to antioxidant properties, MitoQ is also able to attenuate liver fibrosis through the direct inhibition of hepatic stellate cell (HSC) activation. Male C57BL/6J mice treated with carbon tetrachloride to induce liver fibrosis showed decreased necrosis, apoptosis and inflammation. Furthermore, it was reported that there was inhibition of HSC activation and profibrogenic factors such as TGF- β and as such, not only did MitoQ protect against hepatocellular injury there was direct prevention of liver fibrosis, suggesting that there was additional evidence to develop MitoQ for prevention and treatment of liver fibrosis (Rehman *et al.*, 2016). While MitoQ has shown great promise, other methods of treating oxidative stress have also shown promise. Catalase is an endogenously produced antioxidant that successfully scavenges H₂O₂, however, it is not found within mitochondria. Lee et al. found that lean healthy mice with targeted overexpression of the human catalase gene in mitochondria were found to be protected from age induced reduction in mitochondrial function associated with oxidative damage. This suggests that there is potential for targeted antioxidant therapies in the future and it would therefore be of interest to repeat the experiments described here with a mitochondrial targeted antioxidant such as MitoQ in order to establish whether this would improve the viability of cells treated with menadione or troglitazone (Lee *et al.*, 2010).

The data presented here show that there are distinct differences in responses of B-13 and B-13/H cells to known hepatotoxins, menadione and troglitazone. While both drugs are known to be able to initiate redox cycling and generate superoxide, only catalase successfully prevented cell death in B-13/H cells exposed to menadione suggesting that superoxide may have been rapidly dismutated by endogenous antioxidants. Similarly, when exposed to co-treatment of antioxidants and troglitazone, no antioxidant could be seen to maintain cell viability, including mitochondrial permeable CoQ10. This suggested that there may be alternative mechanisms of cell death and ROS may only have a small or secondary role in the cytotoxicity observed.

3.5 References

- Ayala, A., Muñoz, M.F. and Argüelles, S. (2014) 'Lipid peroxidation: Production, metabolism, and signaling mechanisms of malondialdehyde and 4-hydroxy-2-nonenal', *Oxidative Medicine and Cellular Longevity*, 2014.
- Birben, E., Sahiner, U.M., Sackesen, C., Erzurum, S. and Kalayci, O. (2012) 'Oxidative stress and antioxidant defense', *World Allergy Organization Journal*, 5(1), pp. 9-19.
- Bova, M.P., Tam, D., McMahon, G. and Mattson, M.N. (2005) 'Troglitazone induces a rapid drop of mitochondrial membrane potential in liver HepG2 cells', *Toxicology Letters*, 155(1), pp. 41-50.
- Day, C. (1999) 'Thiazolidinediones: A new class of antidiabetic drugs', *Diabetic Medicine*, 16(3), pp. 179-192.
- Fröhlich, E. and Wahl, R. (2015) 'Chemotherapy and chemoprevention by thiazolidinediones', *BioMed Research International*, 2015.
- Funk, C., Ponelle, C., Scheuermann, G. and Pantze, M. (2001) 'Cholestatic potential of troglitazone as a possible factor contributing to troglitazone-induced hepatotoxicity: In vivo and in vitro interaction at the canalicular bile salt export pump (Bsep) in the rat', *Molecular Pharmacology*, 59(3), pp. 627-635.
- Gane, E.J., Weilert, F., Orr, D.W., Keogh, G.F., Gibson, M., Lockhart, M.M., Frampton, C.M., Taylor, K.M., Smith, R.A.J. and Murphy, M.P. (2010) 'The mitochondria-targeted anti-oxidant mitoquinone decreases liver damage in a phase II study of hepatitis C patients', *Liver International*, 30(7), pp. 1019-1026.
- Gitlin, N., Julie, N.L., Spurr, C.L., Lim, K.N. and Juarbe, H.M. (1998) 'Two cases of severe clinical and histologic hepatotoxicity associated with troglitazone', *Annals of Internal Medicine*, 129(1), pp. 36-38.
- Glorieux, C., Zamocky, M., Sandoval, J.M., Verrax, J. and Calderon, P.B. (2015) 'Regulation of catalase expression in healthy and cancerous cells', *Free Radical Biology and Medicine*, 87, pp. 84-97.
- Hargreaves, I.P. (2014) 'Coenzyme Q10 as a therapy for mitochondrial disease', *International Journal of Biochemistry and Cell Biology*, 49(1), pp. 105-111.
- Hauer, H. (2002) 'The mode of action of thiazolidinediones', *Diabetes/Metabolism Research and Reviews*, 18(SUPPL. 2).
- Hewitt, N.J., Lloyd, S., Hayden, M., Butler, R., Sakai, Y., Springer, R., Fackett, A. and Li, A.P. (2002) 'Correlation between troglitazone cytotoxicity and drug metabolic

- enzyme activities in cryopreserved human hepatocytes', *Chemico-Biological Interactions*, 142(1-2), pp. 73-82.
- Hu, D., Wu, C.Q., Li, Z.J., Liu, Y., Fan, X., Wang, Q.J. and Ding, R.G. (2015) 'Characterizing the mechanism of thiazolidinedione-induced hepatotoxicity: An in vitro model in mitochondria', *Toxicology and Applied Pharmacology*, 284(2), pp. 134-141.
- Kohno, H., Yoshitani, S., Takashima, S., Okumura, A., Hosokawa, M., Yamaguchi, N. and Tanaka, T. (2001) 'Troglitazone, a ligand for peroxisome proliferator-activated receptor γ , inhibits chemically-induced aberrant crypt foci in rats', *Japanese Journal of Cancer Research*, 92(4), pp. 396-403.
- Lee, H.Y., Choi, C.S., Birkenfeld, A.L., Alves, T.C., Jornayvaz, F.R., Jurczak, M.J., Zhang, D., Woo, D.K., Shadel, G.S., Ladiges, W., Rabinovitch, P.S., Santos, J.H., Petersen, K.F., Samuel, V.T. and Shulman, G.I. (2010) 'Targeted expression of catalase to mitochondria prevents age-associated reductions in mitochondrial function and insulin resistance', *Cell Metabolism*, 12(6), pp. 668-674.
- Littarru, G.P. and Tiano, L. (2007) 'Bioenergetic and antioxidant properties of coenzyme Q10: Recent developments', *Molecular Biotechnology*, 37(1), pp. 31-37.
- Marek, C.J., Cameron, G.A., Elrick, L.J., Hawksworth, G.M. and Wright, M.C. (2003) 'Generation of hepatocytes expressing functional cytochromes P450 from a pancreatic progenitor cell line in vitro', *Biochemical Journal*, 370(3), pp. 763-769.
- Masubuchi, Y., Kano, S. and Horie, T. (2006) 'Mitochondrial permeability transition as a potential determinant of hepatotoxicity of antidiabetic thiazolidinediones', *Toxicology*, 222(3), pp. 233-239.
- McEneny, J. (2001) 'Lipoprotein Oxidation and Atherosclerosis', *Biochem Soc Trans*, 29, pp. 358-362.
- Narayanan, P.K., Hart, T., Elcock, F., Zhang, C., Hahn, L., McFarland, D., Schwartz, L., Morgan, D.G. and Bugelski, P. (2003) 'Troglitazone-Induced Intracellular Oxidative Stress in Rat Hepatoma Cells: A Flow Cytometric Assessment', *Cytometry Part A*, 52(1), pp. 28-35.
- Owens, D.R. (2002) 'Thiazolidinediones: A pharmacological overview', *Clinical Drug Investigation*, 22(8), pp. 485-505.
- Oyewole (2015) 'Mitochondrial-targeted antioxidants', *the FASEB Journal*, 29(), pp. 1-6.
- Pisoschi, A.M. and Pop, A. (2015) 'The role of antioxidants in the chemistry of oxidative stress: A review', *European Journal of Medicinal Chemistry*, 97, pp. 55-74.

- Probert, P.M.E., Chung, G.W., Cockell, S.J., Agius, L., Mosesso, P., White, S.A., Oakley, F., Brown, C.D.A. and Wright, M.C. (2014) 'Utility of B-13 progenitor-derived hepatocytes in hepatotoxicity and genotoxicity studies', *Toxicological Sciences*, 137(2), pp. 350-370.
- Rachek, L.I., Yuzefovych, L.V., LeDoux, S.P., Julie, N.L. and Wilson, G.L. (2009) 'Troglitazone, but not rosiglitazone, damages mitochondrial DNA and induces mitochondrial dysfunction and cell death in human hepatocytes', *Toxicology and Applied Pharmacology*, 240(3), pp. 348-354.
- Radi, R., Turrens, J.F., Chang, L.Y., Bush, K.M., Crapo, J.D. and Freeman, B.A. (1991) 'Detection of catalase in rat heart mitochondria', *Journal of Biological Chemistry*, 266(32), pp. 22028-22034.
- Rehman, H., Liu, Q., Krishnasamy, Y., Shi, Z., Ramshesh, V.K., Haque, K., Schnellmann, R.G., Murphy, M.P., Lemasters, J.J., Rockey, D.C. and Zhong, Z. (2016) 'The mitochondria-targeted antioxidant MitoQ attenuates liver fibrosis in mice', *International Journal of Physiology, Pathophysiology and Pharmacology*, 8(1), pp. 14-27.
- Sarafidis, P.A. (2008) 'Thiazolidinedione derivatives in diabetes and cardiovascular disease: An update', *Fundamental and Clinical Pharmacology*, 22(3), pp. 247-264.
- Snow, B.J., Rolfe, F.L., Lockhart, M.M., Frampton, C.M., O'Sullivan, J.D., Fung, V., Smith, R.A.J., Murphy, M.P. and Taylor, K.M. (2010) 'A double-blind, placebo-controlled study to assess the mitochondria-targeted antioxidant MitoQ as a disease-modifying therapy in Parkinson's disease', *Movement Disorders*, 25(11), pp. 1670-1674.
- Weydert, C.J. and Cullen, J.J. (2010) 'Measurement of superoxide dismutase, catalase and glutathione peroxidase in cultured cells and tissue', *Nature Protocols*, 5(1), pp. 51-66.
- Yoshida, K., Hirose, Y., Tanaka, T., Yamada, Y., Kuno, T., Kohno, H., Katayama, M., Qiao, Z., Sakata, K., Sugie, S., Shibata, T. and Mori, H. (2003) 'Inhibitory effects of troglitazone, a peroxisome proliferator-activated receptor γ ligand, in rat tongue carcinogenesis initiated with 4-nitroquinoline 1-oxide', *Cancer Science*, 94(4), pp. 365-371.

**Chapter 4: Extracellular Flux Analysis to Determine Differences in
the Metabolic Profile of B-13 and B-13/H Cells**

4.1 Mitochondrial Role in DILI

Mitochondrial DILI is more frequently becoming associated with the aetiology of drug toxicity. However, it has not historically been investigated during pre-clinical studies as it can often be difficult to detect. The sheer number of mitochondria within cells means that they can usually compensate for low level damage. Despite this, in recent years, the focus of pre-clinical testing of NCEs has shifted so that toxicity is discovered earlier in the process and mitochondria are of increasing interest.

The predominant role of mitochondria within cells is to produce energy, in response to demand, in the form of ATP. Mitochondrial function has been studied in other research contexts for many years and there are many available *in vitro* investigations that could be harnessed to detect mitochondrial DILI in a pre-clinical setting, including, but not limited to: oxygen consumption rates during mitochondrial respiration, ETC complex activity, mitochondrial transmembrane potential, measurement of lactic acid levels and assessment of mtDNA integrity. Many drugs have multiple toxicities due to varied mechanisms of damage, furthermore, and particularly in hepatocytes, metabolites of parent compounds may also elicit their own toxicities. Damage to mitochondria is often silent until the number of mitochondria affected reaches a threshold, beyond which damage can manifest itself in a variety of ways. Moderate impairment to respiration can cause cell dysfunction but severe damage can lead to cell necrosis and potentially fibrosis.

4.1.1 Consequences of Mitochondrial Impairment

β -oxidation is the process by which fatty acid molecules are broken down in order to generate acetyl CoA for the Krebs cycle. When this is inhibited, fatty acids can accumulate and become esterified into triglycerides which can accumulate and lead to steatosis. Drugs can either directly inhibit β -oxidation via interaction with FAO enzymes or indirectly (as discussed previously in chapter 1, section 1.7.3) by inhibiting β -oxidation through impairing the ETC.

Ibuprofen is an example of a drug able to directly interact with the enzymes of fatty acid oxidation to elicit toxic damage. By sequestering Co enzyme A in the form of thioester, it becomes unavailable for the formation of fatty Acyl-CoA within the mitochondria (Begrache *et al.*, 2011; Pessayre *et al.*, 2012). Acyl-CoA is crucial in the Krebs cycle for the generation of reduced carrier molecules that transport hydrogen ions to the ETC. Therefore, as a result of blocking fatty acid oxidation, ATP synthesis will decrease which, again, leads to secondary inhibition of fatty acid oxidation and so

a vicious cycle of damage begins. Troglitazone has also been shown to inhibit acyl-CoA synthase, preventing the formation of long chain acyl-CoA (Begrache *et al.*, 2011).

Severe inhibition of mitochondrial β -oxidation causes an increase in the free fatty acids in the cytoplasm. If the fatty acids cannot be sufficiently oxidised they become esterified into triglycerides. The accumulation of triglycerides can form fatty deposits within cells in a process known as steatosis. If hepatotoxicity is acute and severe, microsteatosis occurs, where lipid deposits in the form of small vesicles accumulate in hepatocytes. The lesion is associated with subsequent liver failure. Conversely when the drug toxicity is sustained over a period of time, large fat vacuoles form within hepatocytes and this is known as macrosteatosis (Pessayre *et al.*, 2012). Macrosteatosis is usually a benign lesion in the short term although there are longer term consequences of having these fatty cell deposits. As a result of ATP shortage within the cell there is reduced gluconeogenesis which can lead to hypoglycaemia (Begrache *et al.*, 2011). Furthermore, hampered energy production within a cell can trigger hepatic cytolysis- large scale cell death in the form of necrosis or apoptosis depending on the severity of ATP depletion (Labbe *et al.*, 2008). Apoptotic cells are usually removed via macrophage-based phagocytosis. However, when apoptosis is sustained over a long period of time, inflammatory cells can be recruited to the site which are able to generate ROS and initiate secondary necrosis within cells. Prolonged presence of inflammatory cells can have the knock-on effect of producing a state of cytolytic hepatitis which in its mildest initial stages can result in raised levels of liver specific enzymes such as ALT and AST. In more severe cases it can develop towards liver failure at which point liver transplant may be the only treatment option (Begrache *et al.*, 2011).

Another manifestation of damaged mitochondrial function is the presence of lactate. If the ETC is damaged and the flow of electrons is impeded, it can lead to an accumulation of electrons upstream in the chain. As previously mentioned in chapter 1, section 1.7.2, this can induce a state of oxidative stress due to O_2^- production from the damaged chain which can then lead to the formation of lesions in mtDNA due to oxidative damage. However, there is also a secondary result of blocked electron flow; a switch in production of energy from oxidative phosphorylation to glycolysis. Reduction in electron flow decreases the level of re-oxidation of the electron carrier NADH into NAD^+ . Under normal, aerobic conditions pyruvate is

oxidised to acetyl co A for the Krebs's cycle using NAD^+ and generating NADH.

NADH is then shuttled through the mitochondrial membrane in order to keep levels low, within the mitochondrial membrane it is able to donate electrons to oxidative phosphorylation (Phypers and Pierce, 2006). In a situation of mitochondrial damage NADH remains reduced and therefore due to a high NADH/ NAD^+ ratio, the oxidation of pyruvate by pyruvate dehydrogenase decreases and instead becomes reduced to lactate, the accumulation which can lead to lactic acidosis (Pessayre *et al.*, 2012).

In a state of overdose, paracetamol has been linked to the formation of lactic acidosis; hyperlactaemia is caused by inhibition of oxidative phosphorylation switching the primary energy production pathway to glycolysis and the reduction of pyruvate to lactate (Adeva-Andany *et al.*, 2014). Similarly, the anti-diabetic, phenofornin, was found to induce lactic acidosis due to its ability to cross the mitochondrial membrane and inhibit oxidative metabolism. It was subsequently removed from the market and replaced with metformin, which, due to a low affinity for the mitochondrial membrane cannot cause lactic acidosis despite being capable of inhibiting gluconeogenesis and oxidative phosphorylation (Dykens *et al.*, 2008; Adeva-Andany *et al.*, 2014). Interestingly, there have been numerous clinical cases of patients receiving metformin treatment that have developed lactic acidosis Despite this, however, no causative relationship has been proved (Adeva-Andany *et al.*, 2014).

4.1.2 Current Technologies for Measuring Mitochondrial Respiration

Prediciting the toxicity of a new chemical entitiy (NCE) is a difficult process when all of the complex interactions a drug and its metabolite can have within a cell are considered. In order to investigate mitochondrial liabilities earlier in the development stage and provide meaningful predictive toxicity results, a simple high throughput early stage screen is required (Nadanaciva *et al.*, 2007). The predominant function of mitochondria is the generation of energy from oxidative phosphorylation, and the oxygen consumed by mitochondria can be a useful method for determining dysfuction. Deviations of oxygen consumption away from the norm are indicative of altered metabolism (Dmitriev and Papkovsky, 2012). For over 50 years the main method of assessing mitochondrial respiratory function has been the use of an oxygen sensing Clark electrode. However, with renewed interest in mitochondrial dysfuction with relation to drug development there has been active development over recent years for more sophisticated methods for oxygen measurement.

The Clark electrode, developed by Leland Clark 1953 is the current go-to technique for oxygen sensing (Clark Jr *et al.*, 1953). Working on the basis of amperometry principles, a platinum electrode is covered with an oxygen permeable membrane that, upon applying a voltage, electrochemically reduces oxygen at its surface. The resulting current is proportional to the concentration of oxygen present in the solution (Wolfbeis, 2015). The electrode is placed in a sealed chamber into which a mitochondrial preparation is added through an injection port. Once a steady baseline has been obtained substrates can be added to the chamber and their subsequent effects on respiration can be measured. ADP is generally the first substrate to be added in order to stimulate ATP synthase and accelerate electron transport through the chain and drive ATP production. Following stimulation of respiration, the ATP synthase inhibitor, Oligomycin, can be added to terminate respiration by blocking the re-entry of H⁺ ions which stops production of ATP and slows the passage of electrons through the ETC (Brand and Nicholls, 2011). If there is any residual oxygen consumption, either due to dysfunctional uncoupled ATP synthases or detoxification enzymes requiring oxygen. Complete shut-down of respiration can be achieved by the addition of a combination of electron complex inhibitors which totally shut down any electron transport, usually antimycin A and rotenone. To maximally stimulate mitochondria Carbonyl cyanide-4-(trifluoromethoxy)phenylhydrazone (FCCP) is injected into the mix, FCCP acts to uncouple ATP synthase and maximally drive H⁺ ions through the membrane without the production of ATP (Brand and Nicholls, 2011).

The Clark electrode is a robust and simple method for the determination of mitochondrial function, hence its continued use for over 50 years. Methods have become well established over the years and the Clark electrode is one of the most reliable ways of measuring mitochondrial respiration. Despite this, the Clark electrode would not be suitable for screening for drug toxicity in a high-throughput format due to the short life span of the electrode and, more importantly, the implications of using mitochondrial fraction as a sample (Brand and Nicholls, 2011; Zhang *et al.*, 2012). When not using whole cell samples there is the confounding issue of not having cellular context, while it means that mechanistic studies can be easier as there is no interference from cytosolic factors, without surrounding interaction with other cellular signals and enzymes, a true response might not always be achieved. Furthermore, the isolation process can damage some mitochondria so

that it is possible that some are already dysfunctional before exposure to drug treatment. Using a cell fraction also means that the sample size must be much larger making the use of a Clark electrode impractical for high throughput screening (Zhang *et al.*, 2012).

An accepted alternative to the Clark electrode is the use of optical sensors for oxygen detection. Optical sensors utilise luminescence quenching of a reporter dye to generate a signal that is proportional to the concentration of oxygen present in the sample (Wolfbeis, 2015). Reporter dyes are usually metal-ligand complexes such as phosphorescent Pt (II) and Pd (II) that, upon collisional interaction with oxygen molecules, lose energy and enter a lower excited state. In a lower excited state, the luminophore is deactivated and luminescence intensity decreases. The shorter lifetime the dye has the faster the signal acquisition can be (Dmitriev and Papkovsky, 2012).

While the Clark electrode is better at detecting high levels of oxygen within a sample, the flexibility in design of optical electrodes mean that they can be adapted to detect very small concentrations of oxygen as well as higher levels. In addition to this, by combining different types of sensors, multiple parameters can be sensed at the same time, such as oxygen level and pH. Optical oxygen sensors can therefore provide a wealth of information about mitochondrial respiration. However, the strengths of optical probes also cause weaknesses in the technique; sensor membranes are highly soluble for oxygen and will therefore extract oxygen from the sample being tested. This means that in low oxygen levels or small sample volumes erroneous results may be generated. In addition to this, when using metaloporphyrins, there is the opportunity for artefacts to be generated under conditions of strong photoexcitation (Wolfbeis, 2015).

A development of the optical sensor is the introduction of the oxygen nanosensor. While still very much being developed, a nanosensor for oxygen detection would allow for real time and direct sensing of oxygen within cells. Nanosensors work on the same basis of the optical probes mentioned previously, an indicator probe in a polymer host, the difference being that it is nanoscale. The small size of nanosensors enables non-invasive quantitative measures to be taken within living cells. While this technique uses whole cells and so is more physiologically relevant there are still issues to improve sensitivity as the polymer coating of nanosensors can reduce the signal from the probes (Wolfbeis, 2015).

Regarding predictive toxicology, high throughput screening is essential to be able to assess a large number of compounds in a short space of time and key to aligning toxicity studies with early development studies. There is currently only one technique that has the potential to become a mainstream measure of bioenergetic function- Seahorse extracellular flux analysis (Salabei *et al.*, 2014).

Like other techniques, oxygen sensing is based on the quenching of a probe, in this case an oxygen sensitive fluorophore. The probes are embedded within a polymer and attached to a sensor cartridge, such that when the cartridge is placed on top of the cell culture plate (in either a 24 well or 96 well format) each well has its own sensor (Zhang *et al.*, 2012). Cells are grown in a multi-well plate to which they attach in a monolayer on the bottom. The sensors are brought within 200µm of a cell monolayer to form a transient micro-chamber from which immediate measures can be taken. Fibre optic bundles within the instrument emit light to excite the fluorophore at which point, any oxygen in the sample can quench the fluorescence at a rate proportional to the concentration of oxygen present (Figure 4.1). The pistons within the machine that form the micro-chamber, work reversibly, so that they can be raised to allow the surrounding media to re-equilibrate the system, making it possible to take multiple measures (Ferrick *et al.*, 2008). Within the sensor cartridge there are 4 injection ports for each well, this allows for the sequential addition of 4 different compounds throughout the experiment and real time measures of the oxygen consumption.

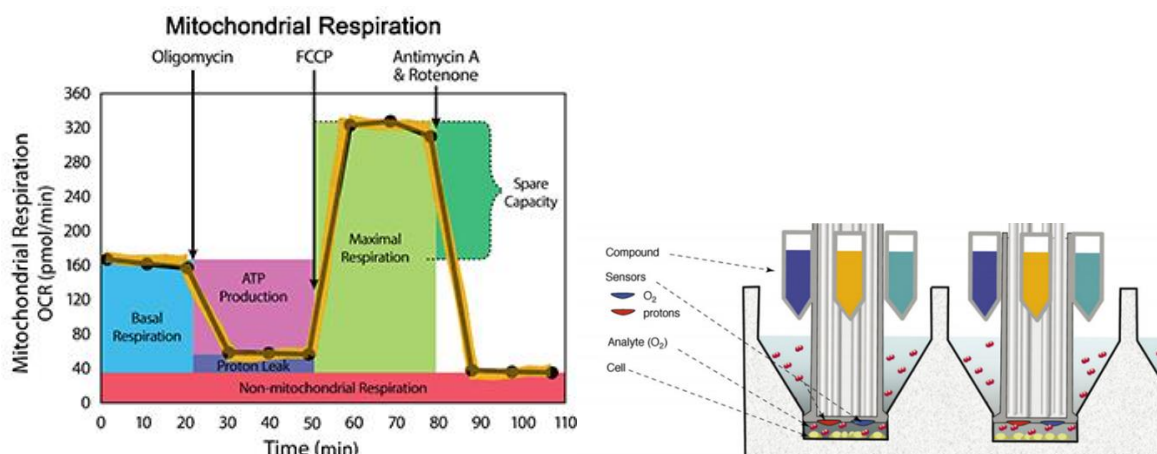


Figure 4.1: The parameters of mitochondrial respiration that can be assessed using a mitochondrial stress test and illustration of a XF microplate and sensor cartridge as depicted by (Ferrick *et al.*, 2008)

The ability to make additions throughout the experiment is perhaps the biggest advantage over the traditional Clark electrode as it allows for multiple parameters of

respiration to be measured in one experiment. Furthermore, in the 96 well format, there is the ability for multiple replicates and multiple experimental conditions allowing for a huge amount of data to be produced in a short space of time. Additionally, with regards to toxicity testing, it also allows for the specific location of mitochondrial dysfunction to be determined (Brand and Nicholls, 2011). Further, measures are taken in whole cells and due to the microplate format, fewer cells than a Clark electrode set up can be used. This does however, present the issue that if the cells are not grown in a uniform monolayer, that measures can be prone to error and lack reproducibility, this is more likely the smaller the area being measured, so in a 96 well format, often more replicates are required than a 24 well format in order to locate erroneous results (Zhang *et al.*, 2012).

Using carefully titrated drugs with known effects on the ETC and oxidative phosphorylation, it is possible to determine particular parameters about mitochondrial function as seen in figure 4.1:

- Basal Respiration: The level of basal oxygen consumption is strongly linked to the demand a cell has for ATP and can therefore change dramatically depending on drugs present in the media.
- Maximal Respiration Rate: reports the maximum activity of electron transport and can be stimulated by uncoupling H⁺ ion transport, allowing it to bypass ATP synthase.
- Spare Capacity: indicates how closely a cell is operating to its energetic limit.
- ATP Turnover: Although not measured directly, the rate in ATP synthesis can be estimated from changes in oxygen consumption following the addition of Oligomycin which inhibits ATP synthase and shifts the entire production of ATP to glycolysis (Brand and Nicholls, 2011).
- Proton Leak: an increase in leak is indicative of mitochondrial damage (Brookes, 2005)

4.1.3 Aims

The aim of this study was to use extracellular flux analysis to investigate potential metabolic differences between B13 and B-13/H. Troglitazone, a known hepatotoxin, was utilised to determine whether there were any mitochondrial liabilities from its use in hepatocyte like B-13/H cells and if so, how do these effects differ to those seen

Chapter 4: Metabolic Differences Between B-13 and B-13/H Cells
prior to differentiation in B-13 cells. Information from extracellular flux analysis was supplemented by complimentary data from ATP and lactate assays.

4.2 Methods

4.2.1 Materials

Assay media and calibrant media were supplied by Seahorse Bioscience (Massachusetts, USA). All other reagents were supplied by Sigma Aldrich (Poole, UK) unless otherwise stated.

4.2.2 Cell Culture

B-13 cells were a gift from Prof. Matthew Wright (Newcastle University). Cells were routinely cultured in low glucose (1000 mg/l) DMEM which was supplemented with 10% FBS, 500 U/ml penicillin and streptomycin, 2 mM L-Glutamine and 1% amphotericin B. Cells were incubated at 37°C in 95% air and 5% CO₂. The medium was changed every 2-3 days.

When cells reached 70-90% confluence, the cells were passaged. The medium was removed from the flask and the cell layer was washed once with pre-warmed PBS to remove traces of media. As cells were adherent, 2 ml of 10x trypsin in EDTA was added to the flask. The flask was gently tilted back and forth and then tapped gently to encourage the detachment of the cell layer from the surface. 8 ml of culture medium was then added to the flask to inhibit the action of the trypsin and the full 10 ml was then transferred to a 15ml falcon tube which was then centrifuged at 2000 rpm for 5 minutes. Supernatant was subsequently removed and the cell pellet was re-suspended in fresh medium for counting using a haemocytometer. Finally, cells were seeded as required, either into a fresh t75 culture flask for maintenance of the stock or for a specific experiment.

For B-13/H cells, B-13 cells were routinely cultured before being seeded at the relevant density into the relevant experimental plate in media containing 10 nM dexamethasone made from a serial dilution of a 100 µM stock in ethanol.

4.2.3 Seahorse Extracellular Flux Optimisation

Cells differ in their growth rates, energy demand and tolerance to stress. Therefore, it is crucial to the success of the experiment that an optimisation experiment is performed prior to undertaking any work. Extracellular flux (XF) assays were optimised for cell seeding density and concentration of injected compounds for a mitochondrial stress test, namely, Oligomycin, FCCP, antimycin A and rotenone. Typically, a working concentration of a drug was optimal when it stimulated the maximal response expected without exhibiting toxicity in its own right. Initially

seeding densities of 5×10^3 and 1×10^4 cells per well were chosen. Oligomycin concentrations of $1 \mu\text{M}$ and $2 \mu\text{M}$ were tested, FCCP concentrations of $0.5 \mu\text{M}$ and $1 \mu\text{M}$ and an excess of rotenone and antimycin A, both at $0.5 \mu\text{M}$. The rest of the mitochondrial stress test was performed as described in Section 4.2.4.

4.2.4 Mitochondrial Stress Test

A mitochondrial stress test was used to assess differences in the mitochondrial responses to troglitazone shown by B-13 and B-13/H cells. Cells were seeded into Seahorse XF 96 cell micro-culture plates at 1×10^4 cells per well for B-13 cells and 5×10^3 cells per well for B-13/H cells as per the results of the optimisation test described in section 4.2.3. Seeding densities often differ between cell types depending upon how metabolically active they are. To account for differences in cell number all results are normalised for protein content (section 4.2.5) to allow for direct comparisons to be made between cell lines. Plates were left to settle for 1 hour before incubating at 37°C overnight for B-13 cells and for 7 days in DEX media for B-13/H cells. 24 hours before testing, a range of troglitazone concentrations were made up at 10x concentration in DMEM before being diluted 1 in 10 in cell containing wells for final concentrations between $0.5 \mu\text{M}$ and $100 \mu\text{M}$. The 4 corner wells were left cell free to be used as control wells. In addition to this a sensor cartridge was hydrated overnight in $200 \mu\text{l}$ / well in Seahorse calibrant at 37°C in a non CO_2 incubator.

Assay media was made fresh on the day of the experiment; Seahorse assay media was supplemented with 10 mM glucose, 1 mM pyruvate and 2 mM L-glutamine. The media was warmed to 37°C and the pH was adjusted to pH7.4. The warmed media was then used to wash the cells twice, before being placed in a non- CO_2 incubator at 37°C for 1 hour. While the cells were in the incubator, mitochondrial stress test compounds were prepared at 100x concentration in assay media for addition to injection ports on the sensor cartridge. $25 \mu\text{l}$ of each compound was added to the injection ports of the microplate sensor cartridge for a final concentration of $1 \mu\text{M}$ oligomycin, $1 \mu\text{M}$ FCCP, $0.5 \mu\text{M}$ antimycin A and rotenone combined in ports A, B and C respectively. Port D was loaded with $25 \mu\text{l}$ of experimental media. The loaded sensor cartridge was then placed in the XF analyser for calibration of oxygen and pH levels. Following calibration, the cells were removed from the incubator and placed in the analyser. Baseline measures of oxygen consumption are determined prior to injections. Each measure that the analyser makes consists of a 3-minute mix time

and a 4-minute read cycle. The mitochondrial stress test was then performed by sequential addition of oligomycin from port A, FCCP from port B, antimycin A and rotenone in port C and media in port D. Three measures of oxygen consumption were taken for each injection.

4.2.5 Normalisation for Protein Content

Wells were normalised for protein content so that results across plates and cell types could be compared. Following the assay, the plate was removed from the analyser and all media was removed from all wells. Complete M lysis buffer (20 µl) was added to each well, cells were then scraped from the surface and placed on ice. A working reagent at a 50:1 ratio was made of bicinchoninic acid and 4% cupric sulphate. 200 µl of the working reagent was added to each well. The full contents of each well was transferred to a clean 96 well, black walled plate with clear bottom. The plate was covered and incubated for 30 minutes at 37°C.

A standard curve was prepared alongside the unknowns. A serial dilution of a 2 mg/ml Bovine Serum Albumin (BSA) was made to produce samples between 0.02 mg/ml and 2 mg/ml. 20 µl of each standard was added in triplicate to a black walled, clear bottom plate and 200 µl of working reagent was added. The plate was incubated at 37°C for 30 minutes.

Plates were read on a Tecan Infinite M200 spectrophotometer (Tecan, Austria) at an absorbance of 562 nm.

4.2.6 ATP Quantification

Intracellular ATP was measured using an ATP content assay (Abcam, Cambridge). Cells were seeded at 1×10^4 cells per well in black walled, clear bottom 96 well plate. B-13 cells were left over-night to attach and B-13/ H cells were left for 7 days in DEX media to transdifferentiate (media changes every 2-3 days). On the day of the experiment troglitazone was added to cells at concentrations between 0 µM and 100 µM. First, cells were washed with PBS before addition of 90 µl unsupplemented experimental media to each well. Troglitazone concentrations were made at 10x concentration and 10 µl was then added to wells. Measures were performed in triplicate. Cells were incubated for 1 hour at 37 °C 5% CO₂. The rest of the assay was performed as described in the manufacturer's instructions. Briefly, 50 µl of detergent was added to each well to lyse cells and stabilise ATP and the plate was shaken on an orbital shaker for 5 minutes. 50 µl of luciferin substrate was added to

each and the plate was shaken again for 5 minutes before a final dark adaptation for 10 minutes. Luminescence was then read using a Tecan Infinite M200 plate reader. The assay is based on the production of light which caused the reaction of ATP with luciferase and D- luciferin. The emitted light is proportional to ATP concentration.

4.2.7 Lactate Quantification

Cells were seeded at 1×10^4 cells per well in 96 well, black walled, clear bottom plates. B-13 cells were left to attach overnight and B-13/H cells were treated for 7 days with DEX media (media changes every 2-3 days). Following attachment or transdifferentiation the media in the wells was replaced with un-supplemented experimental media and cells were treated with a range of concentrations of troglitazone (0 μ M- 100 μ M) for 24 hours. The rest of the assay was performed as per the manufacturer's instructions. Briefly, following troglitazone treatment, samples of the assay media were taken from the wells and diluted 1 in 10,000 with lactate assay buffer and the total volume was adjusted to 50 μ l. A reaction mix for each well was prepared containing 47.6 μ l assay buffer, 0.4 μ l probe and 2 μ l enzyme mix for each well. The plate was incubated at room temperature for 30 minute.

Fluorescence was measured using a Tecan Infinite M200 plate reader at excitation 535 nm and emission 587 nm.

4.3 Results

4.3.1 Optimisation of Extracellular Flux Analysis

The first injection of 1 μM oligomycin was designed to inhibit ATP production and drop oxygen consumption. As oxygen consumption and ATP production are very closely linked, the levels of oxygen consumption should almost drop to zero after oligomycin addition. Figure 4.2 showed that both 1 μM and 2 μM oligomycin additions produced a similar response. Therefore, in subsequent experiments 1 μM oligomycin was chosen as optimal in order to prevent any inadvertent toxicity from higher concentrations of oligomycin. Similarly, for FCCP, 1 μM total concentration was selected for further experiments. 0.5 μM FCCP was not sufficient to maximise oxygen consumption as a further rise in oxygen consumption was seen when a second injection of FCCP was added to the well. A total of 1 μM was therefore selected for subsequent experiments. 2 μM FCCP was shown to decrease oxygen consumption again (data not shown) indicative of toxicity. An excess of rotenone and antimycin A was required. This was shown with 0.5 μM of each. Finally, it was observed that 5,000 cells per well was the optimum number for B-13/H cells compared to 10,000 cells per well for B-13 cells (figure 4.2).

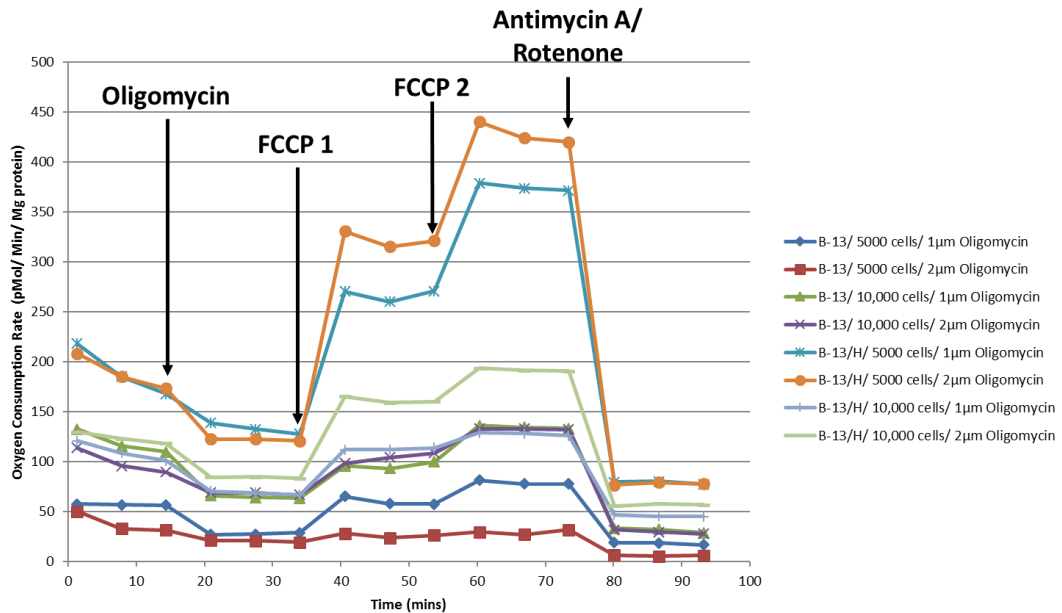


Figure 4.2: Optimisation of Mitochondrial Stress Test. The X^{fe} 96 format allows for optimisation to be completed in one assay. 3 baseline measures of oxygen consumption were measured and a subsequent 3 measures for each injection. The first injection from port A, Oligomycin. The second and third injections from ports B and C were both 0.5 μM FCCP to give a total concentration of 1 μM . The final injection from port D was 0.5 μM Antimycin A and Rotenone combined. 5,000 cells per well was optimum for B-13/H cells. In contrast, a higher response was achieved from 10,000 B-13 cells per well than 5,000.

4.3.2 The Effect of Troglitazone on Mitochondrial Respiration

Hepatocytes are highly metabolically active cells and figure 4.3 clearly demonstrated that the B-13/H hepatocyte like cells were similarly more metabolically active than the B-13 cells. Even without drug treatment, in control cells, there was a marked difference between the oxygen consumption in B-13 cells compared to B-13/H cells. While baseline measures of oxygen consumption were very similar, when stimulated with 1 μ M FCCP, B-13/H cells had a much greater spare capacity and reached a much higher level of maximal respiration. The data showed that B-13 cells were functioning much closer to their metabolic limit than B-13/H cells due to a larger reserve capacity of oxygen consumption.

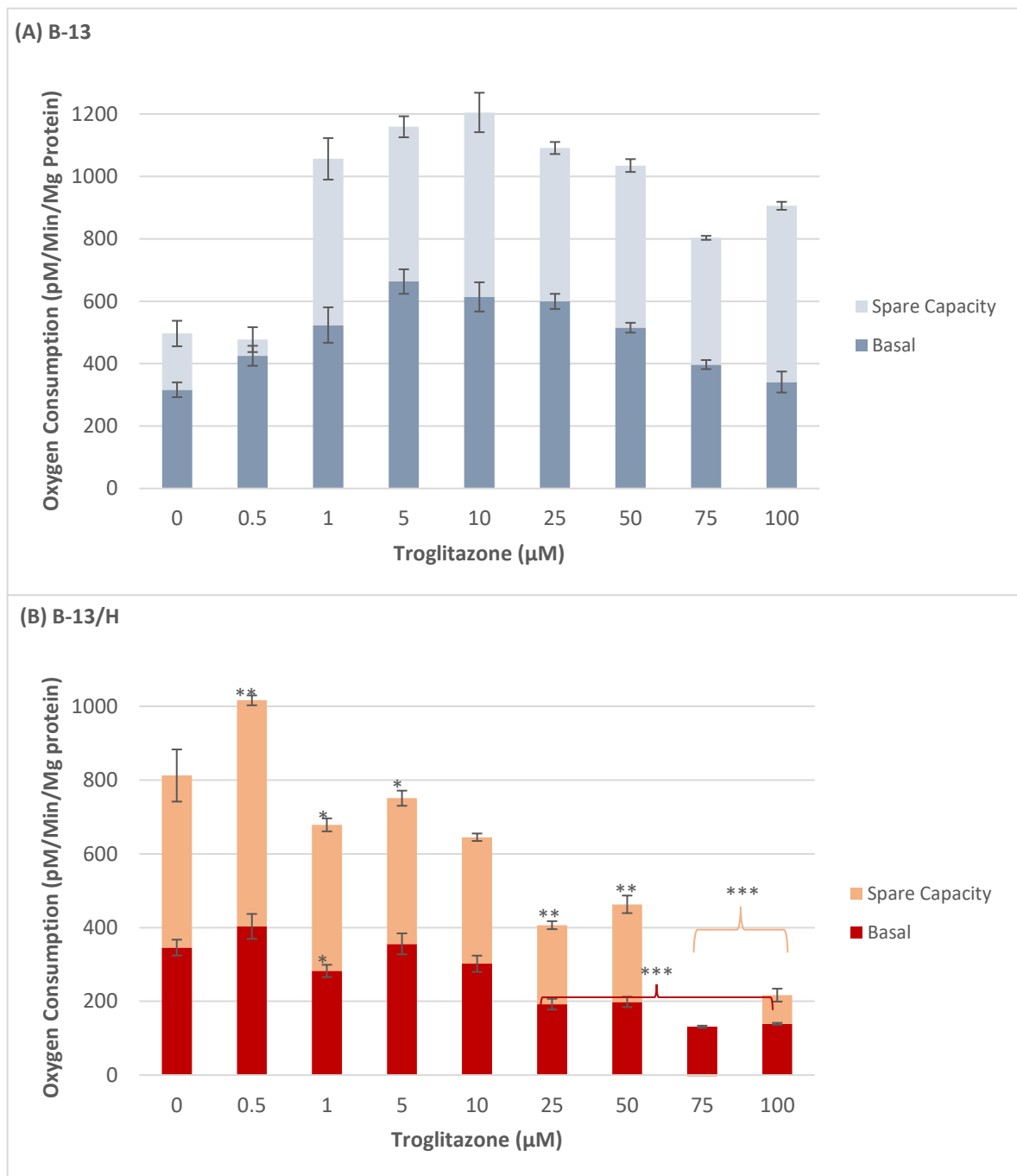


Figure 4.3: Effect of different concentrations of troglitazone on mitochondrial respiration following 24-hour incubation at 37°C. (A) At concentrations between 0.5 μM and 5 μM there was a steady increase in the baseline measures of oxygen consumption. Beyond which point there was a gradual decline up to the maximum concentration of 100 μM (B) Basal oxygen consumption was decreased in B-13/H cells with increased troglitazone concentration. The spare respiratory capacity was reduced at all concentrations apart from 0.5 μM . ($n=8 \pm \text{SEM}$, * $P<0.05$, ** $P<0.01$, *** $P<0.001$).

There were significant differences between B-13 and B-13/H cells in terms of their mitochondrial response to troglitazone. In B-13 cells treated with different concentrations of troglitazone it was observed that at the lower end of the concentration range, 0.5 μM - 5 μM , there was an increase in oxygen consumption. At

concentrations above this there was a gradual decline in oxygen consumption. Rates did not, however, reduce past control levels and even at 100 μM troglitazone the basal level of respiration was not significantly different to that seen in untreated cells. Spare respiratory capacity remained significantly elevated above control levels at concentrations of troglitazone of 1 μM and above. Troglitazone seemed to stimulate an increase in respiration but also worthy of note is that the cells were not functioning closer to their respiratory limit and instead the maximum respiratory capacity increased similarly to basal levels.

In contrast, B-13/H cells were much more susceptible to the effects of troglitazone. There was a concentration dependent decrease in oxygen consumption with an increase in troglitazone concentration. At concentrations of 25 μM and above, the level of oxygen consumption was significantly less than in untreated cells. Furthermore, unlike B-13 cells, at concentrations above 1 μM it was seen that the maximum level of respiration also decreased compared to untreated cells. It was seen that, despite the reductions, cells still operated at approximately 40% of maximal capacity until 75 μM , at which point the mitochondrial activity was much closer to the maximal level.

Figure 4.4A showed that the pattern of oxygen consumption at basal levels of respiration is similar to the pattern of oxygen consumption for ATP production in both B-13 and B-13/H cells. In the B-13 cells there was an increase in oxygen consumption for ATP production up to 5 μM troglitazone, after which point there was a decrease. However, the levels of oxygen consumption did not decrease significantly below control levels other than in cells exposed to the maximum concentration of troglitazone (100 μM). In the B-13/H cells, oxygen consumption for ATP production remained elevated above control levels up to 50 μM at which point there was a significant decline in oxygen consumption.

In addition to this, there was also a decrease in observed in proton leak that was concentration dependent in B-13/H cells, as troglitazone concentration increased there was a decrease in proton leak, this was significantly lower than untreated cells at concentrations above 5 μM . Conversely, in B-13 cells there was a significant increase in proton leak at concentrations above 0.5 μM .

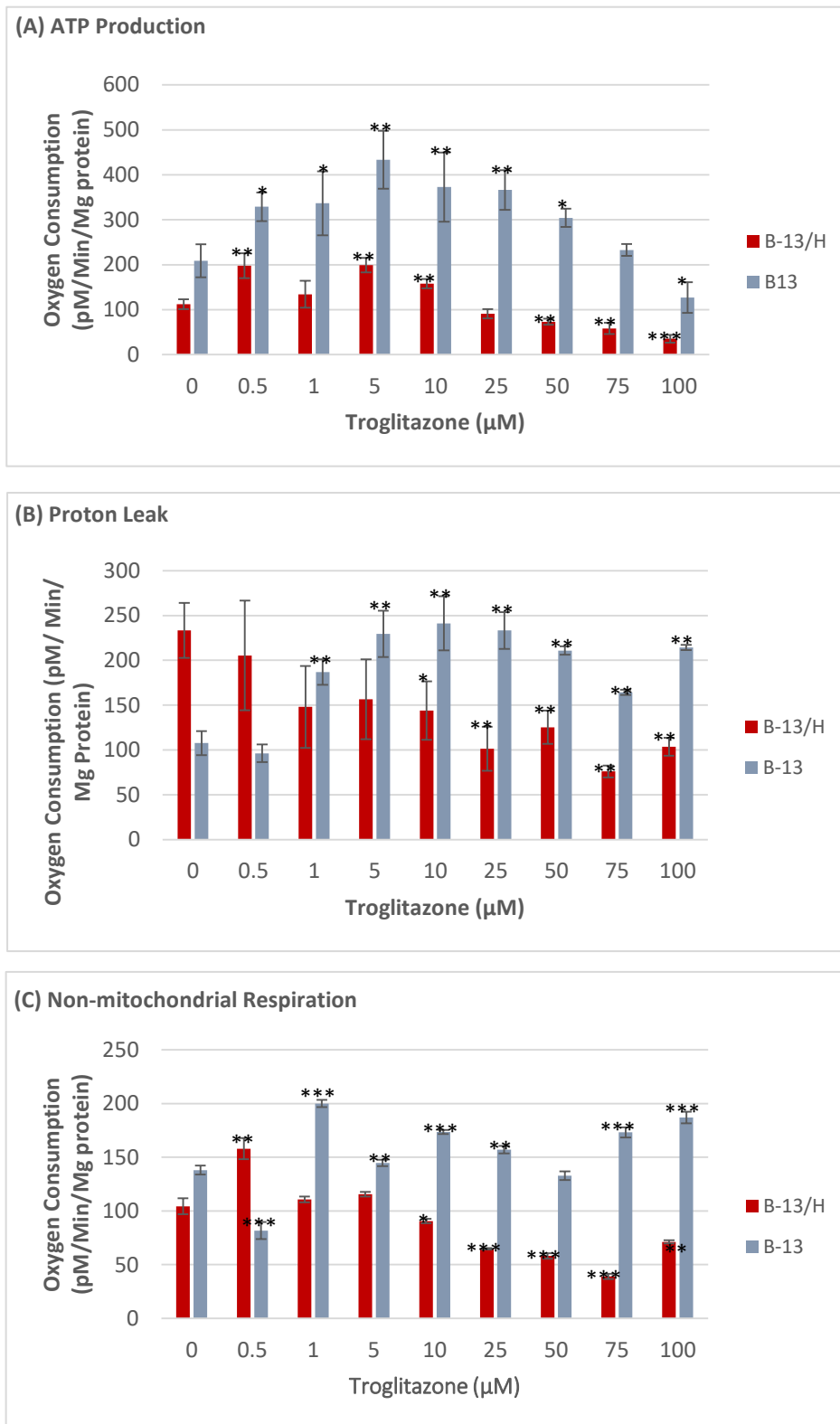


Figure 4.4: Effect of different concentrations of troglitazone on mitochondrial functions following 24 hr incubation at 37°C. (A) ATP Production: B-13 cells showed elevated oxygen consumption above control cells compared to B-13/H cells where there was a steady decline. (B) Proton Leak: In B-13 cells there was a sustained increase in proton leak. In B-13/H cells there was a decrease in proton leak at levels that were significantly lower than control cells at troglitazone concentrations of 10 µM and above. (C) Non-mitochondrial respiration: Oxygen consumed for purposes other than oxidative phosphorylation. (n=8 ±SEM, *P<0.05, **P<0.01, ***P<0.001)

4.3.3 Cellular ATP levels in Response to Troglitazone

The mitochondrial stress test cannot determine ATP levels within cells directly and can only indicate an increase or decrease in the oxygen consumed to produce ATP. Therefore, to clarify extracellular flux data that showed an increase in the oxygen consumption for ATP production in B-13 cells, ATP quantification assays were performed. As seen in figure 4.5 both B-13 and B-13/H cells showed a concentration dependent decrease in levels of ATP within cells. The effect was less pronounced in B-13 cells with only a troglitazone concentration of 50 μM causing a significant reduction below the level of an untreated control. Conversely, all concentrations of troglitazone caused a reduction in ATP levels that were significantly lower than untreated controls in B-13/H cells.

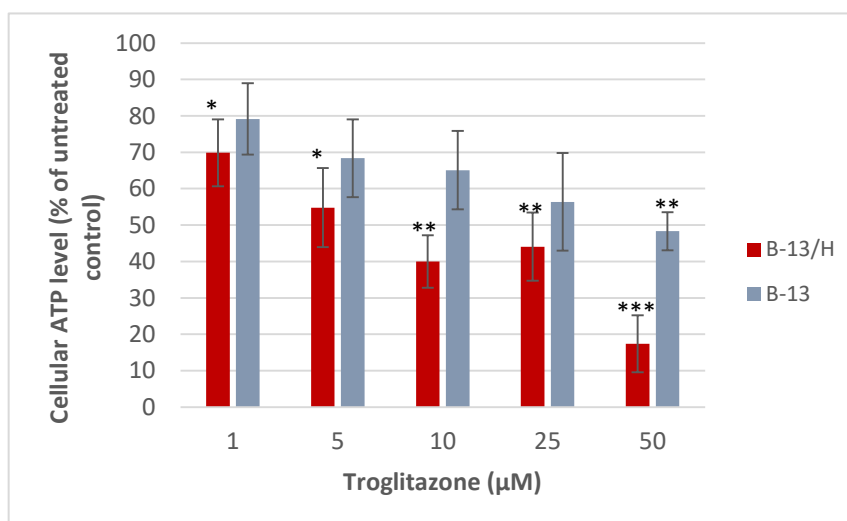
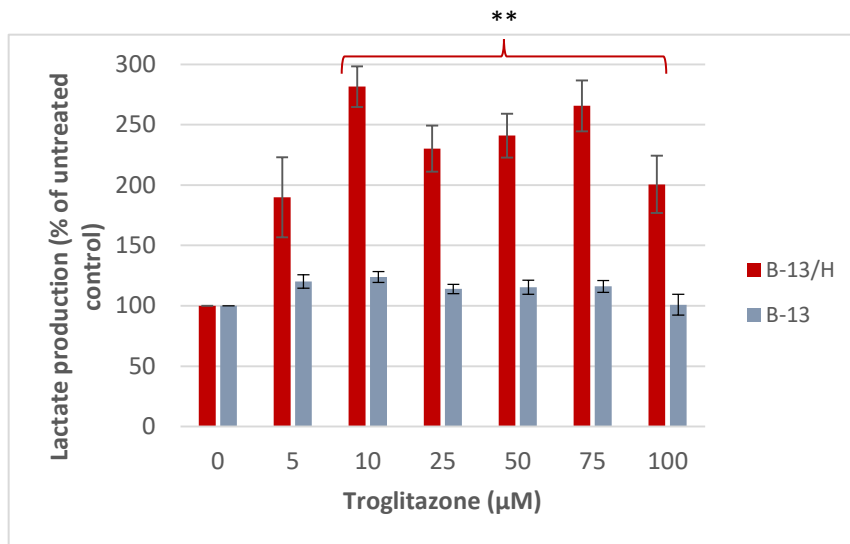


Figure 4.5: Cellular ATP level in response to 1hr troglitazone treatment. Data presented as mean of 3 replicates \pm SD (* $P < 0.05$, ** $P < 0.01$, *** $P < 0.001$)

4.3.4 Lactate Production Following Troglitazone Treatment

There was a significant difference in lactate levels present in the B-13 and B-13/H cells. Figure 4.6 shows that troglitazone had no effect on lactate production in B-13 cells whereas there was an elevated lactate production in B-13/H cells that was significantly higher than untreated controls at concentrations of 10 μM and above.



*Figure 4.6: Effect of troglitazone on lactate production in B-13 and B-13/H cells. Cells were treated for 24 hrs with a range of concentrations of troglitazone. Troglitazone did not significantly change the level of lactate present in B-13 cells at any of the treatment concentrations. There was a significant increase in the levels of lactate present in B-13/H cells following treatment with troglitazone at concentrations of 10 μM and above, however, this was not concentration dependent and there was no linear relationship. Data is presented as mean of 3 replicates ±SD, **P<0.01.*

4.4 Discussion

Mitochondrial dysfunction is more frequently becoming associated with drug induced liver injury and in recent years has been the underlying reason for several high-profile drug withdrawals from the market, including troglitazone in 2000. Therefore, a great deal of work has been done to develop a high throughput screen for mitochondrial liabilities in NCEs in order to provide a more comprehensive overview of potential drug toxicities.

Extracellular flux analysis offers a realistic option for preclinical drug screening. Not only does the technique allow for rapid measurement of oxygen consumption, the unique micro-chamber set up allows for multiple drug additions to be made with the refreshing of media and return to baseline levels before each new addition. This means that multiple mitochondrial parameters can be measured in a single experiment. For example, when studying mitochondrial stress, the technique can provide information on maximum respiratory capacity, reserve respiratory capacity, ATP production and proton leak. The results of a mitochondrial stress test, therefore, can help to determine specific locations of mitochondrial damage or areas for further study. Changes in any of the aforementioned parameters can be indicative of mitochondrial dysfunction.

In order to obtain the most reliable and accurate respiration data, the XF assay first had to be optimised for the specific cell line being used. For example, in the assay described here, both pancreatic acinar cells and hepatic like cells are used. Hepatocyte cells are highly metabolically active due to their role in metabolism of endogenous and exogenous compounds. Hepatocytes contain many more mitochondria than pancreatic acinar cells and will therefore have a different metabolic profile. This was demonstrated in figure 4.2, the largest response was in B-13/H cells at 5,000 cells per well, a similar number of B-13 cells with all other conditions the same showed a baseline oxygen consumption level approximately 4 times smaller. 10,000 B-13 cells per well however, showed the clearly defined responses to the different drug injections that were expected.

Following optimisation under baseline condition cells were subsequently challenged with troglitazone in order to establish its effects on respiration, however, it is also pertinent to mention that even before the addition of troglitazone there were distinct differences between B-13 and B-13/H cells in untreated control conditions. While basal levels of oxygen consumption were very similar, when stimulated with the

uncoupler, FCCP, it was observed that the B-13/H cells had a much greater reserve capacity for respiration than the B-13 cells. This is in line with what would be expected from hepatocyte cells, which, as the first line of defence within the liver, need to be able to respond quickly to external stressors. Furthermore, the B-13/H response could be as a result of them having a greater number of mitochondria than the B-13 cells which would also be expected from highly metabolically active cells such as hepatocytes. This suggests that the B-13/H cells have hepatocyte like behaviour which would be crucial if they were to be used in preclinical testing. Regarding further work in this area, it would be of interest to study the mitochondrial profile of primary hepatocytes to see if there are similar levels of respiration in B-13/H cells and a primary counterpart.

Troglitazone provides an important case study in the argument for the use of mitochondrial testing in drug development. Over the years, the mechanism of toxicity has been widely disputed due to conflicting evidence of damage between cell models. For example, depleted ATP levels are often reported in troglitazone toxicity (Tirmenstein *et al.*, 2002; Rachek *et al.*, 2009; Hu *et al.*, 2015). However Bova *et al.* found that after 24 hours exposure, troglitazone did not significantly alter ATP levels in HepG2 cells (Bova *et al.*, 2005). Furthermore, Narayanan *et al.* argued that damage found to mitochondria was caused by oxidative stress whereas Masubuchi suggested that while oxidative stress might be present in troglitazone toxicity it is secondary to already dysfunctional mitochondria (Narayanan *et al.*, 2003; Masubuchi *et al.*, 2006). In recent years it has become accepted, however, that there is a likely role for mitochondrial dysfunction. As such, B-13 and B-13/H cells were subsequently treated with a range of concentrations of troglitazone and mitochondrial effects were studied. As troglitazone showed only moderate toxicity in B-13 cells compared to B-13/H cells and when mitochondrial stress was studied it was found that there was a stimulatory effect of troglitazone in B-13 cells. At the lower end of the concentration range (0.5 μ M- 5 μ M) there was an increase in basal oxygen consumption after which there was a gradual decline at higher concentrations. However, levels of oxygen consumption did not drop below that seen in untreated cells. An increase in oxygen consumption indicated a drive to produce ATP and this was matched by the oxygen consumption for ATP production profile seen in figure 4.5. Conversely, when ATP levels were measured after an hour there was already shown to be a decline in ATP content within the cells compared to an untreated

control. This suggested that while there was an increase in demand for ATP, it was not matched with an increase in supply. While ATP production cannot be measured directly using the mitochondrial stress test, ATP production is very closely linked to oxygen consumption as the demand for ATP stimulates the ETC and thus oxygen consumption. Therefore, by adding oligomycin to inhibit ATP synthase, the difference in oxygen consumption before and after addition gave a reflection of the changes in ATP production by giving a measure of the oxygen consumed to produce ATP.

When the data for proton leak was analysed it was found that B-13 cells were much 'leakier' than B-13/H cells. This indicated that troglitazone possibly uncoupled proton transport and ATP synthase. It is expected that uncouplers of respiration will increase oxygen consumption within mitochondria (Attene-Ramos *et al.*, 2013). Therefore, it is likely that while troglitazone was not lethal to B-13 cells it was able to elicit damage in cells that made the production of ATP inefficient.

Conversely, B-13/H cells showed that with an increase in troglitazone concentration there was a concurrent decrease in oxygen consumption, associated with an inhibition of electron flow through the ETC. As to be expected from a shut down in electron transport, there was a decrease in oxygen consumed for ATP production. However, unlike B-13 cells, this was corroborated by the ATP quantification assay which showed a significant reduction in ATP levels within cells. A drop in proton leak was observed in the B-13H cells that was concentration dependent in response to troglitazone. This, again, was a different response to that seen in the B-13 cells and, again, indicated a slowdown of transport within the ETC. Fewer H⁺ ions pumped out of the matrix would also reduce the build-up of an electrochemical gradient and reduce the ions available for transport back into the matrix when uncoupled with FCCP. Nandanaciva *et al.* similarly showed that depending upon the cell type being studied; troglitazone can elicit opposing mitochondrial effects. HepG2 cells exposed to troglitazone showed an immediate inhibition of respiration in contrast to cardiomyocytes, which, like the B-13 cells, responded with an increase in oxygen consumption and troglitazone appeared to have a stimulatory effect (Nadanaciva *et al.*, 2012).

Dan et al. reported similar findings to those found in B-13/H cells here. It was found that 24 hours troglitazone pre-treatment of HepaRG cells caused a reduction in respiration rate at basal levels in cells that was lower than observed in untreated

cells. The sensitivity to FCCP was also reduced, as shown by a decrease in the maximum respiratory capacity (Hu *et al.*, 2015).

When oxidative phosphorylation is inhibited, a cell will compensate for reduced energy production by upregulating glycolysis (Dykens *et al.*, 2008) a by-product of which is lactate formation due to a decrease in the oxidation of pyruvate. When lactate was measured in the media of B-13/H cells following 24 hours' exposure to troglitazone, it was found that there was a significant increase in lactate at all concentrations above 10 μ M. The effect was not concentration dependent and it appeared that 10 μ M was a threshold point. However, this suggests that there was a compensatory effect in B-13/H cells where ATP production switched to glycolysis rather than oxidative phosphorylation. It has previously been found that ATP depletion was also linked to an increase in lactate efflux in HepG2 cells that had been treated with phenformin (Dykens *et al.*, 2008). On the other hand, there was no change in lactate concentration in B-13 cells compared to an untreated control, suggesting that oxidative phosphorylation was still functional.

The data presented here showed that, following a transdifferentiation period of 7 days, the cells have a fundamentally different phenotype from the original B-13 cell type. The significant differences in responses to troglitazone by B-13 and B-13/H cells were unexpected as there appeared to be two distinct mechanisms of action-stimulatory in B-13 cells and inhibitory in B-13/H cells. To further understand the mechanisms behind this, additional work would need to be done to elucidate what caused these differences. For example, hepatocytes have a larger variety of drug metabolising enzymes than pancreatic cells. It could therefore be possible that a metabolite of troglitazone rather than the parent compound could be contributing to the mitochondrial toxicities seen in B-13/H cells. To investigate this further it would be possible to use inhibitors of drug metabolising enzymes in order to see how the toxicity of troglitazone is affected. For example, the sulphation inhibitor, phenobarbital, was used by Kostrubsky *et al.*, to investigate the toxicity of parent compound vs metabolite in human hepatocytes. While it was observed that rather than reducing toxicity, inhibition of sulphation aggravated toxicity, there are conflicting arguments and it has previously been reported that sulphate metabolites can induce cellular damage (Kostrubsky *et al.*, 2000; Funk *et al.*, 2001).

The XF assay for mitochondrial stress can provide information on multiple parameters of mitochondrial respiration in a single assay, providing many

advantages over the traditional Clark electrode set up which is low throughput and time consuming. The XF assay provides fast reliable information about mitochondrial function. It is however, limited in its ability to decipher between different complex dysfunctions of the ETC. In order to gain a full overview of mitochondrial function, XF assays must be combined with other techniques that are able to provide information on specific mitochondrial complex toxicities. This has been done previously by measuring the activity of oxidative phosphorylation complexes that have been immunocaptured from mitochondria on 96 well plates coated with monoclonal antibodies raised against complex I, II, III, IV and V. In doing so it was possible to localise drug damage to a specific complex (Nadanaciva *et al.*, 2007; Dykens *et al.*, 2008). Nadanaciva found that troglitazone was able to inhibit complexes II, III, IV and V (Nadanaciva *et al.*, 2007). In addition to this, further information could be gained from adapting the current XF techniques. A simple modification would be the addition of troglitazone during the experiment as an injection rather than as a pre-treatment. This would enable the immediate effects of troglitazone on cells to be established and would also provide more information on the uncoupling ability of troglitazone in B-13 cells to see if it gives a similar response to that seen with FCCP. Furthermore, as well as mitochondrial stress testing, XF assays can also be used to determine extracellular acidification (ECAR) which provides a measure of glycolysis by using pH sensors to detect proton concentration in the sample.

Predictive toxicology is a complex process, there is a great variation in tissue response, and that was clearly highlighted here. The transdifferentiation of a pancreatic cell into a hepatocyte like cell produced vastly different metabolic profiles with differing responses to a known toxin. Furthermore, due to the nature of the many detoxifying reactions that generate metabolites that can be toxic in their own right within hepatocytes as well as the ability of cells to compensate for injury, it is difficult to attribute a mechanism of action. However, the data shown here also show the importance of investigating mitochondrial dysfunction early in the drug development stage as there can be stark differences in cellular response to a compound. Finally, the XF analyses were also able to show that there are metabolic differences following transdifferentiation of the B-13 cells into B-13/H cells adding further weight to the argument that this cell line has the potential to be developed into an alternative cell model for the study of drug toxicity.

4.5 References

- Adeva-Andany, M., López-Ojén, M., Funcasta-Calderón, R., Ameneiros-Rodríguez, E., Donapetry-García, C., Vila-Altesor, M. and Rodríguez-Seijas, J. (2014) 'Comprehensive review on lactate metabolism in human health', *Mitochondrion*, 17, pp. 76-100.
- Attene-Ramos, M.S., Huang, R., Sakamuru, S., Witt, K.L., Beeson, G.C., Shou, L., Schnellmann, R.G., Beeson, C.C., Tice, R.R., Austin, C.P. and Xia, M. (2013) 'Systematic study of mitochondrial toxicity of environmental chemicals using quantitative high throughput screening', *Chemical Research in Toxicology*, 26(9), pp. 1323-1332.
- Begrache, K., Massart, J., Robin, M.A., Borgne-Sanchez, A. and Fromenty, B. (2011) 'Drug-induced toxicity on mitochondria and lipid metabolism: Mechanistic diversity and deleterious consequences for the liver', *Journal of Hepatology*, 54(4), pp. 773-794.
- Bova, M.P., Tam, D., McMahon, G. and Mattson, M.N. (2005) 'Troglitazone induces a rapid drop of mitochondrial membrane potential in liver HepG2 cells', *Toxicology Letters*, 155(1), pp. 41-50.
- Brand, M.D. and Nicholls, D.G. (2011) 'Assessing mitochondrial dysfunction in cells (Biochemical Journal (2011) 435, (297-312))', *Biochemical Journal*, 437(3), p. 575.
- Brookes, P.S. (2005) 'Mitochondrial H⁺ leak and ROS generation: An odd couple', *Free Radical Biology and Medicine*, 38(1), pp. 12-23.
- Clark Jr, L.C., Helmsworth, J.A., Kaplan, S., Sherman, R.T. and Taylor, Z. (1953) 'Polarographic measurement of oxygen tension in whole blood and tissues during total by-pass of the heart', *Surgical forum*, 4, pp. 93-96.
- Dmitriev, R.I. and Papkovsky, D.B. (2012) 'Optical probes and techniques for O₂ measurement in live cells and tissue', *Cellular and Molecular Life Sciences*, 69(12), pp. 2025-2039.
- Dyken, J.A., Jamieson, J., Marroquin, L., Nadanaciva, S., Billis, P.A. and Will, Y. (2008) 'Biguanide-induced mitochondrial dysfunction yields increased lactate production and cytotoxicity of aerobically-poised HepG2 cells and human hepatocytes in vitro', *Toxicology and Applied Pharmacology*, 233(2), pp. 203-210.
- Ferrick, D.A., Neilson, A. and Beeson, C. (2008) 'Advances in measuring cellular bioenergetics using extracellular flux', *Drug Discovery Today*, 13(5-6), pp. 268-274.

- Funk, C., Ponelle, C., Scheuermann, G. and Pantze, M. (2001) 'Cholestatic potential of troglitazone as a possible factor contributing to troglitazone-induced hepatotoxicity: In vivo and in vitro interaction at the canalicular bile salt export pump (Bsep) in the rat', *Molecular Pharmacology*, 59(3), pp. 627-635.
- Hu, D., Wu, C.Q., Li, Z.J., Liu, Y., Fan, X., Wang, Q.J. and Ding, R.G. (2015) 'Characterizing the mechanism of thiazolidinedione-induced hepatotoxicity: An in vitro model in mitochondria', *Toxicology and Applied Pharmacology*, 284(2), pp. 134-141.
- Kostrubsky, V.E., Sinclair, J.F., Ramachandran, V., Venkataramanan, R., Wen, Y.H., Kindt, E., Galchev, V., Rose, K., Sinz, M. and Strom, S.C. (2000) 'The role of conjugation in hepatotoxicity of troglitazone in human and porcine hepatocyte cultures', *Drug Metabolism and Disposition*, 28(10), pp. 1192-1197.
- Labbe, G., Pessayre, D. and Fromenty, B. (2008) 'Drug-induced liver injury through mitochondrial dysfunction: Mechanisms and detection during preclinical safety studies', *Fundamental and Clinical Pharmacology*, 22(4), pp. 335-353.
- Masubuchi, Y., Kano, S. and Horie, T. (2006) 'Mitochondrial permeability transition as a potential determinant of hepatotoxicity of antidiabetic thiazolidinediones', *Toxicology*, 222(3), pp. 233-239.
- Nadanaciva, S., Dykens, J.A., Bernal, A., Capaldi, R.A. and Will, Y. (2007) 'Mitochondrial impairment by PPAR agonists and statins identified via immunocaptured OXPHOS complex activities and respiration', *Toxicology and Applied Pharmacology*, 223(3), pp. 277-287.
- Nadanaciva, S., Rana, P., Beeson, G.C., Chen, D., Ferrick, D.A., Beeson, C.C. and Will, Y. (2012) 'Assessment of drug-induced mitochondrial dysfunction via altered cellular respiration and acidification measured in a 96-well platform', *Journal of Bioenergetics and Biomembranes*, 44(4), pp. 421-437.
- Narayanan, P.K., Hart, T., Elcock, F., Zhang, C., Hahn, L., McFarland, D., Schwartz, L., Morgan, D.G. and Bugelski, P. (2003) 'Troglitazone-Induced Intracellular Oxidative Stress in Rat Hepatoma Cells: A Flow Cytometric Assessment', *Cytometry Part A*, 52(1), pp. 28-35.
- Pessayre, D., Fromenty, B., Berson, A., Robin, M.A., Lettéron, P., Moreau, R. and Mansouri, A. (2012) 'Central role of mitochondria in drug-induced liver injury', *Drug Metabolism Reviews*, 44(1), pp. 34-87.
- Phypers, B. and Pierce, J.M.T. (2006) 'Lactate physiology in health and disease', *Continuing Education in Anaesthesia, Critical Care and Pain*, 6(3), pp. 128-132.

Rachek, L.I., Yuzefovych, L.V., LeDoux, S.P., Julie, N.L. and Wilson, G.L. (2009) 'Troglitazone, but not rosiglitazone, damages mitochondrial DNA and induces mitochondrial dysfunction and cell death in human hepatocytes', *Toxicology and Applied Pharmacology*, 240(3), pp. 348-354.

Salabei, J.K., Gibb, A.A. and Hill, B.G. (2014) 'Comprehensive measurement of respiratory activity in permeabilized cells using extracellular flux analysis', *Nature Protocols*, 9(2), pp. 421-438.

Tirmenstein, M.A., Hu, C.X., Gales, T.L., Maleeff, B.E., Narayanan, P.K., Kurali, E., Hart, T.K., Thomas, H.C. and Schwartz, L.W. (2002) 'Effects of troglitazone on HepG2 viability and mitochondrial function', *Toxicological Sciences*, 69(1), pp. 131-138.

Wolfbeis, O.S. (2015) 'Luminescent sensing and imaging of oxygen: Fierce competition to the Clark electrode', *BioEssays*, 37(8), pp. 921-928.

Zhang, J., Nuebel, E., Wisidagama, D.R.R., Setoguchi, K., Hong, J.S., Van Horn, C.M., Imam, S.S., Vergnes, L., Malone, C.S., Koehler, C.M. and Teitell, M.A. (2012) 'Measuring energy metabolism in cultured cells, including human pluripotent stem cells and differentiated cells', *Nature Protocols*, 7(6), pp. 1068-1085.

Chapter 5: Human Equivalents

5.1 Introduction

5.1.1 Extrapolation of animal data to humans

The data presented in previous chapters have so far displayed the potential of B-13/H cells to provide an alternative hepatocyte model that requires no animal donor and can be supplied on demand and in potentially unlimited numbers. These cells represent an important advance in drug screening technology. However, to have clear clinical relevance and optimise the advantages offered by this new approach a human equivalent model of the B13/H cell system is required.

Before a new drug can be tested in humans, extensive research must first be done in animal models in order to establish exposure limits and dosage. Typically this includes 2 mammalian species, one rodent and one non-rodent (Peters, 2005).

While whole animal studies are typically the most informative, there is an important role for *in vitro* test models in preclinical development. In order to identify potential tissue specific toxicities in whole animal studies, *in vitro* cell models can be used to highlight 'at risk' tissues. *In vitro* assessments can be carried out quickly and inexpensively as cell based assays lend themselves to high throughput screening (McKim Jr, 2010). Once these preliminary assessments have been completed, then human cells and the data derived from them becomes much more important. Whilst many important drug metabolising enzymes are conserved between species, their highly substrate specific nature means that slight differences in structure can cause huge differences in functionality.

One of the most important questions in pre-clinical toxicology is "can data generated from animal models be successfully extrapolated to humans?". Pharmacokinetic data is reasonably well extrapolated when there is a clear idea of the endpoint being studied and when considerations for body weight are taken into account. For example, rodents have a short life span and can be produced in large numbers, therefore, are useful in early preliminary studies where a large amount of data is needed quickly. In addition to this, a short life span means rodents are useful for generating data regarding acute exposure to drugs. Large animals, such as dogs, live much longer than rodents and can therefore provide useful information in longitudinal studies of chronic toxicity and due to being a more similar size to humans it gives the opportunity to adjust dosage for size (Martignoni *et al.*, 2006).

Most drugs and chemicals induce hepatic cytochrome P450 enzymes (Graham and Lake, 2008). CYP enzymes are one of the most highly conserved entities between

humans and animals and are found in virtually all organs (predominantly the liver). CYP enzymes are therefore critical in metabolism and consequently in pharmacokinetic studies. However, small changes in CYP isoform structure and expression profile can lead to large differences in metabolic capacity making extrapolation of data between animals and humans quite complicated (Martignoni *et al.*, 2006).

CYP 2E1 is an isoform expressed in the liver that is well conserved between humans and rats. It is only inducible by a few drugs including ethanol and caffeine. With regard to CYP 2E1, the rat is therefore a good model of human response and data extrapolation holds well (Martignoni *et al.*, 2006).

The CYP 1A subfamily of enzymes plays a role in the metabolism of environmental carcinogens, polyaromatic hydrocarbons and arylamines. The CYP 1A subfamily is also well conserved between humans and rats, showing 80% similarity. However, it also provides an important example of how extrapolation does not always work. The anti-ulcer drug, omeprazole, induced CYP 1A2 in humans but not in rats, therefore this would not have been noticed in rodent based pre-clinical studies (Martignoni *et al.*, 2006).

The CYP 3A family is the most important CYP family in humans. It accounts for 30% of all microsomal CYP content and plays a role in the metabolism of 50% of all drugs as well as the metabolism of some endogenous compounds including steroids and bile acid (Graham and Lake, 2008). In humans there are 4 main isoforms: CYP 3A1, 3A23, 3A2, 3A9, 3A18 and 3A62. There is not a lot of parity between the human and rat CYP 3A family and as such the rat does not provide an effective model of CYP 3A expression. Although CYP 3A is highly inducible in rats, the most abundant CYP isoform in the rat liver is CYP 2C and in addition to this, the typical inducer of CYP 3A in research in humans is rifampicin which is unable to induce CYP 3A in rats (Martignoni *et al.*, 2006).

There are other important considerations when extrapolating data besides metabolising enzymes. When extrapolating data, it is important to understand the effect of size and weight on metabolism. Rats have a much larger liver to body weight ratio. The percentage of liver weight as total body weight is much higher in rats than in humans, this means that rats can often metabolise and clear drugs quicker than humans due to a higher content of microsomal CYP enzymes per gram

of body weight (Martignoni *et al.*, 2006). This is thought, in part, to explain why troglitazone toxicity was not observed during *in vivo* experiments in rats. Troglitazone showed hepatotoxicity in the clinic, but experimentally, only 'acceptable' levels of toxicity were seen which included microvesicular steatosis and liver enlargement in monkeys (Bedoucha *et al.*, 2001; Smith, 2003; Boelsterli and Lim, 2007). No toxicity was observed in rats, possibly due to faster clearance in rats and less exposure to the drug. Interestingly, it has been reported that while toxicity is not observed in rats *in vivo*, rat cells grown *in vitro* are susceptible to troglitazone when grown in monolayer, thought to be due to a reduced rate of clearance. Subsequently rat hepatocytes were grown in 3D culture and exposed to lower concentrations of troglitazone for 21 days. These experiments showed that *in vivo* and *in vitro* data correlated, which suggested that gel entrapment of cells could be the way forward in terms of generating reliable data that reflects *in vivo* effects (Shen *et al.*, 2012). Furthermore, it is known that troglitazone is primarily metabolised by CYP 3A in humans, which, as previously stated, is not well modelled in rats.

Understanding the differences in metabolism between rats and humans can help inform studies to ensure that the data generated is as valuable as possible. Using *in vitro* and *in vivo* animal experiments to combine data along with computational *in silico* simulations, enables a tiered and comprehensive system to be developed for preclinical tests that can inform clinical dosage regimens. There is also a considerable drive to reduce the number of animals used in medical research, including pre-clinical toxicology and to that end developing alternative *in vitro* models that can successfully predict toxicity in humans is of paramount importance (as evidenced by The National Centre for the Replacement, Refinement and Reduction of Animals in Research).

The B-13/H cell line has shown great promise in providing an unlimited, on demand supply of hepatocytes without the need for a donor. Despite this, a human alternative would provide much more relevant data, especially if supplementary whole animal studies are to be reduced. Furthermore, the successful development of a human hepatocyte cell line would also have potential in cell replacement therapy and transplantation.

Anecdotally, it has been observed that patients on long term steroid treatment have the development of hepatocyte like cells within their pancreas. In addition to this, it was found by Fairhall *et al.* that pancreatic tissue taken from a patient on long term

systemic glucocorticoid therapy (at least 20 years) contained hepatocyte like cells that were not seen in the cells of patients who were not exposed to glucocorticoid therapy. These cells also expressed liver markers at levels comparable to human hepatocytes (Fairhall *et al.*, 2013b). This work was built upon with the observation that human pancreatic acinar cells (HPAC) showed a slowed proliferation in response to dexamethasone in a manner similar to B-13/H cells and thus indicated that there may be other similarities between the two cell lines. It was therefore hypothesised that HPAC cells could provide a human alternative to the B-13/H cell line (Fairhall, 2013). HPAC cells are a pancreatic adenocarcinoma epithelial cell line that was derived from a pancreatic adenocarcinoma after engraftment into nude mice. The HPAC cell line was also the first reported human adenocarcinoma cell line to express a functional glucocorticoid receptor (GR) (Norman *et al.*, 1994). It was first found by Norman *et al.* in 1994 that DEX could slow the growth of HPACs (Norman *et al.*, 1994). In addition to this, Sumitran-Holgersson *et al.* found that human foetal pancreatic (HFP) cells were treated with fibroblast growth factor 2 and DEX, a liver phenotype was induced. When characterised for pancreatic and hepatic markers it was found that the cells had lost pancreatic markers and expressed the hepatic markers albumin and cytokeratin 19 at the mRNA and protein level. Cells were also successfully grafted into nude mice in which they retained their hepatic phenotype (Sumitran-Holgersson *et al.*, 2009). Fairhall has also reported that cell morphology changed following DEX treatment, becoming more tightly packed and rounded in shape with distinct cell boundaries (Fairhall *et al.*, 2013b).

Therefore, it was hypothesised that the hepatic-like cells derived from the DEX treatment of HPACs could potentially be developed into a human version of the B-13/H cell line. Unpublished work by the Wright group at Newcastle University has shown that two variants of the differentiated HPAC cell line have been produced to date, known as the H-13 and H-14 cells lines. Both cell lines are transfected with slightly different DNA plasmids expressing different liver markers prior to transdifferentiation in DEX media. H-13 cells are transfected with HNF4a and H-14 cells with HNF1a. HNF4a and HNF1a are human nuclear factors that regulate the expression of several hepatic genes and are mostly involved in early development of the liver (Pontoglio, 2000; Babeu and Boudreau, 2014). Specifically, HNF4a is involved in the transcription of genes involved in the regulation of metabolism, cell junctions, differentiation and proliferation; it is crucial for early embryonic

development and subsequent function of the adult liver (Babeu and Boudreau, 2014). HNF1a, on the other hand, is a key regulator of glucose homeostasis and is involved in the regulation of albumin, beta fibrinogen and α 1 antitrypsin (Pontoglio, 2000).

Despite initial promising findings, there have also been problems with the maintenance of a differentiated phenotype suggesting that there is still a great deal of development to be done before the HPACs can provide a suitable progenitor to hepatocyte like cells (Fairhall, 2013). However, if a greater understanding of the differentiation process can be established there is huge potential for the development of a human cell model for preclinical toxicology.

5.1.2 Aims

- To test two variants of differentiated HPACs, H-13 and H-14 to investigate their responses to the hepatotoxin troglitazone.
- To investigate if H-13 and H-14 cells responded in a similar way to B-13/H cells following exposure troglitazone.

5.2 Methods

5.2.1 Materials

Unless otherwise stated all materials were supplied by Sigma Aldrich (Poole, UK)

5.2.2 Cell Provision

HPAC, H-13 and H-14 cells were a gift from Prof. Matthew Wright (Newcastle University), cells were maintained and cultured by Dr. Emma Fairhall (Newcastle University) before being provided for experimentation as a confluent monolayer in 96-well plates.

5.2.3 HPAC Cell Culture

HPAC cells originate from a 64-year old Caucasian female. Cells were derived in 1985 from a nude mouse xenograft of the primary tumour. HPAC cells were routinely cultured in low glucose (1000 mg/l) DMEM which was supplemented with 10% FBS, 500 U/ml penicillin and streptomycin, 2 mM L-Glutamine and 1% amphotericin B. Cells were incubated at 37°C in 95% air and 5% CO₂. The medium was changed every 2-3 days.

When cells reached 70-90% confluence, the cells were passaged. The medium was removed from the flask and the cell layer was washed once with pre-warmed PBS to remove traces of media. As cells were adherent, 2 ml of 10x trypsin in EDTA was added to the flask. The flask was gently tilted back and forth and then tapped gently to encourage the detachment of the cell layer from the surface. 8 ml of culture medium was then added to the flask to inhibit the action of the trypsin and the full 10 ml was then transferred to a 15ml falcon tube which was then centrifuged at 2000 rpm for 5 minutes. Supernatant was subsequently removed and the cell pellet was re-suspended in fresh medium for counting using a haemocytometer. Finally, cells were seeded as required, either into a fresh t75 culture flask for maintenance of the stock or for a specific experiment.

5.2.4 H-13 and H-14 Cell Culture

H-13 and H-14 cells were routinely cultured before being seeded at the relevant density into the relevant experimental plate in media containing 10 nM dexamethasone made from a serial dilution of a 100 µM stock in ethanol.

5.2.5 Resazurin Cell Viability Assay

HPAC, H-13 and H-14 cells were routinely cultured and seeded into 96 wells plates by Dr Emma Fairhall prior to experimentation. On the day of the experiment, the media was removed and cells were washed with PBS, media was replaced with unsupplemented DMEM containing a range of concentrations of troglitazone (1 μ M-500 μ M). Cells were incubated at 37 °C for 3, 6 and 24 hours. Cell viability was measured by adding resazurin (0.03% w/v) to each well. Resorufin, produced as a result of bio-reduction of resazurin was measured fluorometrically at excitation 530 nm and emission 590 nm using the Tecan-I plate reader.

5.2.6 ATP Quantification

Intracellular ATP was measured using an ATP content assay (Abcam, Cambridge). On the day of the experiment troglitazone was added to cells at concentrations between 0 μ M and 100 μ M. First, cells were washed with PBS before addition of 90 μ l unsupplemented experimental media to each well. Troglitazone concentrations were made at 10x concentration and 10 μ l was then added to wells. Measures were performed in triplicate. Cells were incubated for 1 hour at 37 °C 5% CO₂. The rest of the assay was performed as described in the manufacturer's instructions. Briefly, 50 μ l of detergent was added to each well to lyse cells and stabilise ATP and the plate was shaken on an orbital shaker for 5 minutes. 50 μ l of luciferin substrate was added to each and the plate was shaken again for 5 minutes before a final dark adaption for 10 minutes. Luminescence was then read using a Tecan Infinite M200 plate reader. The assay is based on the production of light which was caused by the reaction of ATP with luciferase and D- luciferin. The emitted light was proportional to ATP concentration.

5.3 Results

It was observed in the H-13 cells that while the responses were not linear and there were some anomalous points (figure 5.1B, 10 μ M and 25 μ M), there was a definite trend to suggest that troglitazone was toxic. While 5 μ M- 25 μ M troglitazone appeared to have similar levels of toxicity, at concentrations of ≥ 50 μ M, cytotoxicity was concentration dependent. There was no obvious time effect of troglitazone and maximum viability at concentrations of ≥ 100 μ M was approximately 40% at 3, 6 and 24-hour time points.

Figure 5.1 showed that there was a difference in response observed between the cells before and after differentiation. While toxicity was observed in the HPAC cells, they were less susceptible than the differentiated H-13 cells at all time points, for example at a 3-hour time point troglitazone concentrations below 100 μ M did not cause a reduction in viability in the undifferentiated HPAC cells whereas a decrease in viability was seen at all concentrations in the H-13 cells. Furthermore, unlike the H-13 cells there was a time effect of troglitazone. Maximum levels of toxicity, however, were comparable to those levels seen in the H-13 cells. The response of H-14 cells to troglitazone treatment was slightly different to that observed in the H-13 cells.

Although toxicity was observed in H-14 cells and there was vulnerability to troglitazone, the H-14 cells did not display significantly different toxicity to that observed in the undifferentiated HPAC cells at 3 hours and 6 hours (figure 5.2A and B). The response was, however, concentration dependent. Interestingly, at a 24-hour time point, it appeared that troglitazone was more toxic to the HPAC cells than the H-14 cells (figure 5.2C).

Compared to H-13 cells, the H-14 cells produced more consistent responses and responded in a concentration dependent manner to troglitazone. The time effect of troglitazone toxicity only occurred between 3 hours and 6 hours. Unexpectedly, troglitazone toxicity did not continue to worsen.

Figure 5.3 compared the response seen in the B-13/H cells to those seen in the HPAC progenitor cells and the differentiated HPACs at a 24-hour time point. It was observed that the B-13/H cells showed a much more consistent response and were also much more susceptible to troglitazone toxicity, at all concentrations of troglitazone, viability was less than that observed in either the H-13 or H-14 cells.

The biggest difference was observed at 50 μM where B-13/H viability was 60% less than that seen in H-14 cells (which showed no loss of viability) and 30% less than the H-14 cells. H-13 cells showed a response more similar to the B-13 cells than the H-14 cells in that there was a concentration dependent decrease in viability in response to troglitazone, however at concentrations $> 5 \mu\text{M}$ the response in B-13 cells was approximately 20% lower than H-13 cells. Conversely, in the undifferentiated state it was the H-14 cells that showed the most similarity with the B-13 cells, comparable responses were seen between B-13 and undifferentiated H-14 cells, there was a concentration dependent decline in viability. In undifferentiated H-13 cells there was no drop in viability observed until a troglitazone concentration of 75 μM .

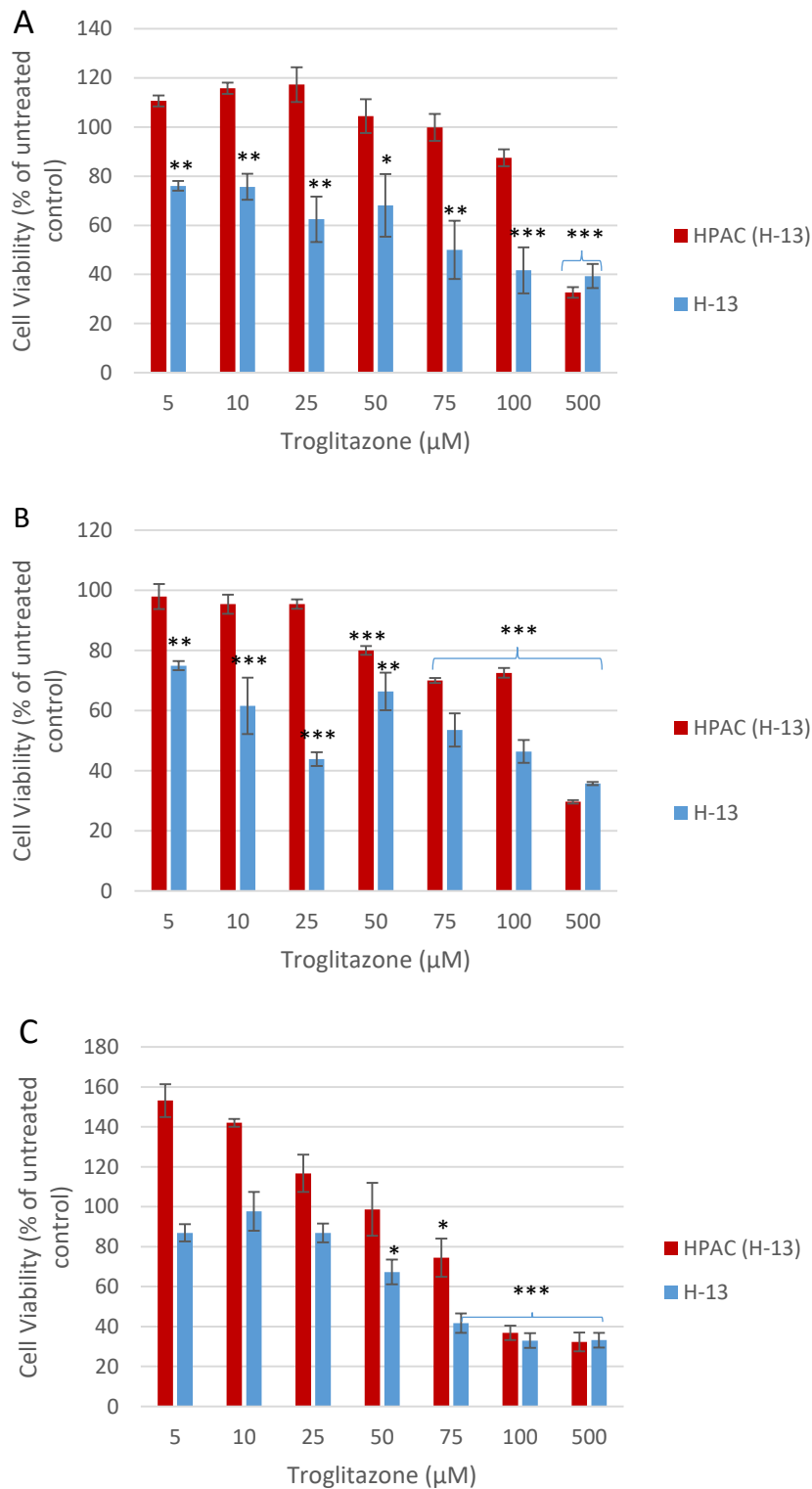


Figure 5.1: The comparison of troglitazone toxicity in H-13 with their undifferentiated counterparts over 24 hours. At concentrations of 50 μM and above there was a concentration and time dependent effect observed in the H-13 cells. H-13 cells were more susceptible to the toxic effects of troglitazone than their undifferentiated HPAC counterpart, this was most evident at a 3-hour time point as viability in the undifferentiated cells were not significantly lower than an untreated control until the maximum concentration of 500 μM was reached. (A) 3-hours (B) 6- hours (C) 24-hours. (* $P < 0.05$, *** $P < 0.001$)

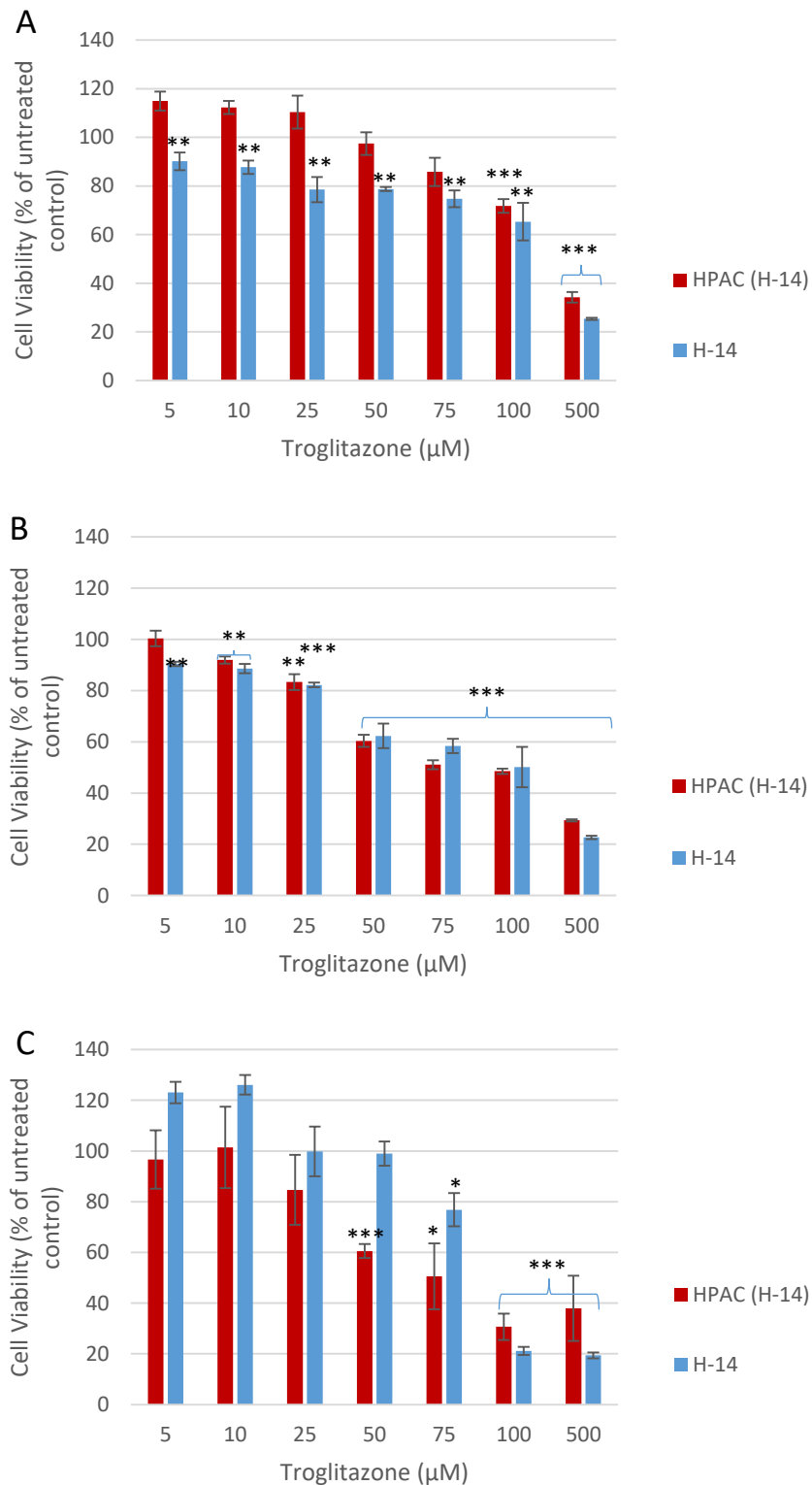


Figure 5.2: The comparison of troglitazone toxicity in H-14 with their undifferentiated counterparts over 24 hours. The H-14 cells showed a time and concentration dependent decrease in viability, in the undifferentiated counterpart, a concentration dependent decrease in viability was only observed at a 24-hour time-point. (A) 3-hours, (B) 6-hours, (C) 24-hours. (* $P < 0.05$, ** $P < 0.01$, *** $P < 0.001$)

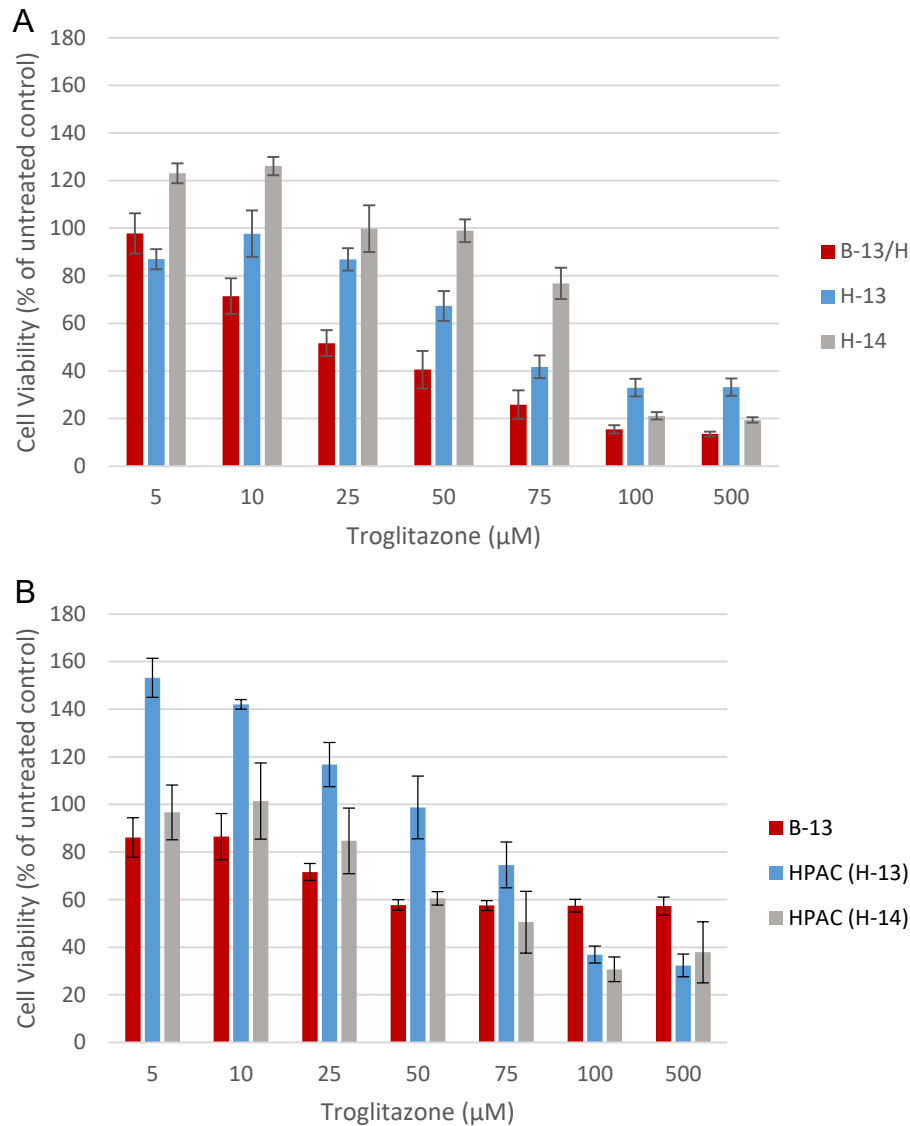


Figure 5.3: Comparison of troglitazone toxicity after 24-hour exposure between rodent and human cells lines. (A) In B-13/H cells there was a concentration dependent decrease in cell viability, this same concentration dependent response was observed in H-13 and H-14 cells, however, the effect was most significant in the B-13/H cells, H-14 cells were least susceptible to the toxic effects of troglitazone. (B) B-13 cells showed a plateau in viability at concentrations of 50 μM and above. HPAC cells showed a concentration dependent drop in viability with the undifferentiated H-14 cells being more susceptible to the effects of troglitazone than the H-13 cells.

It was hypothesised that troglitazone might cause B-13/H cell death via mitochondrial damage. Part of the assessment of mitochondrial damage was to measure the ATP levels within cells. This was repeated, therefore, in the H-13 and H-14 cells in order to determine whether comparable damage occurred in the presence of troglitazone. Similar to the B-13/H cells it was shown in figure 5.4 that as the troglitazone concentration increased there was a decline in ATP concentration

within cells. The effect was more pronounced in the H-13 cells than the H-14 cells with ATP levels typically 10-15% greater in the H-13 cells at troglitazone concentrations between 1 μ M and 50 μ M. In the H-13 cells at concentrations \geq 25 μ M ATP levels were less than 50% of those observed in control cells without troglitazone treatment.

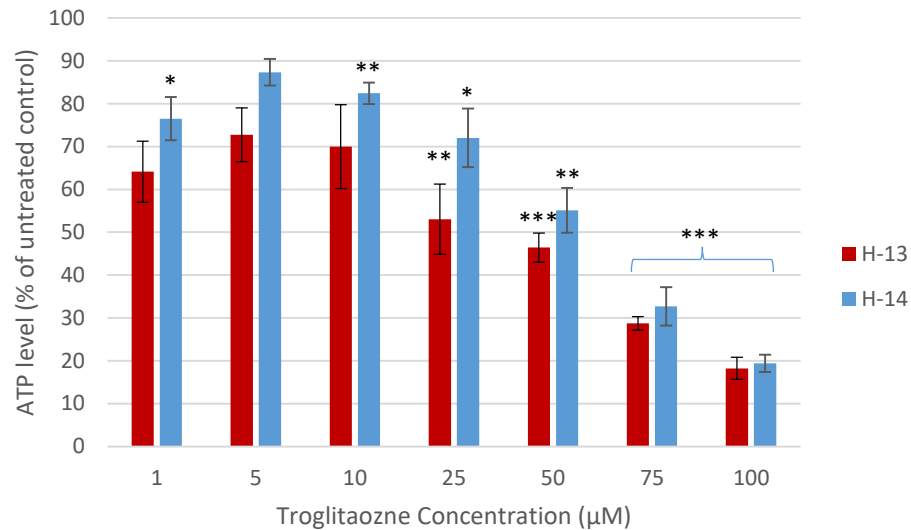


Figure 5.4: ATP levels in H-13 and H-14 cells treated with troglitazone for 1 hour. At concentrations of 5 μ M and above there was a concentration dependent decrease in ATP levels present in both H-13 and H-14 cells. A similar pattern of ATP reduction was seen in both cells lines. (P <0.05, ** P <0.01, *** P <0.001)*

5.4 Discussion

The data presented here support the initial findings by the Wright group that HPAC cells respond in a similar way to B-13 cells when treated with DEX to produce a hepatic like phenotype. Interesting differences were noted however, between the H-13 and H-14 cells. While H-14 cells were shown to be susceptible to troglitazone toxicity in a concentration dependent manner, this was not significantly different to the toxicity seen in the HPAC cells prior to differentiation. This raised the question of whether the HPAC cells were susceptible to troglitazone or whether the differentiated H-14 cells were less susceptible than other hepatocyte like cells. When compared to undifferentiated H-13 and B-13 cells it was observed that undifferentiated H-14 cells had a similar toxicity profile to B-13 cells up to concentrations of 75 μM . However, when data from the differentiated cells was compared to B-13/H cells and H-13 cells, the H-14 cells were not as susceptible to toxicity from troglitazone. This suggested that the H-14 cells had not fully differentiated or that their hepatocyte profile did not contain a full complement of functional drug metabolising enzymes. This is a common problem seen with many other human hepatocyte models (Guillouzo *et al.*, 2007; Hart *et al.*, 2010; Gerets *et al.*, 2012). Conversely it was seen that the H-13 cells were susceptible to troglitazone. While the response at 6 hours was variable it was observed that there was a decline in cellular viability with higher concentrations of troglitazone; this effect was seen at each time point. At a 3 and 24-hour time point, there was a concentration dependent decrease in viability in response to troglitazone exposure. The response at 6 hours was variable at the lower end of the concentration range, however, a decline in viability at concentrations of 50 μM and above was observed. This suggested that troglitazone was toxic to the H-13 cells and, when compared to undifferentiated HPAC cells, H-13 cells were significantly more susceptible. In addition to this, it appeared that troglitazone caused acute toxicity in H-13 cells as toxicity at concentrations $\geq 100 \mu\text{M}$ was not time dependent and toxicity did not worsen after 3 hours up to a maximum of 24 hours. Furthermore, it is also worthy of note that there appeared to be troglitazone-dependent *increase* H-13 progenitor HPAC cells. This is likely to be due to a continuation in proliferation of the cells and a lack of troglitazone related toxicity.

When compared to B-13/H cells at a 24-hour time point it was observed that the H-13 cells were less susceptible to troglitazone than the rodent B-13/H cells. This could possibly be due to the B-13/H cells being hypersensitive due to being grown in

monolayer. As previously discussed in section 5.1.1, the artificial environment in which cells are tested has led to false positive results with regards to troglitazone toxicity (Shen 2011). This highlights the importance of differences between human and animal models. It has been suggested that troglitazone toxicity might have been missed in animal studies due to the nature of the rodents chosen. Healthy, physiologically normal animals were employed in drug screens but patients receiving troglitazone treatment were diabetic and usually obese. This patient group may already have disease related mitochondrial dysfunction which would predispose them to being more vulnerable to troglitazone toxicity (St. Peter *et al.*, 2001; Smith, 2003). However, toxicity was observed in H-13 cells that was greater than in undifferentiated HPAC cells suggesting that DEX caused fundamental genotypic changes in the cells that caused them to become more hepatic.

With that in mind, subsequently ATP levels in H-13 and H-14 cells were measured in order to begin to establish if similar outcomes of toxicity were observed in the differentiated HPACs as was observed in the B-13/H cells. It is widely reported that troglitazone elicits toxicity through mitochondrial damage (Tirmenstein *et al.*, 2002; Masubuchi *et al.*, 2006; Rachek *et al.*, 2009; Nadanaciva *et al.*, 2012; Hu *et al.*, 2015). An indicator of mitochondrial dysfunction is a drop in ATP content as damaged mitochondria with a dysfunctional electron transport chain no longer effectively produce ATP. It was shown in Chapter 4 that in the B-13/H cells there was a drop in ATP levels that was supported by extracellular flux analysis which showed a concomitant drop in oxygen consumed for ATP production. It was found that there was a concentration dependent decrease in ATP levels seen with increasing troglitazone concentration in both H-13 and H-14 cells. The effect was more pronounced in the H-13 than the H-14 cells, suggesting that there was a greater degree of mitochondrial dysfunction in the H-13 cells. This, combined, with the toxicity data might suggest that the H-13 cells were a more susceptible alternative to H-14 cells as they appear from these initial experiments to behave more like hepatocytes. It has previously been found that troglitazone is similarly able to reduce ATP levels in human hepatocytes; however, the decrease was far greater in the human hepatocytes. Rachek *et al.* found that concentrations of troglitazone $\geq 10 \mu\text{M}$ reduced ATP levels to less than 50% of an untreated control and a maximum concentration of $50 \mu\text{M}$ reduced levels to approximately 4% of that seen in an untreated control (Rachek *et al.*, 2009). The data presented here suggest that

troglitazone produced some degree of mitochondrial damage that affected ATP production in both the H-13 and H-14 cells. This suggested that troglitazone might be able to elicit cellular damage but is not lethal. It is also interesting to note that the only difference between the H-13 and H-14 cells are the transcription factors used to create the cells. HNF4a is known to be required for PXR and CAR mediated transcriptional activation of CYP3A4 (Hwang-Verslues and Sladek, 2010). It is also known that CYP3A4 is the primary CYP enzyme involved in the metabolism of troglitazone (He *et al.*, 2001; Hewitt *et al.*, 2002; Sahi *et al.*, 2003). Therefore, it is possible that this explains the greater susceptibility of H-13 cells than H-14 cells to the toxic effects of troglitazone. This would also suggest a role for metabolism in the mechanism of troglitazone toxicity. Before these cells can be fully characterised, however, there is much work that remains to be done. The response to troglitazone wasn't linear in the H-13 cells at 6 hours due to an anomalous result suggesting that perhaps the cells behave inconsistently.

Work reported here has shown that the B-13/H cell line can be humanised, thus limiting the problems faced with further drug extrapolation. Probert *et al* reported that the B-13 cell line could be stably transfected with human CYP 1A2 and the subsequently derived B-13/H cells expressed functional CYP 1A2 at the mRNA and protein level. This was shown by their ability to metabolise methoxyresorufin, an inducer of CYP 1A2 in humans (Probert *et al.*, 2014). Until the time when a human cell line is fully developed, a humanised line would offer a useful alternative.

The data presented here add to the current body of research for the development of a human alternative to the B-13/H cell line. The growth factors used appear to have a marked effect on the functionality of differentiated cells. The H-13 cells which were transfected with HNF4a were far more susceptible to the effects of troglitazone than H-14 cells which showed no marked difference in cytotoxicity from the undifferentiated HPAC cells. While it is possible that this may be due to the fact that HNF4a is required for the activation of the main troglitazone metabolising CYP enzyme, CYP3A4, investigating CYP induction could be important in understanding why these differences occur and crucial in optimising the process of differentiation and ultimately in producing a new cell line.

Given time constraints it was not possible to test the undifferentiated HPACs for ATP content in response to troglitazone. This would have been the obvious next step in

order to make comparisons following differentiation and to understand if similar damage was seen in response to troglitazone prior to DEX treatment. Ideally more detailed experiments would be performed on the H-13 and H-14 cells so that a full comparison with the B-13/H cells could also be made, including extracellular flux analysis and lactate assays to determine if mitochondrial damage was also a contributing factor to the cytotoxicity observed.

5.5 References

- Babeu, J.P. and Boudreau, F. (2014) 'Hepatocyte nuclear factor 4-alpha involvement in liver and intestinal inflammatory networks', *World Journal of Gastroenterology*, 20(1), pp. 22-30.
- Bedoucha, M., Atzpodien, E. and Boelsterli, U.A. (2001) 'Diabetic KKAy mice exhibit increased hepatic PPAR γ 1 gene expression and develop hepatic steatosis upon chronic treatment with antidiabetic thiazolidinediones', *Journal of Hepatology*, 35(1), pp. 17-23.
- Boelsterli, U.A. and Lim, P.L.K. (2007) 'Mitochondrial abnormalities-A link to idiosyncratic drug hepatotoxicity?', *Toxicology and Applied Pharmacology*, 220(1), pp. 92-107.
- Fairhall, E.A. (2013) *Hepatocyte generation from pancreatic acinar cell lines*. Newcastle University
- Fairhall, E.A., Wallace, K., White, S.A., Huang, G.C., Shaw, J.A., Wright, S.C., Charlton, K.A., Burt, A.D. and Wright, M.C. (2013) 'Adult human exocrine pancreas differentiation to hepatocytes - Potential source of a human hepatocyte progenitor for use in toxicology research', *Toxicology Research*, 2(1), pp. 80-87.
- Gerets, H.H.J., Tilmant, K., Gerin, B., Chanteux, H., Depelchin, B.O., Dhalluin, S. and Atienzar, F.A. (2012) 'Characterization of primary human hepatocytes, HepG2 cells, and HepaRG cells at the mRNA level and CYP activity in response to inducers and their predictivity for the detection of human hepatotoxins', *Cell Biology and Toxicology*, 28(2), pp. 69-87.
- Graham, M.J. and Lake, B.G. (2008) 'Induction of drug metabolism: Species differences and toxicological relevance', *Toxicology*, 254(3), pp. 184-191.
- Guillouzo, A., Corlu, A., Aninat, C., Glaise, D., Morel, F. and Guguen-Guillouzo, C. (2007) 'The human hepatoma HepaRG cells: A highly differentiated model for studies of liver metabolism and toxicity of xenobiotics', *Chemico-Biological Interactions*, 168(1), pp. 66-73.
- Hart, S.N., Li, Y., Nakamoto, K., Subileau, E.A., Steen, D. and Zhong, X.B. (2010) 'A comparison of whole genome gene expression profiles of HepaRG cells and HepG2 cells to primary human hepatocytes and human liver tissues', *Drug Metabolism and Disposition*, 38(6), pp. 988-994.

- He, K., Woolf, T.F., Kindt, E.K., Fielder, A.E. and Talaat, R.E. (2001) 'Troglitazone quinone formation catalyzed by human and rat CYP3A: An atypical CYP oxidation reaction', *Biochemical Pharmacology*, 62(2), pp. 191-198.
- Hewitt, N.J., Lloyd, S., Hayden, M., Butler, R., Sakai, Y., Springer, R., Fackett, A. and Li, A.P. (2002) 'Correlation between troglitazone cytotoxicity and drug metabolic enzyme activities in cryopreserved human hepatocytes', *Chemico-Biological Interactions*, 142(1-2), pp. 73-82.
- Hu, D., Wu, C.Q., Li, Z.J., Liu, Y., Fan, X., Wang, Q.J. and Ding, R.G. (2015) 'Characterizing the mechanism of thiazolidinedione-induced hepatotoxicity: An in vitro model in mitochondria', *Toxicology and Applied Pharmacology*, 284(2), pp. 134-141.
- Hwang-Verslues, W.W. and Sladek, F.M. (2010) 'HNF4 α -role in drug metabolism and potential drug target?', *Current Opinion in Pharmacology*, 10(6), pp. 698-705.
- Martignoni, M., Groothuis, G.M.M. and de Kanter, R. (2006) 'Species differences between mouse, rat, dog, monkey and human CYP-mediated drug metabolism, inhibition and induction', *Expert Opinion on Drug Metabolism and Toxicology*, 2(6), pp. 875-894.
- Masubuchi, Y., Kano, S. and Horie, T. (2006) 'Mitochondrial permeability transition as a potential determinant of hepatotoxicity of antidiabetic thiazolidinediones', *Toxicology*, 222(3), pp. 233-239.
- McKim Jr, J.M. (2010) 'Building a tiered approach to in vitro predictive toxicity screening: A focus on assays with in vivo relevance', *Combinatorial Chemistry and High Throughput Screening*, 13(2), pp. 188-206.
- Nadanaciva, S., Rana, P., Beeson, G.C., Chen, D., Ferrick, D.A., Beeson, C.C. and Will, Y. (2012) 'Assessment of drug-induced mitochondrial dysfunction via altered cellular respiration and acidification measured in a 96-well platform', *Journal of Bioenergetics and Biomembranes*, 44(4), pp. 421-437.
- Norman, J., Franz, M., Schiro, R., Nicosia, S., Docs, J., Fabri, P.J. and Gower Jr, W.R. (1994) 'Functional glucocorticoid receptor modulates pancreatic carcinoma growth through an autocrine loop', *Journal of Surgical Research*, 57(1), pp. 33-38.
- Peters, T.S. (2005) 'Do preclinical testing strategies help predict human hepatotoxic potentials?', *Toxicologic Pathology*, 33(1), pp. 146-154.
- Pontoglio, M. (2000) 'Hepatocyte nuclear factor 1, a transcription factor at the crossroads of glucose homeostasis', *Journal of the American Society of Nephrology*, 11(SUPPL. 16).

- Probert, P.M.E., Chung, G.W., Cockell, S.J., Agius, L., Mosesso, P., White, S.A., Oakley, F., Brown, C.D.A. and Wright, M.C. (2014) 'Utility of B-13 progenitor-derived hepatocytes in hepatotoxicity and genotoxicity studies', *Toxicological Sciences*, 137(2), pp. 350-370.
- Rachek, L.I., Yuzefovych, L.V., LeDoux, S.P., Julie, N.L. and Wilson, G.L. (2009) 'Troglitazone, but not rosiglitazone, damages mitochondrial DNA and induces mitochondrial dysfunction and cell death in human hepatocytes', *Toxicology and Applied Pharmacology*, 240(3), pp. 348-354.
- Sahi, J., Black, C.B., Hamilton, G.A., Zheng, X., Jolley, S., Rose, K.A., Gilbert, D., Lecluyse, E.L. and Sinz, M.W. (2003) 'Comparative effects of thiazolidinediones on in vitro P450 enzyme induction and inhibition', *Drug Metabolism and Disposition*, 31(4), pp. 439-446.
- Shen, C., Meng, Q. and Zhang, G. (2012) 'Species-specific toxicity of troglitazone on rats and human by gel entrapped hepatocytes', *Toxicology and Applied Pharmacology*, 258(1), pp. 19-25.
- Smith, M.T. (2003) 'Mechanisms of troglitazone hepatotoxicity', *Chemical Research in Toxicology*, 16(6), pp. 679-687.
- St. Peter, J.V., Neafus, K.L., Khan, M.A., Vessey, J.T. and Lockheart, M.S.K. (2001) 'Factors associated with the risk of liver enzyme elevation in patients with type 2 diabetes treated with a thiazolidinedione', *Pharmacotherapy*, 21(2), pp. 183-188.
- Sumitran-Holgersson, S., Nowak, G., Thowfeequ, S., Begum, S., Joshi, M., Jaksch, M., Kjaeldgaard, A., Jorns, C., Ericzon, B.G. and Tosh, D. (2009) 'Generation of hepatocyte-like cells from in vitro transdifferentiated human fetal pancreas', *Cell Transplantation*, 18(2), pp. 183-193.
- Tirmenstein, M.A., Hu, C.X., Gales, T.L., Maleeff, B.E., Narayanan, P.K., Kurali, E., Hart, T.K., Thomas, H.C. and Schwartz, L.W. (2002) 'Effects of troglitazone on HepG2 viability and mitochondrial function', *Toxicological Sciences*, 69(1), pp. 131-138.

Chapter 6: General Discussion

6.1 General Discussion

High attrition rates and a pressure to reduce the number of animal used in pharmacokinetic studies are driving reform of preclinical testing. It has been reported that in recent years expenditure by the pharmaceutical industry on research and development has increased by 80% whereas productivity has decreased by 43% (Ahuja and Sharma, 2014). This lack of efficiency has largely been attributed to a failure to predict toxicity in the early screening process, with 40% of NCEs failing to progress past the preclinical safety testing phase (McKim Jr, 2010). Furthermore, it has been suggested that cardiac and hepatic toxicity contribute disproportionately to drug withdrawals from the market (Stevens and Baker, 2009). Therefore, a hepatic cell model that does not require an animal donor would represent a significant development in this reform. While many hepatic models do exist for this purpose they are fraught with reliability issues owing to a lack of functional metabolic enzyme profiles and while human hepatocytes are available for studies they have a tendency to dedifferentiate in culture and have an inability to proliferate (Marek *et al.*, 2003). The B-13 cell line presents a potential alternative as a progenitor to a hepatocyte-like cell line, B-13/H. It is a donor free cell line that can be produced in unlimited numbers, on demand.

The primary aims of this thesis was to investigate and characterise the B-13/H toxicity profile when tested with known hepatotoxins. Particular focus was placed on identifying mitochondrial dysfunction, as this is increasingly becoming implicated in the aetiology of drug induced toxicity and particularly hepatotoxicity. Troglitazone was withdrawn from the market in 2000 after reports of severe liver injury. Mitochondrial liabilities have since been associated with the toxicity that resulted in its withdrawal (Dykens and Will, 2007; Ahuja and Sharma, 2014). Troglitazone, therefore, presented the ideal challenge for the B-13 and B-13/H cells in order to study its potential for mitochondrial dysfunction in hepatocytes.

Menadione is a chemical that is commonly used for research purposes to produce cytotoxicity. It has a well characterised toxicity profile and elicits damage through a redox cycling mechanism due to a quinone moiety in its chemical structure (Klotz *et al.*, 2014). It is known that the chemical structure of troglitazone also contains a quinone moiety and thus it was hypothesised that troglitazone may also be capable of causing oxidative stress through a redox cycling mechanism.

As a general assessment of the differences between the B-13 and B-13/H cells when exposed to troglitazone, a viability assay was performed. If DEX treatment had caused a functional hepatic genotype within the B-13/H cells it was anticipated that a drug with known hepatotoxic effects would elicit greater toxicity in the B-13/H cells than the B-13 cells. It was subsequently found that menadione caused much greater cytotoxicity in the B-13/H cells compared to a minimal loss in viability shown by B-13 cells. This finding supported the idea that following transdifferentiation, B-13/H cells developed a significantly different metabolic profile. This was supported by data generated from a troglitazone viability assay. This time, while there was cytotoxicity observed in both cell lines the drop in viability was much greater in the B-13/H cells than the B-13. A plateau was observed in B-13 cells exposed to troglitazone, beyond which there was no further loss. This was an interesting finding as it suggested that troglitazone could be toxic to B-13 cells without the need for metabolism by the abundant CYP enzymes found in hepatocytes and consequently that the parent compound itself may elicit damage. This finding could also suggest that troglitazone toxicity might be a cumulative effect of the parent drug *and* its metabolites. This could be investigated by using inhibitors of metabolic enzymes such as CYP3A which is known to be the primary CYP family that metabolises troglitazone in rodents (He *et al.*, 2001). Therefore, if metabolism played a role in hepatocyte toxicity, this would be inhibited and any maintenance of cell viability would indicate a role for metabolism in toxicity. For example, it was found that troglitazone sulphate, to a much greater extent than troglitazone, could elicit damage through competitive inhibition of the BSEP in rats (Funk *et al.*, 2001).

It is known that menadione can undergo redox cycling and is thought that due to similar structural features, troglitazone and quinone metabolites of troglitazone will also be able to redox cycle. The most common accepted technique for measuring ROS is the use of fluorescent dyes which undergo redox reactions to form a fluorescent by-product. The amount of fluorescence detected is proportional to the amount of ROS produced. This technique is unreliable and has a tendency to lack specificity for the ROS species of interest, often showing cross reactivity with multiple ROS (Yazdani, 2015). Therefore, one of the aims of this project was to develop a platform with which O_2^- production could be measured intra- and extracellularly. Knowing that the most common site of ROS production is the mitochondria due to a leak in the channel of electrons along the electron transport chain forming O_2^- within

the mitochondrial matrix it would represent a major step forward if ROS could be measured near the site of production intracellularly as O_2^- is rapidly dismutated by endogenous antioxidants making extracellular detection quite difficult. A combined platform in which O_2^- could be detected both intracellularly using PEBBLE nanosensors and extracellularly using electrochemistry would give a much better understanding of drug induced ROS.

Unfortunately, as shown by the data presented in Chapter 2, the development of a functional nanosensor to detect ROS was far more challenging than anticipated and while progress was made in understanding the limitations and the requirements for a functional sensor, no experimental data was able to be obtained from the intracellular environment of B-13 or B-13/H cells. Dye retention within the sensor matrix appeared to be the main issue with the sensor development. The nature of ROS responsive dyes means that their chemical structure is compact and makes the dye molecules smaller than the gaps in the polyacrylamide matrix. This led to a situation during the washing stages of the manufacture process where the dye was rinsed from the nanosensor mix into the solvent. Subsequently, in calibration experiments, it was observed that the sensors did not respond to an enzyme system in which O_2^- was produced. It was shown as a proof-of concept that a pH nanosensor could be successfully calibrated and it has been shown previously that PEBBLE nanosensors can be successfully utilised in the detection of changes in pH in cellular lysosomal compartments (Zhang *et al.*, 2015) and in whole *C. elegans* worms (Chauhan *et al.*, 2013). Therefore, with further developmental work it is hoped that a ROS nanosensor can also be developed. Future work on this aspect of the project would require investigating how to make the dye molecules larger without affecting functionality of the dye, this could possibly be achieved by the covalent binding of dextran, an inert carbohydrate chain, to the dye molecule which should make it physically larger thus preventing the leaching from the dye matrix. Following on from successful dye entrapment it would be pertinent to produce a calibration curve in a cell free system to optimise the signal obtained. At this stage it would then be possible to internalise the nanosensors into the cells to obtain measures of the intracellular environment.

The electrochemistry for the measures of the extracellular environment also saw some variable results. While it was possible to obtain a response from B-13/H cells to menadione it was found that the signal obtained was 100 times smaller than that

seen in calibration experiments so whether this was a true response or not is unclear. Furthermore, no signal at all could be obtained from cells used past 5 days transdifferentiation or with the use of troglitazone. The extracellular sensing method, therefore, may not have been sensitive enough to detect O_2^- using the experimental set up described. The calibration curve was produced using a stirred system and it is suspected that this may be key to the erratic signals obtained from the cell based system which was unstirred and thus there may not have been even distribution of the drug throughout the medium.

Further methods for assessing drug-induced mitochondrial dysfunction were assessed. Mitochondrial functionality can be examined using measures of oxygen consumption as oxygen is required for the production of ATP in healthy mitochondria. A change in oxygen consumption rate is indicative of mitochondrial dysfunction. Traditionally these measures have been made using a Clark electrode, however, in recent years, significant progress has been made in the development of new technologies for oxygen sensing. The Seahorse Extracellular Flux Analyser offers a wide range of mitochondrial assessment criteria which added significant value to this research. The technique allows for high throughput screening by using a 96-well plate format and a multiple injection strategy allows for multiple measures from a single well allowing for large amounts of data to be generated in a short amount of time (Brand and Nicholls, 2011). This would be a particular benefit in the preclinical testing environment as resources have to be accurately targeted.

The Extracellular Flux Analyser was used to perform mitochondrial stress tests on the B-13 and B-13/H cells in response to troglitazone challenge. Previously data suggested that troglitazone elicited greater loss of viability in B-13/H cells than the B-13 cells. It was hypothesised that this difference was due to DEX treatment creating a hepatic-like phenotype in the B13/H cells. Subsequently, troglitazone would be expected to cause mitochondrial dysfunction that would be shown as a concentration dependent drop in oxygen consumption rate. The findings produced from B-13/H cells analysis supported these assertions. A concentration dependent decrease in oxygen consumption rate was observed suggesting a depression of mitochondrial respiration which was indicative of mitochondrial dysfunction. This finding was supported by an ATP quantification assay which showed a concentration dependent decrease in the total ATP content within the cells following troglitazone exposure.

Results obtained from B-13 cells were unexpected. Troglitazone was seen to be significantly less toxic to the B-13 cells when compared to B13/H cells. This would suggest that there would be negligible differences in the oxygen consumption rate seen when B13 cells were incubated with troglitazone. Whilst B13 cell oxygen consumption rate did not fall below levels seen in untreated cells there was an increase in oxygen consumption seen with lower concentrations of troglitazone. ATP quantification assays showed that there was a slight decrease in cellular ATP levels despite the oxygen consumption rate for ATP production increasing. This suggested that there were inefficiencies in the electron transport chain and the transport of electrons may not have been linked to the production of ATP. This was supported by an observed increase in proton leak. A lactate assay showed that in the B-13 cells there was a large increase in the amount of lactate present in cells suggesting that B-13 cells were using glycolysis as a mechanism to produce ATP as a compensatory mechanism for the dysfunction in mitochondria.

The extracellular flux data was particularly interesting as it displayed distinct functional differences between the B-13 and B-13/H cells and suggested that the DEX treatment did cause the cells to undergo genotypic as well as phenotypic changes. To confirm the suggestion that glycolysis played a compensatory role for ATP production in cells, further work would utilise the glycolysis stress test function of the Extracellular Flux Analyser to measure the extracellular acidification rate in cells as lactate production is the main contributor to acidification within cells (Dykens and Will, 2007).

Currently in development is a human cell line derived from HPAC cells. While still in the very early stages of development, the preliminary results here have already highlighted a difference in response between the two hepatic cell lines, H-13 and H-14, to troglitazone treatment. The H-13 cells showed a greater tendency for hepatic behaviour than the H-14 cells. Toxicity observed in the H-14 cells was not significantly different to that seen in the undifferentiated HPAC cells. The potential for further work on the H-13 and H-14 cells is beyond the scope of this one project. However, with regards to troglitazone it would be interesting to establish a profile for mitochondrial respiration within the cells. It was found that, despite hepatocytes being much more metabolically active than pancreatic cells, that the B-13 and B-13/H cells showed remarkably similar basal levels of respiration until challenged with a toxin. Therefore, further work could involve extracellular flux analysis of the H-13 and

H-14 cells to see if their basal levels of respiration are different and if, when treated with troglitazone, there was a difference in mitochondrial response. If the H-13 still behaved more like hepatocytes than H-14 cells it would be expected that their oxygen consumption rate would decrease in response troglitazone.

One of the greatest challenges that pharma companies face when doing preclinical toxicity testing is extrapolating the data generated in animals to humans. Indeed, while the data presented here, from a rat cell line, supports the reports in current literature that troglitazone is hepatotoxic, this was not seen in the preclinical toxicity studies in whole rat models. It has been suggested that rodent hepatocytes grown in monolayer are more sensitive due to a reduced rate of clearance and thus show a false positive result. Further work could be done to investigate this by growing the B-13 cells in 3D culture. It has previously been shown by Richter *et al.* that when B-13 cells were grown in a 3D bioreactor that they were able to successfully transdifferentiate into B-13/H cells and aggregate in a 3D configuration. Hepatocyte formation was confirmed by an increase in expression of hepatocyte specific markers; albumin, cytokeratin 18, CEBP- β and CYP2E1. The B-13/H cells were stably maintained for a 2-week period (Richter *et al.*, 2015). It would therefore be of interest to study the effects of troglitazone on the B-13/H cells grown in 3D culture in order to determine whether the cells showed a comparable response to those seen in whole animal studies. Finally, it would ultimately be of interest to try and grow the H-13 and H-14 cells in a 3D bioreactor in order to determine if a response can be generated that is similar to the response seen in humans following troglitazone treatment.

The data presented here show that the B-13 cell line represents an *in vitro* cell model with huge developmental potential as a progenitor of B-13/H hepatocyte like cells. The hepatic response of the B-13/H cells to challenge with a known hepatotoxin opens the door for further development of the cell line as an alternative *in vitro* model that could potentially inform the use of further animal models, thus reducing the number of animals required. The ultimate goal however, still remains to be the development of a human hepatocyte cell line that can be produced on demand and in unlimited numbers. Initial work using the HPAC cell line is promising but many challenges still remain and elucidating the molecular mechanisms behind differentiation is crucial in forming a robust *in vitro* model for preclinical toxicity testing and beyond.

6.2 References

- Ahuja, V. and Sharma, S. (2014) 'Drug safety testing paradigm, current progress and future challenges: An overview', *Journal of Applied Toxicology*, 34(6), pp. 576-594.
- Brand, M.D. and Nicholls, D.G. (2011) 'Assessing mitochondrial dysfunction in cells (Biochemical Journal (2011) 435, (297-312))', *Biochemical Journal*, 437(3), p. 575.
- Chauhan, V.M., Orsi, G., Brown, A., Pritchard, D.I. and Aylott, J.W. (2013) 'Mapping the pharyngeal and intestinal pH of *Caenorhabditis elegans* and real-time luminal pH oscillations using extended dynamic range pH-sensitive nanosensors', *ACS Nano*, 7(6), pp. 5577-5587.
- Dykens, J.A. and Will, Y. (2007) 'The significance of mitochondrial toxicity testing in drug development', *Drug Discovery Today*, 12(17-18), pp. 777-785.
- Funk, C., Ponelle, C., Scheuermann, G. and Pantze, M. (2001) 'Cholestatic potential of troglitazone as a possible factor contributing to troglitazone-induced hepatotoxicity: In vivo and in vitro interaction at the canalicular bile salt export pump (Bsep) in the rat', *Molecular Pharmacology*, 59(3), pp. 627-635.
- He, K., Woolf, T.F., Kindt, E.K., Fielder, A.E. and Talaat, R.E. (2001) 'Troglitazone quinone formation catalyzed by human and rat CYP3A: An atypical CYP oxidation reaction', *Biochemical Pharmacology*, 62(2), pp. 191-198.
- Klotz, L.O., Hou, X. and Jacob, C. (2014) '1,4-naphthoquinones: From oxidative damage to cellular and inter-cellular signaling', *Molecules*, 19(9), pp. 14902-14918.
- Marek, C.J., Cameron, G.A., Elrick, L.J., Hawksworth, G.M. and Wright, M.C. (2003) 'Generation of hepatocytes expressing functional cytochromes P450 from a pancreatic progenitor cell line in vitro', *Biochemical Journal*, 370(3), pp. 763-769.
- McKim Jr, J.M. (2010) 'Building a tiered approach to in vitro predictive toxicity screening: A focus on assays with in vivo relevance', *Combinatorial Chemistry and High Throughput Screening*, 13(2), pp. 188-206.
- Richter, M., Fairhall, E.A., Hoffmann, S.A., Tröbs, S., Knöspel, F., Probert, P.M.E., Oakley, F., Stroux, A., Wright, M.C. and Zeilinger, K. (2015) 'Pancreatic progenitor-derived hepatocytes are viable and functional in a 3D high density bioreactor culture system', *Toxicology Research*, 5(1), pp. 278-290.
- Stevens, J.L. and Baker, T.K. (2009) 'The future of drug safety testing: expanding the view and narrowing the focus', *Drug Discovery Today*, 14(3-4), pp. 162-167.
- Yazdani, M. (2015) 'Concerns in the application of fluorescent probes DCDHF-DA, DHR 123 and DHE to measure reactive oxygen species in vitro', *Toxicology in Vitro*, 30(1), pp. 578-582.

Zhang, M., Søndergaard, R.V., Kumar, E.K.P., Henriksen, J.R., Cui, D., Hammershøj, P., Clausen, M.H. and Andresen, T.L. (2015) 'A hydrogel based nanosensor with an unprecedented broad sensitivity range for pH measurements in cellular compartments', *Analyst*, 140(21), pp. 7246-7253.